Analytical and Numerical analysis of extrusion force, stress and strain development during extrusion Al-SiC composite

A thesis submitted by

Fentahun Workie Zeleke

(GSR/0084/09)

Advisor:

Dr. C. Venkatesh

For the Partial fulfillment of the

Requirement for the award of degree

Of

Master of Science

In Manufacturing Engineering

Advisor:

Dr. Venkatesh

Mechanical Design & Manufacturing Engineering Program

School of Mechanical, Chemical and Materials Engineering

Adama Science and Technology University

June, 2018

ADAMA, ETHIOPIA

School of Mechanical Chemical and Materials Engineering

Mechanical Design and Manufacturing Engineering Program

Analytical and Numerical analysis of extrusion force, stress and strain development during extrusion Al-SiC composite

By

Fentahun Workie Zeleke

Approved by board of examiners

Chair, department graduate committee	Signature	Date
______________________________	_____________	____________
Advisor	Signature	Date
Dr.C.Venkatesh	_________	____________
Internal examiner	Signature	Date
Dr.Desalegn Wagaso	__________	_________
External examiner	Signature	Date
Dr.Asmamaw Tegegne	________	_______

DECLARATION

I hereby declare that the work which is being presented in this thesis entitled **"Analytical and Numerical analysis of extrusion force, stress and strain development during extrusion Al-SiC composite"** in partial fulfillment of the requirement for the award of the degree of Masters of Science in Manufacturing Engineering is my own work carried out **September to June 2018** under the supervision of **Dr.C.Venkatesh**, program of Mechanical Design and Manufacturing Engineering, Adama Science and Technology University, Adama, Ethiopia.

The matter embodied in this thesis has not been submitted by me for the award of any other degree or diploma. All relevant resources of information used in this thesis have been duly acknowledged.

Fentahun Workie Zeleke ID NO: GSR/0084/09 ______________ _____________

Candidate Signature Date

This is to certify that the above declaration made by the candidate is correct to the best of my knowledge and belief. This thesis has been submitted for examination with my approval.

Dr.C.Venkatesh ______________ _______________

Advisor Signature Date

ACKNOWLEDGEMENT

First of all my deep gratitude goes to the almighty GOD for everything he did to me in all the way I path through, then after for my advisers Dr.C.Venkatesh including Mechanical Design and Manufacturing Engineering Department staff members for their continues and progressive support, advice and guide me to do better work and give me a reference materials and initiate me for my work. In addition, I would like to thanks Dr.PJR. to help for DEFORM 3D software and I would like to thank my classmates and friends for sharing their ideas and materials. In addition, I would like to thank my families to help for this study.

ABSTRACT

Aluminium based metal matrix composite with silicon carbide as particle reinforcements called discontinuous reinforced metal matrix composites have excellent mechanical properties like high yield strength, wear resistance, corrosion resistance and vibration resistance .During the development of discontinuous reinforcement metal matrix composites compression process like, extrusion is an advisable secondary process for homogenous distribution of the reinforcements materials through the metal matrix. This research was investigated the metal flow behaviour of extrusion load, stress and strain distribution of Al/Sic based discontinuous reinforcement metal matrix composite billets extruded from round billet to square shape through two different die profiles namely, third order polynomial and cosine die profiles by taking 30%, 60% and 90% area reductions. Depends on these three different area reductions were analyzed analytically and numerically by using upper bound and DEFORM 3D finite element analysis method respectively. Due to these different area reductions, the extrusion load was minimum in cosine die profiles both analytical and numerical results. In 30% of area reduction cosine die profile has optimum load (878.59N) and it used to extrude Al6063/20%SiC composite billet materials from 20mm input diameter to 14.8x14.8mm output square sides.

Keywords*:* Metal Matrix composite, Extrusion, force, strain and DEFORM-3D

TABLE OF CONTENT

Contents **page**

LIST OF FIGURE

LIST OF TABLE

NOMENCLATURE

Symbols

L	Length of the die
m	Friction factor
P_{ave}	Average extrusion load
r, z,θ	Cylindrical coordinate system
R (z)	Die profile
R' (z)	First order derivation of R(z)
R'' (z)	second order of R(z)
R_1	Radius at the entry
R_2	Radius at the exist
V_0	Ram velocity
V_r, V_z, V_θ	Velocity components in r, z and θ
εij	Strain rate tensor
ξ	Stream function constant
σ_y	Yield stress value of the material
ψ	Stream function
J	Total power
WI	power losses due to the plastic deformation

ABBREVIATION

AMC	Aluminium Matrix Composite
MMCs	Metal Matrix Composites
SiC	Silicon Di Carbide
DB	Data Bas
DRMM	Discontinuous reinforcement metal matrix
FEM	Finite Element Method
CAD	Computer Aided Design

CHAPTER ONE

INTRODUCTION

1.1 General backgrounds

Metallic matrix composites are combinations of two or more different metals, inter metal compounds or second phases in which dispersed phases are embedded within the metallic matrix. They are produced by controlling the morphologies of the constituents to achieve optimum combination of properties. Properties of the composites depend on the properties of the constituent phases, their relative amount, and dispersed phase geometry including particle size, shape and orientation in the matrix. AMCs have found wide applications in our daily life. There are some advantages in using particles reinforced AMCs materials than unreinforced materials such as- greater strength and high specific modulus, improved stiffness, light weight, low thermal expansion coefficient, high thermal conductivity, tailored electrical properties, increased wear resistance and improved damping capabilities. Reinforcing constituents can be incorporated within the matrix in the form of particles, short fibers, continuous fibers or mono filaments (Md. Halibut Rahmana (2014)). Now it is used in aerospace, thermal management areas, industrial products, automotive applications such as engine piston, break disc etc. Md.Halibut et al (2014)

There are two primary processes to develop AMC fabrication systems which are among at depend on temperature such as liquid phase processing techniques such as casting and solid phase processing techniques including powder metallurgy routes. After the primary fabrication methods, there are also secondary processing techniques to develop AMC materials such as extrusion, rolling or forging are necessary for consolidating the composites and decreasing their porosity. Extrusion is a very effective step to improve the density and mechanical properties of MMCs. The extruded microstructures have a more uniform distribution of the SiC particles and the eutectic silicon by comparison with as-cast microstructures. Evaluation of the mechanical properties show that the extruded samples have strength and ductility values superior to those of the as-cast counterparts. In the extruded samples the addition of increasing amounts of particulate SiC increases the yield and tensile strength and decreases the ductility. The ductility level of the extruded samples is found to be higher than those of the forged and as cast samples Jabbar Kasim Jabbar (2010).

1.2 Extrusion

Extrusion is an often used forming process among the different metal forming operations and its industrial history dates back to the 18th century. A billet (work piece) is placed in the container and pressed by the punch, after pressing the metal to flow through a die with an opening. In process of extrusion, a billet is placed in an enclosed chamber. The chamber has an opening through which the excess material escapes as the volume of chamber is reduced when pushed by ram (punch). The escaped material has a uniform cross section identical with that of the opening. In general extrusion process is used to produce cylindrical bars or hollow tubes. A large variety of irregular cross sections are also created by this process using dies of complex shapes. The process has accuracy and firmness, in this process large reduction achieved even at high strain rates has made it one of the fastest growing metal working methods. In extrusion process more force is required. The most metals are extruded hot when the deformation resistance of this metal is low. However cold extrusion is also possible for many metals and has become an important commercial process. The reaction of the workspace with the container and the die result in high compressive stress that effectively reduces cracking of the materials during primary breakdown from ingot. This is an important reason for increased commercial adaptation of extrusion in the working of metal difficult to such as stainless steel, nickel, nickel based alloy and other high temperature materials. More than 10 years ago researchers started to attracted by the 3D problems in metal forming now-a-days 3D modeling (Singh Pachalasiya (2013)) is still regarded as a highlighted and difficult problem. The different methods of analysis extended to 3D, among which the finite element analysis is most commonly used. Most of the results that have been published on three dimensional finite element method simulations are based on software package like DEFORM-3D.Plastic deformation process in which a block of billet is forced to flow by compression through the die opening of a smaller cross-sectional area. Show in Fig.1.1 below

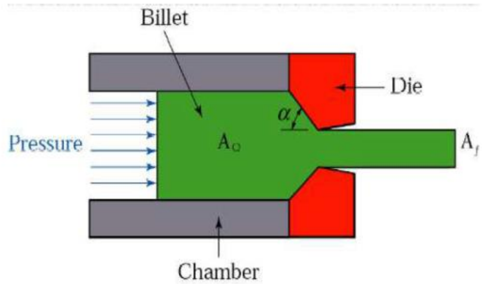

Figuer.1. 1 Principal of extrusion process, [www.scribd.com]

The forcing of solid metal or work piece through a suitable shaped orifice under compressive forces, extrusion is slightly similar to squeezing toothpaste through a tube, although some cold extrusion processes more nearly look like forging, which also deforms metals by application of compressive forces. Most metals can be extruded, although the process may not be economically feasible for high-strength alloys. The most widely used method for producing extruded shapes is the direct, hot extrusion process. In this process, a heated billet of metal is placed in a cylindrical chamber or rectangular chamber and then compressed by a hydraulically operated ram. The extrusion of cold metal is variously termed cold pressing, cold forging, cold extrusion forging, extrusion pressing and impact extrusion.

The cold extrusion has become popular in the steel fabrication industry, while is widely used in the nonferrous field. The advantages of cold extrusion are higher strength because of severe strain-hardening, good surface finish, dimensional accuracy and economy of the product and minimize the machining requirement of the output product. Singh Pachalasiya (2013)

1.2.1 Classification of extrusion processes

There are several ways to classify metal extrusion processes;

- By direction:-Direct / indirect extrusion or forward /backward extrusion
- By operating temperature: - Hot /cold extrusion.
- By equipment: - Horizontal and vertical extrusion.
- Others

1.2.1.1Direct and Indirect extrusions

1 Direct extrusion

In direct extrusion the metal billet is placed in a container and driven through the die by the ram or punch and friction is at the die and container wall requires higher pressure than indirect extrusion process. The dummy block or pressure plate is placed at the end of the ram in contact with the billet. Fig.1.2 below shows a direct extrusion process.

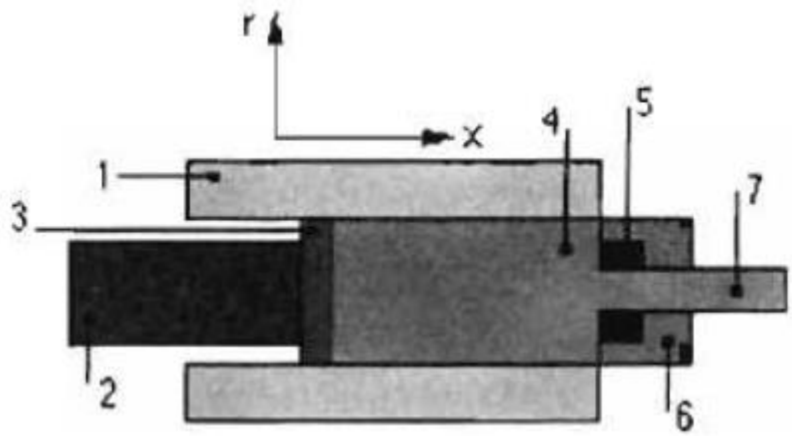

1 Container 2 Ram 3 Dummy blocks 4 Billets

5 Die 6 Die holders 7 Extrude products

Figuer.1. 2 Direct Extrusion (Singh Pachalasiya (2013))

2 Indirect extrusions

The hollow ram containing the die is kept stationary and container with the billet is caused to move and the friction at the die only (there is no relative movement at the container wall) requires constant pressure and the hollow ram limits the applied load. Fig.1.3 below shows the indirect extrusion process.

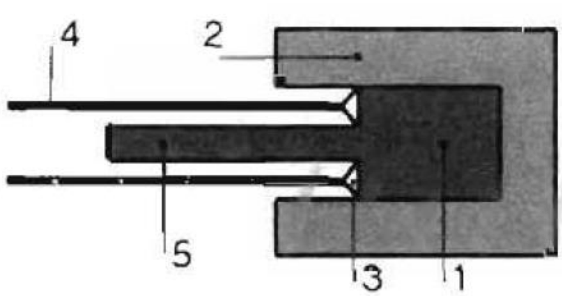

1. Billet
2. Container
3. Die
4. Ram
5. Extruded product

Figuer.1. 3Indirect Extrusion (Singh Pachalasiya (2013))

1.2.1.2 Combination of backward and forward extrusion

In this process Metal is forced to flow into two direction of the punch movement both opposite and similar direction of the punch.

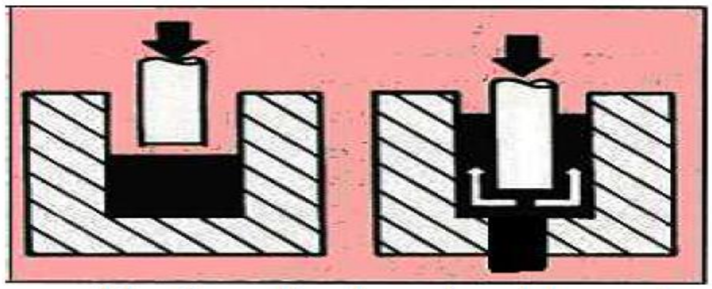

Figuer.1. 4 Combination of backward and forward extrusion

1.2.1.3 Cold extrusion and hot extrusions (Singh Pachalasiya (2013))

1. Cold extrusion

Cold extrusion process done at room temperature or slightly elevated temperatures. This process can be used for most material subject to designing strong sufficient tooling that can withstand the stresses crested by extrusion. The metals that can be extruded are lead, tin, aluminum alloy, copper, titanium, molybdenum, vanadium and steel. Examples of cold extruded part are collapsible tubes aluminum can, cylinders gear blanks, etc. C.S Ramesh (2012)

2. Hot extrusion

Hot extrusion is done at high temperatures about 50 - 70 % of the melting point of the work piece material. The most commonly used extrusion process is the hot direct extrusion process the cross-section shape of the extrusion is defined by the shape of the die. High temperatures and pressures affect die life as well as other components. In hot extrusion process, good lubrication is required. Oil and graphite work at low temperatures whereas at higher temperatures glass powder is used. . C.S Ramesh (2012)

1.2.1.3 Hydrostatic and impact extrusions

1. Hydrostatic extrusion

In hydrostatic extrusion process the billet is smaller in diameter than the chamber, which is filled with a fluid and the pressure is transmitted to the billet by a ram or punch and during this process billet does not come in contact with the piston and the material is deformed due to development of hydrostatic pressure within the fluid hydrostatic pressure increase the ductility, and very good quality products can be extruded by this process.

Hydrostatic extrusion can be done hot warm or cold and can be used to extrude brittle materials. That cannot be handled by conventional extrusion process. It can be seen in the fig.1.5 given below.

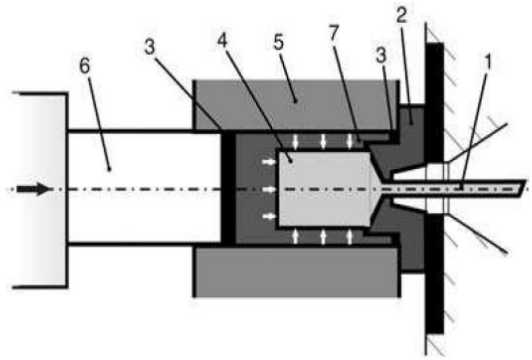

1. Extrusion 2. Die 3. Seal
4. Billet 5. Container 6. Stem 7. Hydrostatic medium

Figuer.1. 5 Hydrostatic extrusion (Singh Pachalasiya (2013))

2. Impact extrusion

Impact extrusion comes into cold extrusion process, in this process a heavy punch is allowed to fall over the material and material takes the shape of the die by following the clearance between punch and die. This is used to make collapsible tubes of soft alloys as tooth paste containers made by this process. This process is limited to soft and ductile materials. It can be seen in the fig.1.6 shown below;

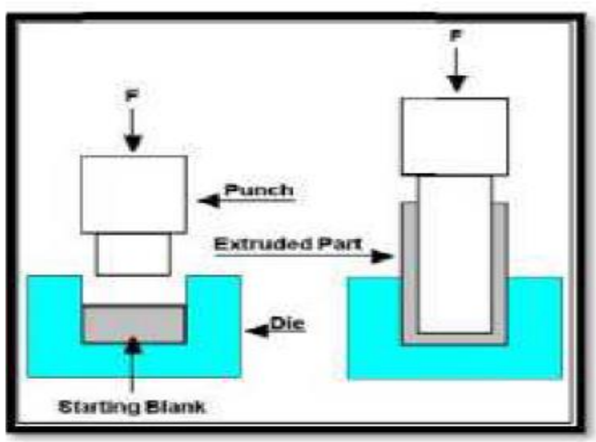

Figuer.1. 6 Impact extrusions (Singh Pachalasiya (2013))

1.2.2 Advantage of extrusion

In the different metal forming processes, Extrusion has definite advantages over others for the production of three dimensional section shapes. Now it is becoming essential to pay more attention to the extrusion of section rod from round stock. The process is also attractive because press machines are readily available and the necessity to purchase expensive section stock corresponding to a multiplicity of required sections is eliminated.

There are many (Singh Pachalasiya (2013)) advantage of extrusion as follows;

- Uniform cross-section areas obtain in whole process.
- Strain and hardness are increased due to strain hardening.
- Low cost of die and it's economical to make small quantities of a shape and size.
- Good surface finish obtained by any other metal forming process.

1.2.3 Limitation of Extrusion

- Extrusion is limited to only a few metals and cannot be done any chosen material.
- Most materials require high temperature and pressure which makes equipment costly.
- During extrusion process die material should be able to withstand the load, high temperature and wear.
- In the case of steel extrusion process the equipment is costlier due to the magnitude of temperature to which the metal must be heated (2300F).
- In indirect extrusion complicates the handling of extruded or output parts.

Additionally, on the extrusion process there are some defects like particle cracking and micro porosity. These defects can appear inappropriate processing parameters, such as die design, applied load, extrusion temperature, extrusion ratio has been exists. To minimize this extrusion defects upper bound die design technique is one method. It has different geometrical techniques such as third-order polynomial, fourth-order polynomial, cosine, elliptical, hyperbolic and conical geometry die profiles. Many researchers has done this techniques to solve the extrusion defects by using different die shapes like circular, square, rectangular and hexagonal with different billet shape materials. Analysis the extrusion stress and strain analytically and numerically which is used to determine the applied load. Numerical methods provide a general tool to analyze arbitrary geometries and loading condition. Among the numerical methods, FEM has been extensively used with success; however, this kind of analysis requires the generation of a large set of data in order to obtain reasonably accurate results and consumes large investment in engineering time and computer resources. The FEM for elastic - plastic material property is considered to be an accurate method, but is generally not very well suited for the severe material deformation typical in many metal forming processes.

The finite element method can be briefly described through taking the system for the purpose of solution when the system is divided for elements connected with some points are called nodes. There are different shapes of elements which are used in the systems. They depend on system shape and complexity degree, which can be shaped (triangle walled at three nodes, square or rectangle are walled at four nodes) and another type is found from elements which is called axisymmetiric element which is used in this study. Goveiaa et al. (2000)

Generally, analytical and numerical analysis of extrusion force, stress and strain are used to minimize the extrusion defects on the fabrication of Al/SiC composite materials through circular billet to square shape die profile. In addition, for this work hot forward extrusion process is better as seen as above extrusion process type.

1.2.4 Application of extrusion

Extrusion is one of the most important methods of metal forming process and is used to produce many products of high industrial applications with good quality. Some of the applications of the extrusion process are given below;

- ✓ Railing for sliding doors.
- ✓ Tube for various cross-sections.
- ✓ Structure and architectural shapes.
- ✓ Doors and window frames.
- ✓ Extrusion process used to make collapsible tubes of soft alloys such as tooth paste containers.

1.3 Statements of the problem

Because of improved mechanical properties such as; greater strength, high specific modulus, improved stiffness, light weight, low thermal expansion coefficient, high thermal conductivity, increased wear resistance and improved damping capabilities, the metal matrix composites are most preferable in the field of aerospace, thermal management areas, industrial products, automotive applications and electronic products(Md. Halibut Rahmana (2014)). But the problem involving with manufacturing of advanced metal matrix composite is nonhomogeneous distribution of reinforced particle. Hence, the extrusion process considered to be a secondary process for the quality composite material. Normally, extrusion process and its design tools become heuristic in nature. Therefore, during the extrusion of composite materials, development of die profile and prediction of extrusion force, stress development and strain development also complex to select optimal die profile.

1.4 Significance of the Study

- Used to study the plastic deformation of composite material during the extrusion of any other die profiles.
- Used to predict the extrusion load, stress development and strain development during extrusion.
- Used to develop ductile and higher tensile strength composite materials than casting.
- Used to identify the die profile at minimum extrusion load
- Used to transfer knowledge's about MMC materials which is Al/SiC, extrusion process, optimal die identification and FEM

1.5 Objectives of the Study

1.5.1 Main objective

- To Analysis the extrusion forces, stress and strain during extrusion of Al/SiC both analytically and numerically method.

1.5.2 Specific objectives

- To select the optimal die profile
- To determine the velocity components of plastic deformation
- To determine the extrusion force required, stress induced and strain developed
- To simulate the extrusion process by incorporating the developed die profile
- To validate the analytical results through numerical package DEFOEM-3D.

1.6 Scope of the research

The scope of the research is comprised the objective and specific objective in details. In general, this research focuses to identify an optimal die profile to extrude round billet to square billet. Investigation of extrusion forces, stress development, and strain gradient during the plastic deformation through known analytical way of upper bound technique and extends to validate the analytical results through numerical technique.

1.7 Limitation

There are some limitations presented in working this research; such as there no internet availability for some months to searching necessary data, lack of resources related to this research and lack of advisors.

CHAPTER TWO

LITERATURE REVIEW

2.1 Introduction

Conducting the literature review is done prior to undertaking the research. This is critically provide as much information as needed on the technologies available and methodologies used by other research counter parts around the world on the topic. This chapter provides the summary of the literature reviews on topics related to the extrusion of round to square shape die profiles.

Gouveia et al. (2000) were studied the numerical and experimental analysis of the round-to-square extrusion of a model material by using combined Eulerian-Lagrangian formulation and updated Lagrangian formulation for analyzing a steady-state metal forming process. The numerical results in both flow pattern and strain distribution have been shown to be in good agreement with the results obtained from the physical modeling experiments. In terms of numerical modeling, it can also be concluded that combined Eulerian-Lagrangian mesh models are more efficient for the analysis of steady-state metal forming processes, because the steady-state metal forming conditions are directly included in the finite element formulation. Finally, it should be noted that the combined Eulerian-Lagrangian formulation is computationally more efficient than the updated Lagrangian formulation for analyzing a steady-state metal forming process, as it requires much less CPU time.

Celik et al. (2000) were studied based on the upper-bound theory, for the design of three dimensional off-centric extrusions of arbitrarily shaped dies were applied to the off-centric extrusion of square sections from initially round billets with experimental verifications. A computer program was written to obtain optimum die design which yields the lowest upper-bound for a given reduction in area, die length, off-centric positioning and frictional conditions. Computations were carried out both for the converging (ruled-surface) and smooth curved (advanced surface) dies. The theoretical predictions were observed to be in good agreement with the experimental results.

C.W. Wu et al. (2000) were presented a model based on upper-bound theorem to analyze the extrusion of composite clad rods with non-axisymmetric cross-section. Velocity fields for both core and sleeve are generated with the assistance of a product's cross-sectional profile functions. Products with rectangular, hexagonal and octagonal sections are chosen as the study objects. Also discussed herein are numerical results for various process variables such as semi-die angle, reduction of area, frictional condition of die, and product shape complexity. According to these results, the extrusion pressure and product dimensional change are closely related to the process variables.

Gouveia et al. (2001) were studied the physical and numerical modeling, which are intended to serve as design aids of three dimension forward extrusion process. A comparative examination between different modeling techniques has been performed under the theoretical and experimental analysis of round-to- square forward extrusion of a model material. Experimental results confirm that physical modeling is capable of providing relative quantitative information on the behavior of a complex three -dimensional extrusion process, especially the strain distribution. Update Lagrangian finite element numerical simulation show a good agreement with the results of the physical modeling experiment in terms of replicating the flow pattern and the distribution of strain.

R. K. Sahoo et al. (2009) were found an upper bound solution for the extrusion of channel section from round billet through the taper die. The rigid-perfectly plastic model of the material is assumed, and the spatial elementary rigid region (SERR) technique is presented for which the kinematically admissible velocity field is found out by minimizing the plastic dissipation of power. The presented analysis allows for specification of process control parameters and their relation to extrusion load, equivalent die angle, reduction ratios and friction factor.

Joseph S et al. (2009) were studied upper bound elemental technique (UBET) for prediction of extrusion pressure in three-dimensional forward extrusion process is presented. Using square/rectangular billets, the study of the effect of die land length has been extended for the evaluations of extrusion pressures to extrude sections such as circular, square and rectangular shaped sections with power of deformation due to ironing effect at the die land taken into account. The extrusion pressure contributions due to the die land evaluated theoretically for these shaped sections considered are found to increase with die land lengths for any given percentage reduction and also increase with increasing percentage die reductions at any given die land length. The effect of die land lengths on the extrusion pressures increases with increasing complexity of die openings geometry with rectangular section giving the highest extrusion pressure followed by circular with square section die opening, giving the least extrusion pressure for any given die reduction at any given die land lengths. The proper choice of die land length is imperative if excessive pressure buildup at the emergent section is to be avoided so as to maintain good quality and metallurgical structure of the extrudes.

K. Abrinia et al. (2009) were designed for profiled sections such as square, rectangular, elliptical and cross shapes. These dies force the material to flow sideways and spread so as to extrude sections with wider dimensions than the initial billet or the maximum container diameter. The geometry of the deforming zone in the die was formulated and based upon that, a kinematically admissible velocity field was derived. Using this velocity, estimated the field upper bound on extrusion power. Profile sections with different aspect ratios were investigated and the influence of other process parameters such as friction and reduction of area on the extrusion pressure were studied. Optimum die lengths for each die were calculated so as to minimize the extrusion pressure. Finite element analysis for the numerical simulation of the process was also carried out. The finite element results were also used as an aid to the design process of the extrusion dies. Dies were manufactured for different sections such as square, rectangle, and ellipse and cross shapes. Experiments were carried out to obtain data to verify the theory. Comparison of the results showed good agreement between the theoretical, numerical and experimental data. It was concluded the present method could be used to design dies for the spread extrusion of different shaped dies.

Kumar Rout et al. (2010) were investigated a numerical analysis of extrusion through cosine die profile using DEFORM software for plane strain deformation using rigid plastic material. The extrusion load has been predicted. The effective stress, strain, strain rate and velocity distribution have been determined. It is proposed to investigate the evolution of uniform microstructure and the effect of strain hardening in the extrusion process in future work.

Avinash Kumar (2011) was studied an upper bound solution has been developed for three-dimensional extrusion of circular sections from a circular bar through cosine die. It is concluded that the extrusion dies based on cosine profile is superior to straightly converging and concave circular profile. It is further observed that the cosine profile based die needs lower plastic deformation work, die surface friction and total power consumption compared to straightly converging die for all the values of relative die length compared to straightly converging die. It is also seen that the upper bounds calculated for concave dies are always greater than those for convex dies, due to the greater deformation volumes enclosed by these latter dies.

A. K. Rout et al.(2012)were investigated a numerical FEM modeling has been carried out for extrusion of triangular section from round billet through a curved die using DEFORM-3D software for steady state deformation using rigid plastic material. The extrusion load has been predicted. The effective stress, strain, strain rate velocity and temperature distribution have been determined. An experimental test rig has been fabricated. The experimental results are compared with the theoretical results. The results of computations are found to be in good agreement with those of the experiments.

F. GhaemI eT al.(2013) were studied an optimum extrusion die profiles through implementation of slab analysis in a computational algorithm. Moreover, extrusion process through both optimum conical and curved die has been performed experimentally and also by finite element method. It has been demonstrated that material work hardening characteristics and friction condition have remarkable effects on the optimum streamlined die profile. Also, results prove that the streamlined die profile designed based on the developed approach, is superior to the conventional conical dies from both metallurgical and manufacturing perspectives. Consequently, the proposed method can be regarded as an efficient and reliable tool for designing streamlined die profiles. Hence, this technique can be used to produce desirable conditions in both process and product quality in terms of extrusion force, deformation homogeneity and die wear.

Aue-u-lan Y. et al. (2013) were studied effect of extrusion speed on the extrusion load, temperature distributions and the stress concentration in the pothole die. The aluminium square hollow profile size 1.7x1.7 inch with the wall-thickness of 0.7 mm was used in this study. The aluminium initial billet was made of AA6063-T5, which has the diameter of 127 mm and length of 508 mm. This process has the extrusion ratio of about 106, which is considered to be extremely high. Viscos plastic Finite Element Modeling (FEM) was employed to simulate the aluminium hot extrusion process and investigate the results. The simulation results demonstrated that the extrusion load and temperature over the whole extrusion process was not uniform, and the die stress analysis could predict the weak area in the porthole die.

Debabrata Rath et al. (2013) were studied the changes of die angle, area reduction in dies, loading rate on the final extruded products, extrusion pressures of lead of circular cross sections has been investigated experimentally. The proposed method is successfully adapted to the forward extrusion of the equilateral triangular section from round billet through converging dies of different area reductions. Computation of extrusion pressure at various area reductions was found that extrusion pressure increases with increase in reduction and calculations of different parameters (stress, strain etc.) in wet condition.

Maity et al. (2013) were investigated a die profile is designed for extrusion of square section from round billet with a cosine die profile. It is proposed to carry out FEM modeling using DEFORM-3D software for lead and aluminum.

Singh pachalasiya (2013) was studied anon-linear converging cosine dies profiles are used for square to square extrusion process. Extrusion through mathematically contoured die plays a critical role in improvement of surface finish of extruded product. The cosine die profile designed using CATIA, Solidworks and MATLAB was used to find out the coordinate of the cosine die profile and solid model was generated using CATIA the STL files of extrusion dies generated by solid work and CATIA. Extrusion was assumed to be isothermal condition, for extrusion purpose Al- 6062 work material are used in DEFORM-3D Software. FEM modeling determine damage Strain-effective (mm/mm), strain rate-effective ((mm/mm)/sec), stress effective (MPa), stress-Max principal (MPa), Velocity Total Vel (mm/sec) and Temperature (C_0). The results optioned during FEM simulation of Al-6062[FEA] are compared with the FEM simulation results of Tellurium Led [FEA]. For Extrusion process of Al-6062, the Extrusion load and pressure are more as compared to extrusion of Tellurium Lead under same percentage of Reductions and comparisons of load and pressure between Aluminum and Tellurium Lead during deformation process.

Venkatesan et al. (2014) were investigated the metal flow behavior of Al-B_4C based DRMM composite extruded from round to hexagon through six different die profiles namely third order polynomial, fourth order polynomial, cosine, elliptical, hyperbolic and conical geometry. Extrusion load, stress and strain distribution, and metal flow for above said die profiles are predicted by using analytical approach upper bound technique and compared with finite element method. Cosine and third order polynomial profiles are found to be most optimal in terms of homogenous and minimal extrusion load requirement.

Venkatesh et al. (2014) were investigated the metal flow behavior of Al–SiC based DRMM composite extruded from round to hexagon through six different die profiles namely third-order polynomial, fourth-order polynomial, cosine, elliptical, hyperbolic and conical geometry. Extrusion load, stress and strain distribution, and metal flow for above said die profiles are predicted using analytical approach upper bound technique and numerical technique finite element method. Cosine and third order polynomial profiles are found to be most optimal in terms of homogenous and less extrusion load requirement.

Pathak et al. (2014) were studied, die angle of the square rod extrusion process was optimized to produce micro structurally sound product at maximum production speed and minimum left out material in the die. The design problem is formulated as a nonlinear programming problem which is solved using genetic algorithm. Selection of the processing parameters is carried out using dynamic material modeling (DMM). Using this approach a square rod extrusion problem is successfully designed.

S. T. Oyinbo et al. (2015) were investigated using linearly converging die profiles, the extrusion of simple and advanced polygons such as circular, square, triangular, hexagonal, heptagonal, octagonal, L-, T-, and H- sections from round billet have been numerically simulated. Mathematical equations describing the die profiles were evaluated. A solid CAD model for the linearly converging die profile was made using Autodesk Inventor 2013 software and numerical analysis using DEFORM 3D software for extrusion of the above sections from round billet was then performed to determined, for dry and lubricated condition, the load prediction, effective stress, effective strain, strain rate, velocity and temperature distribution during the deformation. It is found that the predictive loads for advance (asymmetric) shapes are found to be higher than that of the simple shapes. While there is no marked difference between the predictive load for simple (axisymmetric) shapes, the L-section has the highest extrusion load, followed by T-section and the H-section given the least pressure.

A. García-Domínguez, et al. (2014) were presented a comparative study of extrusion processes (solid and cup extrusion), considering both direct and indirect forming conditions and showing the most interesting differences between them. The comparison is realized by Finite Element simulation of the processes, using the code DEFORM F2. The material is a low carbon steel (AISI-1010) and the same extrusion ratio and ram displacement are considered in all cases. By comparing the required forces it can be concluded that required loads are higher in cup extrusion processes than in solid extrusion ones. Regarding the friction load, the maximum contribution due to the die-billet contact in cup extrusion is much higher than in the case of solid extrusion. On the contrary, the maximum friction load contribution due to the container wall is much higher in the case of solid extrusion than in cup extrusion.

Peyman Karam et al. (2014) were provided a new formulation for the analysis of the extrusion process for non-axisymmetric sections. The upper bound theorem has been used to obtain a generalized kinematically admissible velocity field. The geometry of the deforming region has been formulated considering variation of the dead zone size at different angular positions and three-dimensional curved surfaces have been employed to define the entry and exit surfaces of the deformation zone. Using this analytical method, extrusion of square, rectangular and L-shaped sections were analyzed and the effect of shape complexity on material flow and dead material zone (DMZ) formation under different conditions has been investigated. Physical Modeling experiments and finite element analysis were carried out to reveal the capability of the proposed theoretical method.

H.H. Kim et al. (2014) were studied multiwall CNT/Al2O3 preform-based aluminum hybrid composites were fabricated using the infiltration method. Then, the composites were extruded to evaluate changes in its mechanical properties. In addition, the dispersion of reinforcements was investigated using a hardness test. The required extrusion pressure of hybrid MMCs increased as the Al2O3/CNT fraction increased. The deformation resistance of hybrid material was over two times that of the original A356 aluminum alloy material due to strengthening by the Al2O3/CNTs reinforcements. In addition, an unusual trend was detected; primary transition was induced by the hybrid reinforcements, as can be observed in the pressure–displacement curve. Increasing temperature of the material can help increase formability. In particular, temperatures under 623 K (350^{0}C) and over-incorporating reinforcements (Al2O3 20 pct, CNTs 3 pct) are not recommended owing to a significant increase in the brittleness of the hybrid material.

Beata Pawłowska1 (2014) was presented the analysis of nature of metal flow during extrusion of non-circular sections and determining the relationship between extrusion force and geometrical parameters of extrude (the shape of extrude). Experimental procedure was carried out for the simplest cases of non-circular profiles (triangle, square, rectangular) of various geometrical parameters. The extrusion load and punch displacement have been registered during experimental work. By determining parameters of metal plastic flow (the depth of plastic zone Lp and the dead zone angle αsm) it has been shown the difference in nature of metal flow during extrusion product differing in non-circular sections. This differentiation results in the complex nature of flow consequential from change with circular section of the billet to non-circular section of extrude. It has been shown that flow resistance can be different with regard to appearing configurations of deformation zones (the size and shape of plastic zone, dead and shear zones) and dependent from for example geometrical parameters of a die (shape and size of an die orifice).

Kumar Mohapatra et al.(2015)were investigated simulation of extrusion of square section from a square billet (AA-6XXX) through converging die has been carried out using DEFORM-3D commercial package and the effect of few state variables on the process has been studied. The simulation was performed by both linear converging and cosine die profile, to ascertain extrusion load, effective stress, effective strain and temperature distribution. To decipher the effect of die length, ram velocity and extrusion ratio on the process, simulations were carried out by varying the variables in a wide range for both type of dies. The optimum die length for cosine die is a bit larger than linear converging die for a particular reduction. The investigation reveals that extrusion through cosine die is more favorable than shear faced die and linear converging die profile. Lesser velocity relative difference at cosine die exit causes lesser load requirement for extrusion process.

S. K. Mohapatra et al. (2016**)** were studied the effect of various process parameters for determining extrusion load has been studied for square to square extrusion of Al-6061 alloy, a most used aluminium alloy series in forming industries. Parameters like operating temperature, friction condition, ram velocity, extrusion ratio and die length have been chosen as an input variable for the above study.

Twenty five combinations of parameters were set for the investigation by considering aforementioned five parameters in five levels. The simulations have been carried out by

Deform-3D software is predicting maximum load requirement for the complete extrusion process. Effective stress and strain distribution across the billet has been checked. Operating temperature, extrusion ratio, friction factor, ram velocity and die length have the significant effect in decreasing order on the maximum load requirement.

Marcelo et al. (2017) were examined and validated the novel numerical scheme to calculate the velocity, stress, strain, pressure and strain rate fields of metal plastic flow in direct extrusion processes by employing the finite volume method, FVM by using the Explicit MacCormack Method in structured, fixed and collocated mesh. SIMPLE method was applied to attain the necessary pressure-velocity coupling. These new numerical scheme was applied to the analysis of direct hot extrusion process of Al 6351 and Al 6060 aluminium alloys. The velocity and other variables fields achieved fast convergence and a good agreement with experimental results from Visio plasticity tests by the grid stripe pattern technique and Forge 2008 software.

2.2 Research Gaps

Researchers have done round billet to square shape die profiles by using different mathematical techniques with different extruded materials to improve the materials property and minimize the extrusion force. There is a research gap in Al/SiC composite material extrusions from round to square die shape. No one done the extrusion of Al/SiC composite materials from round to square shape die profiles by comparing cosine dies and 3^{rd} order polynomial dies. The reason of comparing two dies is used to extrude Al/SiC composite materials in optimal extrusion load.

In the present work, consider two die profiles (like;3^{rd} order polynomial and cosine dies) in three dimensional extrusions through non-linear converging die for extrusions of Al6063/20%SiC composite materials from round billet to square die profile by using both upper bound method and finite element modeling.

CHAPTER THREE

MATERIALS AND METHODS

3.1 Material selection

The primary data sources are interviewing experienced persons, previous gained information and knowledge.

Secondary data sources; review and assess different previous literatures such as, journals, conference papers, websites, books and related research works.

Using collecting data and literature review, material selection depends on its mechanical, physical and thermal properties. So, for this research the following materials were used.

Depend on;

- Availability
- Machinability
- Cost
- High strength
- High corrosion resistance

3.1.1 Aluminium6xxx – (Al-Mg-Si) Alloys

- ➢ Heat treatable
- ➢ High corrosion resistance, excellent extrudability moderate strength
- ➢ Building & construction, highway, automotive, marine application
- ➢ Representative alloys: 6061,6063, 6111

The 6xxx alloys are heat treatable, and have moderately high strength coupled with excellent corrosion resistance. They are readily welded. A unique feature is their extrudability, making them the first choice for architectural and structural members where unusual or particularly strength- or stiffness-criticality is important.

Alloy 6063 is perhaps the most widely used because of its extrudability; and is used for the automotive space frame parts. Due to this property and the availability of Al6063 is used as the working material. **(**The Aluminum Association, Inc., www.aluminum.org)

Table.3. 1 Al 6063 properties, S.T.Oyinbo et al. (2015)

No.	**Physical properties**	value
1	Density (x1000kg/m^3)	2.7
2	Melting point	655^0c
3	Electrical Resistivity(Ω .m)	0.033 $x10^{-6}$
4	Emissivity	0.02-0.1
5	Electrical Resistivity	52%IACS
	Mechanical properties	
1	Poisson's Ratio	0.33
2	Elastic Modulus (GPa)	70-80
3	Tensile Strength (MPa)	90
4	Yield Strength (MPa)	48
5	Hardness (HB500)	25
6	Shear Strength (MPa)	68
7	Fatigue Strength (MPa)	55
	Thermal property	
1	Thermal Expansion (10^{-6}/^{0}c)	23.4
2	Thermal Conductivity (w/m-k)	218
3	Specific heat capacity (J/g-^{0}c)	0.9

3.1.2 Silicon carbide

Silicon carbides are used for particulate reinforcement materials in the aluminium metal matrix composite.

Table.3. 2 Silicon carbide properties,[www.ferroceramic.com.]

S/No.	Physical properties at room Temperature	Value
1	Density	3.12 g/cm^3
2	Crystal Structure	hexagonal
3	Color	dark gray
4	Water Absorption %	0.0
5	Melting point	2730^0c
	Mechanical Properties	
1	Hardness	9-10 Mohs or 2800 kg/mm2
2	Compressive Strength MPa	1725-2500
3	Tensile Strength MPa	310
4	Modulus of Elasticity(Young's Modulus) G Pa	476
5	Flexural Strength (MOR) MPa	324

6	Poisson's Ratio	0.19
7	Fracture Toughness, MPa x m1/2	
	Thermal properties	
1	Max. Use Temperature (in air) ºC	1400
2	Thermal Shock Resistance ΔT (ºC	50-500
3	Thermal Conductivity W/m-K	41
4	Coefficient of Linear Thermal Expansion, α1 (μm/m-ºC)	5.12
5	Specific Heat, J/g-ºC	0.15

3.1.3 High stainless steel [H13]

Chromium hot-work tool steels are classified as group H steels by the AISI classification system. This series of steels start from H1 to H19. Chromium hot-work steel (H13) is widely used in hot and cold work tooling applications. Due to its excellent combination of high toughness and fatigue resistance H13 is used more than any other tool steel in tooling applications.

Table.3. 3 **AISI H13 Steel** Properties [www.azom.com]

S.No.	**Mechanical properties at room Temperature**	value
1	Tensile strength, ultimate	1200-1590 MPa
2	Tensile strength, yield	1000-1380MPa
3	Reduction of area	50%
4	Modulus of elasticity	215GPa
5	Poisson's ratio	0.27-0.30
	Thermal Properties Conditions	
1	Thermal expansion @ **T (ºC)** 20-100	10.4 x 10^{-6}/ºC
2	Thermal conductivity @ **T (ºC)** 215	28.6 W/m-K
	Physical Properties	
1	Density	7.80 g/cm^3
2	Melting point	1427°C

3.2 Methodology

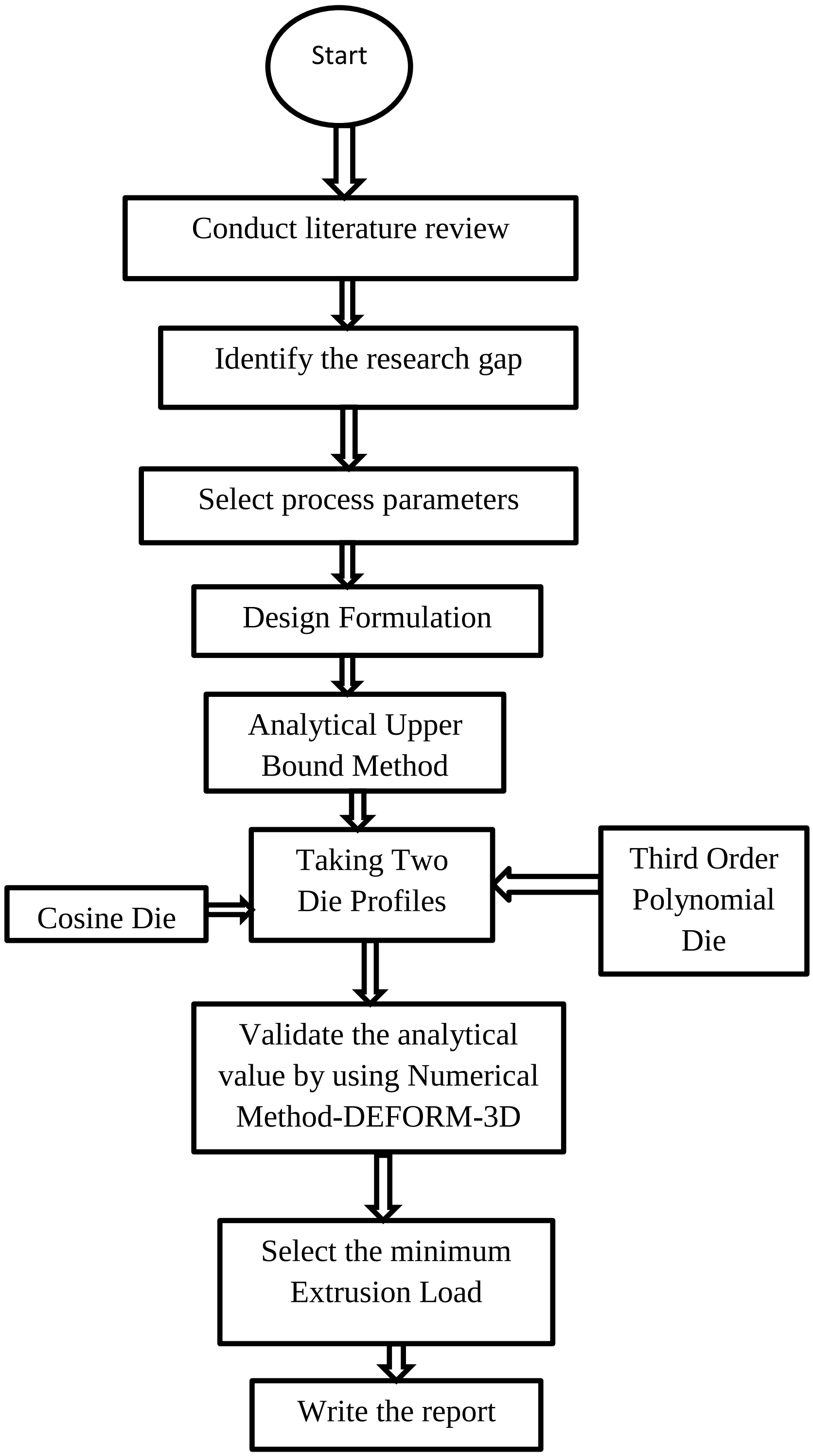

Figure.3. 1 Flow chart of over methodology

3.3 Specification of the dimension of the die and Sample Sizing

- (Kumar Mohapatra (2015) was proved low ram velocity needs to extrude minimum extrusion load. Similarly, Low Die land required low extrusion load to extrude billets. Depends on this statement
  - Initial velocity, V_0=2mm/s
  - Entrance radius, R1=10mm
  - Die land, L=10mm
  - ξ=1(N.Venkata Reddy et al. (1995)) were used ξ=0 at the center of the die and ξ=1 at the surface of the die.
  - Assume friction coefficient m= 0.1 and H13 is used as die materials. Moreover, hot forward extrusion process and vertical die arrangement is used for this research.

3.3.1Estimate volume percentage of reinforcements and matrix

Both Al and SiC were used for to develop the metal matrix composite materials. 20 wt. % SiC reinforced AMC materials (Md.Halibut et al (2014)) showed maximum hardness and tensile strength.

Volume of reinforcement estimated by measuring weight then calculated volume from it.

$$Mf=\rho_f * v_f$$

$$V_f = mf/ \rho f$$

Density of SiC alloy=3.12g/cm^3

Volume= (area X length) of composite = (πr^2) ×11=34.56cm^3

Where: A is area of billet container and

L is length of billet container

V= volume of billet container

For addition of 20% of SiC

Weight of aluminum alloy = (80/100) X34.56X2.72= 75.19grams

Weight of SiC = (20/100)X34.56X3.12= 21.57grams

3.3.2 Sample Sizing

1. for 30% area reduction

Volume of Billet container=Volume of Extruded

34557.52cm3=14.8x14.8xh

h=157.77mm

2. for 60% area reduction

Volume of Billet container=Volume of Extruded

34.56cm3=11.2x11.2xh

h=219.04mm

3. for 90% area reduction

Volume of Billet container=Volume of Extruded

34.56cm3=5.6x5.6xh

h=1101.96mm

To calculate flow stress of Al/SiC composite materials

σ_y =A16063=48MPa

σ_y= sic = 324MPa

σ_y of Al/SiC (80% and 20%) composition

=48x86%+324x20%

= 38.4+64.8

σ_y Al sic =103.2MPa

3.3 Theoretical and Mathematical Analysis

3.3.1 Upper Bound methods for Three-Dimensional Metal Deformation Problems

For problems relating to many metal working operations, exact solution for the load to cause unconstrained plastic deformation is either non-existent or is too difficult to compute. In such cases, approximate analysis is available to establish the deformation load. Two such approximate methods have found extensive application in the analysis of quasi-static metal forming process, i.e., the upper bound and the lower bound techniques.

The upper-bound theorem predicts the power necessary to perform the desired metal forming at the prescribed velocities. However, since the velocity field for a given problem is generally not known, the power for any velocity field as calculated by the upper-bound theorem is greater than or equal to the actual power.

The development also applies to any velocity field which satisfies the boundary and plasticity requirements. Thus for any possible velocity field there also exists an associated total power. The actual velocity field is that which minimizes the associated total power and the actual total power is the minimum associated total power. The formal statement of the upper-bound theorem is that amongst all kinematically admissible velocity fields, the actual field minimizes the work-function *J*, where, J is the total power consumptions required to deform the circular billet into square section through the two different die profile and is denoted as the sum of the power losses due to the plastic deformation inside the die (Wi), due to the velocity discontinuities at the entry (We) and at the exit (W_f) and due to the frictional resistance at the interface between die and material (Ws).So,

$J= W_I+We+Wf+Ws$ (C.Venkatesh et al. (2014)) (1)

But streamlined die profile is concerned, that the velocity components at the entry and exit are uniform, then the equation becomes as

J = WI+Ws (2)

Power loss due to internal deformation;

$$W_I=(\frac{2\sigma_0}{\sqrt{3}})\int_v \sqrt{(\varepsilon_{ij}\varepsilon_{ij})}dv$$

$$W_I=\frac{2\sigma y}{\sqrt{3}}\int_0^z\int_0^r\int_0^\theta \sqrt{\frac{\varepsilon_{rr}^2+\varepsilon_{\theta\theta}^2+\varepsilon_{zz}^2+\varepsilon_{r\theta}^2+\varepsilon_{\theta z}^2+\varepsilon_{rz}^2}{2}}\, d_\theta d_r d_z$$ (C.Venkatesh et al. (2014)) (3)

Where ε_{rr}^2 –Strain rate in radial direction

$\varepsilon_{\theta\theta}^2$- Strain rate in angular direction

ε_{zz}^2- Strain rate in axial direction

$\varepsilon_{r\theta}^2$- Strain rate in both radial and angular direction

$\varepsilon_{\theta z}^2$- Strain rate in both angular and axial direction

ε_{rz}^2- Strain rate in both radial and axial direction

Power loss due to frictional resistance:

$$Ws=\frac{m\sigma_y}{\sqrt{3}}\int_0^z\int_0^\theta\sqrt{V_r^2+V_\theta^2+V_z^2}\sec\alpha\ d_\theta d_z$$ (C.Venkatesh et al. (2014)) (4)

Were V_r^2- Velocity in radial direction

V_θ^2 -Velocity in angular direction

V_z^2 -Velocity in axial direction

M - Friction factor

σ_y -Flow stress

The angle α is the angle of inclination of the element of the die surface for all two die profiles with respect to the projected surface of the element on the rz plane. Knowing the velocity components, strain rate components of the individual die profile of the two different profiles, the volume integral was carried out using Simpson's one-third techniques. The average extrusion load (P_{ave}) and effective stress can be determined from the total power consumption as follows,

$$P_{ave}=\frac{J}{\pi R_1^2 V_0}$$ (C.Venkatesh et al. (2014)) (5)

3.3.2 Equation of velocity and strain rate fields

During an execution of upper bound technique to analyses plastic deformation, an efficiently formulated velocity field is required to ensure the accuracy of the final solution. The velocity components must satisfy the incompressibility condition in order to be kinematically admissible. The billet material is assumed to be rigid at the outside, the entry and the exit of the die section, hence the velocity profiles at these sections are assumed to be uniform. An assumption is extended that the flow pattern of the material in the deformation zone can be represented in the same functional form as the die profile. In the present work, the geometric shape of the die profile is considered to be a key variant for optimal effect. Hence, two different die profile geometries have been considered and the stream surface in the deformation zone (N.Venkata Reddy et al. (1995)) is given by:

$$r = \xi R(z)$$ (6)

Where constant ξ represents a stream-line with value ranging from zero at the axis to unity at the die surface and R (z) represents the cosine and 3^{rd} order polynomial die profiles in eqn. 7 and 8 respectively.

X=Y=R (z) $=\frac{R1+R2}{2}+\frac{R1-R2}{2}\cos(\frac{\pi z}{L})$ (7)

R (z) $=R_1+(R_1-R_2)\,[2\frac{Z^3}{L^3}-3\frac{Z^2}{L^2}]$ (8)

Since the stream function has to satisfy the condition of uniform axial velocity V_0 at the entry section (radius R1) and the symmetry condition at $\xi = 0$, it can be assumed as:

$\psi=\frac{V_0R_1^2\xi^2}{2}$ (9)

The velocity components Vr, Vθ and Vz are analytically derived in terms of the die profile from the derivatives of the stream function for the six different profile functions as: C.Venkatesh et al. (2014)

$V_z=\frac{\partial\psi}{r\partial r}=\frac{V_0R_1^2}{R^2(z)}$ (C.Venkatesh et al. (2014)_ (10)

$V_r=-\frac{\partial\psi}{r\partial z}=\frac{\xi V_0R_1^2R'(z)}{R^2(z)}$ (C.Venkatesh et al. (2014)) (11)

$V_\theta=\frac{V_r}{r}=\frac{V_0R_1^2R'(z)}{R^3(z)}$ (C.Venkatesh et al. (2014) (12)

From the velocity field eqn. 10, 11and 12 the strain rate components can be derived as follows:

$\varepsilon_{rr}=\frac{\partial V_r}{\partial r}=\frac{V_0R_1^2R'(z)}{R^3(z)}$ (C.Venkatesh et al. (2014)) (13)

$\varepsilon_{zz}=\frac{\partial V_z}{\partial z}=-\frac{V_0R_1^2R'(z)}{R^3(z)}$ (C.Venkatesh et al. (2014)) (14)

$\varepsilon_{\theta\theta}=\frac{1}{r}\left[\frac{\partial V_\theta}{\partial\theta}+Vr\right]=2\frac{V_0R_1^2R'(z)}{R^3(z)}$ (C.Venkatesh et al. (2014)) (15)

$\varepsilon_{r\theta}=\frac{\partial V_\theta}{2\partial\theta}-\frac{V_\theta}{r}+\frac{\partial V_r}{r\partial\theta}=-\frac{V_0R_1^2R'(z)}{2R^3(z)}-3\xi$ (C.Venkatesh et al. (2014)) (16)

$\varepsilon_{\theta z}=\frac{\partial V_\theta}{2\partial z}+\frac{\partial V_\theta}{r\partial\theta}=-\frac{3V_0R_1^2R''(z)}{2R^4(z)}$ (C.Venkatesh et al. (2014)) (17)

$\varepsilon_{rz}=\frac{\partial V_r}{2\partial r}+\frac{\partial V_z}{\partial r}=-\frac{V_0R_1^2R'(z)}{R^3(z)}[1+\frac{1}{\xi}]$ (18)

Where $R'(z)=\frac{dR(z)}{dz}$ and $R''(z)=\frac{d^2R(z)}{dz^2}$

Strain rate effective, (Tahir Altinbalik et al. (2013)) $\acute{\varepsilon}_{eff}=\frac{2}{\sqrt{3}}\sqrt{\frac{\varepsilon_{rr}^2+\varepsilon_{\theta\theta}^2+\varepsilon_{\theta\theta}^2+\varepsilon_{r\theta}^2+\varepsilon_{\theta z}^2+\varepsilon_{rz}^2}{2}}$ (19)

Strain, (N.Venkata Reddy et al. (1995)) $\varepsilon=\int\frac{\acute{\varepsilon}}{Vz}dz=\int\frac{\frac{2}{\sqrt{3}}\sqrt{\frac{\varepsilon_{rr}^2+\varepsilon_{\theta\theta}^2+\varepsilon_{\theta\theta}^2+\varepsilon_{r\theta}^2+\varepsilon_{\theta z}^2+\varepsilon_{rz}^2}{2}}}{Vz}dz$ (20)

Where ε-strain

$\acute{\varepsilon}$-strain rate effective

Vz-velocity in the axial component

Using the above equation to calculate the two die profiles (3rd op and cosine) consumption power, extrusion load, strain and die geometry at three different percentage of area reduction (i.e.30%, 60% and 90%).

3.4 Cosine Die profile

1. **At 30% area reduction**

$30\% = \frac{A0 - A+}{A0} \times 100\%$

Extrude radius $R_2 = 7.4$mm

This die profile is represented by the function;

$$R(z) = \frac{R1+R2}{2} + \frac{R1-R2}{2}\cos\frac{\pi z}{L}$$

$$\text{Then } R(z) = \frac{10+7..4}{2} + \frac{10-7.4}{2}\cos\left(\frac{\pi z}{10}\right)$$

$$= 8.7 + 1.3\cos(0.314z)$$

$$R'(z) = -0.41\sin(0.314z)$$

$$R''(z) = (-0.41)(0.314)\cos(0.314z)$$

$$= -0.128\cos(0.314z)$$

$$R^2(z) = (8.7 + 1.3\cos(0.314z)$$

$$= 1.69\cos^2(0.3142z) + 22.62\cos(0.314z) + 75.69$$

$$R^3(z) = (8.7 + 1.3\cos(0.314z))^3$$

$$= 2.2\cos^3(0.314z) + 44.1\cos^2(0.314z) + 291.2\cos(0.314z) + 638.5$$

$$R^4(z) = (8.7 + 1.3\cos(0.314z))^4$$

$=3.86\cos^4(0.314z) + 79.47\cos^3(0.3142) + 767.46\cos^2(0.314z) + 1112.25\cos(0.314z)$

$+5728.95$

$(R^3(z))^2 = 8.84\cos^9(0.314z) + 194.04\cos^6(0.314z) + 3243.68\cos(0.314z) +$

$28934.04\cos^3(0.314z) + 145222.74\cos^2(0.314z) + 388778.4\cos(0.314z) + 433\,622.253$

$(R^4(2))^2 = 8.18\cos^{16}(0.314z) + 437.4\cos^{12}(0.314z) + 5847.88\cos^9(0.314z) + 4389.88\cos^8(0.314z) + 117375\cos^6(0.314z) + 6362\cos^3(0.314z) + 16030580\cos^2(0.314z) + 12744049.28\cos(0.314z) + 32820868.$

a. Velocity of the billet in different components

- To calculate the power consumption (J) in this die profile first could be calculated the velocity and the strain rate of the cosine die profile at different components.

1. Velocity in the axial direction(z), from eqn.(10)

$$V_z = \frac{R_1^2 V_0}{R^2(z)} = \frac{2\,(10)2}{R^2(z)} = \frac{200}{R^2(z)}$$

$$V_z^{\,2} = \frac{200}{1.69\cos 2\,(0.314z) + 22.62\cos(0.314z) + 75.69)}$$

$$= \frac{40000}{2.9\cos^4(0.314z) + 76\cos^3(0.314z) + 767.7\cos^2 2/0.314z)\ 3424\cos(0.314z) + 5728.98}$$

2. Velocity in the radial direction(r), from eqn.(11)

$$V_r = \frac{\xi V_0 R_1^2 R\prime(z)}{R^2(z)} = \frac{(1)(2)(10)2(-0.4\sin(0.314z))}{R^2(z)}$$

$$= -\frac{82\sin(0.314z)}{1.69\cos^2(0.314z) + 22.62\cos(0.314z) + 75.69}$$

$$V_r = \frac{6724\sin^2(0.314z)}{2.9\cos^4(0.314z) + 76\cos^3(0.314z) + 767.7\cos^2(0.314z) + 3424\cos(0.314z) + 5728.98}$$

3. Velocity in the angular direction (θ), from eqn.(12)

$V_\theta = \frac{V_0 R_1^2 R\prime(z)}{R^3(z)}$

$= \frac{(2)\,(10)\,(-0.41 \sin(0.314z))}{R^3(z)}$

$= \frac{-82 \sin(0.314z)}{R^3(z)}$

$V_\theta^2 = \frac{6724\sin(0.3142)}{0.84\cos^9(0.314z) + 194\cos^6(0.314z) + 3243.68\cos^4(0.314z) + 28934\cos^3(0.314z) + 145222.74\cos^2(0.314z) + 388778.4\cos(0.314z) + 433622.25}$

b. Strain rates in different direction

1. Strain rate in radial directions (r) from eqn.(13)

$\varepsilon_{rr} = \frac{V_0 R_1^2 R\prime(z)}{R^3(z)} = \frac{(2)\,(40)^2\,(-0.41 \sin(0.314z))}{R^3(z)}$

$= -\frac{82 \sin(0.314z)}{R^3(z)}$

$\varepsilon_{rr}^2 = \frac{(-82 \sin(0.314z))^2}{(R^3(z))^2} = \frac{6724 \sin^2(0.314z)}{(R^3(z))^2}$

$= \frac{6724 \sin^2(0.314z)}{4.84\cos^6(0.314z) + 3243.68\cos^4(0.314z) + 28934\cos^3 0.314z) + 145222.74\cos^2(0.314z) + 388778.4\cos(0.314z) + 43622.25}$

2. Strain rate in axial direction (z), from eqn.(14)

$\varepsilon_{zz} = -\frac{V_0 R_1^2 R'(z)}{R^3(z)}$

$= \frac{164 \sin(0.314z)}{R^3(z)}$

$\varepsilon_{zz}^2 = \frac{26896 \sin^2(0.314z)}{(R^3(z))^2}$

3. Strain rate in angular direction(θ), from eqn.(15)

$\varepsilon_{\theta\theta} = 2\frac{V_0 R_1^2 R'(z)}{R^3(z)} =$

$= \frac{164 \sin(0.314z)}{R^3(z)}$

$\varepsilon_{\theta\theta}^2 = \frac{26896 \sin^2(0.314z)}{(R^3(z))^2}$

4. Strain rate in both radial and angular direction (r θ), from eqn.(16)

$\varepsilon_{r\theta} = -\frac{V_0 R_1^2 R'(z)}{2R^3(z)} - 3\xi$

$= \frac{41 \sin(0.314z) - 3R^3(z)}{R^3(z)}$

$\varepsilon_{r\theta}^2 = \frac{43.56 \cos^9(0.314z) + 1746.36 \cos^6(0.314z) + 29193.21 \cos^4(0.314z) + 256446.36 \cos^3(0.314z) + 13070004.66 \cos^2(0.314z) + 3499005.6 \cos(0.314z) + 541.2 \sin(0.314z)\cos^3(0.314z) - 10848.6 \sin(0.314z)\cos^2(0.314z) - 72619.2 \sin(0.314z)\cos(0.314z) + 1681 \sin^2(0.314z) - 161991 \sin(0.314z) + 3902600.25}{(R^3(z))^2}$

5. Stain rate in both angular and axial direction (r θ), from eqn.(17)

$\varepsilon_{\theta z} = -\frac{3V_0 R_1^2 R''(z)}{2R^4(z)}$

$= \frac{3(2)(10)^2(0.128\cos(0.314z))}{R^3(z)}$

$= \frac{38.4 \cos(0.3142)}{R^4(z)}$

$\varepsilon_{\theta z}^2 = \frac{1471.56 \cos^2(0.314z)}{8.18 \cos^{16}(0.314z) + 437.4 \cos^{12}(0.314z) + 5847.66 \cos^9(0.314z) + 4389.88 \cos^8(0.314z) + 117375 \cos^6(0.314z) + 6362 \cos^5(0.314z) + 791871.97 \cos^4(0.314z) + 2583400.39 \cos^3(0.314z) + 10030580 \cos^2(0.314z) + 12744099.28 \cos(0.314z) + 31820868}$

6. Stain rate in both radial and axial direction(rz) ,from eqn.(18)

$\varepsilon_{rz} = -\frac{V_0 R_1^2 R'(z)}{R^3(z)}\left[1 + \frac{1}{\xi}\right] = \frac{2(2)(10)^2(0.41 \sin(0.314z))(1 + \frac{1}{\xi})}{R^3(z)}$

$= \frac{164 \sin(0.314z)}{R^3(z)}$

$$\varepsilon_{rz}^{2} = \frac{26896 \sin^{2}(0.314z)}{(R^{3}(z))^{2}}$$

Then by applying Simpsons 1/3 integration techniques can be calculated W_I
By substituting the above strain rates in to eqn. (3) can be calculated power loss due to internal deformation for cosine die profile

$$WI= \frac{2\sigma y}{\sqrt{3}}\int_0^z\int_0^r\int_0^\theta \sqrt{\left(\frac{\begin{array}{c}(43.66 \cos 9\,(0.314z \\ +746.36 \cos 6\,(0.314z)+ \\ 291293.21 \cos 4\,(0.314z) \\ +256446.4 \cos 3\,(0.314z)+ \\ 1307004.7 \cos 2\,(0.314z) \\ +3499005.6 \cos\,(0.314z) \\ +541.2 \sin(0.314z)\cos 3(0.314z) \\ -10848.6 \sin(0.314z)\cos 2\,(0.314z) \\ -72619.25 \sin(0.314z)\cos(0.314z) \\ +89093 \sin 2\,(0.314z) \\ -161991 \sin(0.314z) \\ +3707600.25\end{array}}{(R3\,(2))2}\right) + \left(\frac{1474.56 \cos 2\,(0.314z)}{(R4\,(2))\,2}\right)}\ d\theta drdz \;**$$

Substituting the above velocities in to eqn. (4) could be calculated power loss friction resistance.

$$Ws=\frac{m\sigma y}{\sqrt{3}}\int_0^z\int_0^\theta \sqrt{\left(\frac{6724 \sin^2(0.314z)+40000}{\begin{array}{c}2.9 \cos 4\,(0.314z)+76 \cos 3 \\ (0.314z)+767.7 \cos 2\,(0.314z) \\ +3424 \cos(0314z)+5778.98\end{array}}\right) + \left(\frac{6724 \sin^2(0.3412)}{\begin{array}{c}4.84 \cos 9\,(0.314z) \\ +194 \cos 6(0.314z) \\ +3243.6 \cos 4(0.314z) \\ +145222.74 \cos 3(0.314z) \\ +388778.4 \cos 2(0.314z) \\ +388778.4 \cos(0.314z)+ \\ 433622.25\end{array}}\right)}\ d\theta dz \;***$$

Then by applying Simpson's 1/3 integration rule;

$$\int_a^b R(z)\,dz= \frac{h}{3}\,[R\,(a) +4R\,((b+a)/2) + R\,(b)] \text{ Where } h= (a+b)/2$$

Where WI=R (z) in eqn. ** above

$$R\,(0) = \frac{2x103.2\,x1.1}{\sqrt{3}} = 131.65 \text{ MPa}$$

$$R\,(5) = \frac{2x\,103.2\,x1.2}{\sqrt{3}} =142.99\text{MPa}$$

$$R\,(10) = \frac{2x\,103.2\,x1.12}{\sqrt{3}}= 133.46\text{MPa}$$

$$W_I = \frac{5}{3}\,[R\,(0) +4R\,((b+a)/2) + R\,(b)]$$

$$= 5/3\,(131.65+4(142.99) +133.46)$$

$$= 1395.12 \text{ MPa}$$

$$Ws = \frac{h}{3}\left[(R(0) + 4R\left(\frac{10+0}{2}\right) + R(10)\right]$$

Where Ws =R (z) in eqn. *** above;

$$R(0) = \frac{0.3 \times 103.2 \times 2}{\sqrt{3}} = 35.75\text{Mpa}$$

$$R(5) = \frac{0.3\text{x}103.2\text{x}2.1}{\sqrt{3}} = 35.54\text{MPa}$$

$$R(10) = \frac{0.3 \times 103.2 \times 2}{\sqrt{3}} = 35.75\text{ MPa}$$

$$Ws = \frac{5}{3}(35.75+4(35.54)+35.75)] = 362.06\text{MPa}$$

From eqn. (2) J = W1+ Ws = 1395.12+362.06 = 1757.18MPa

From eqn. (5) $P_{ave} = \frac{J}{\pi V_o R_1^2} = \frac{1757.18}{\pi(2)(10)^2} = 2.8$ MPa

$F=P_{ave}$ x Area =2.8 x100 π =878.59N

σ = F/Area, Where σ =effective stress at different z values.

From eqn. (19) $\varepsilon_{eff}=\frac{2}{\sqrt{3}}\sqrt{\frac{\varepsilon_{rr}^2+\varepsilon_{\theta\theta}^2+\varepsilon_{zz}^2+\varepsilon_{r\theta}^2+\varepsilon_{\theta z}^2+\varepsilon_{rz}^2}{2}}$ to calculate ε_{eff} at z=0, could be calculated six different strain rate components at this z values.

Where $\varepsilon_{rr}^2 = \frac{6724 \sin^2(0.314z)}{4.84 \cos^6(0.314z) + 3243.68 \cos^4(0.314z) + 28934 \cos^3 0.314z) + 145222.74 \cos^2(0.314z) + 388778.4 \cos(0.314z) + 43622.25}$

And similarly, could be calculated $\varepsilon_{\theta\theta}^2$, ε_{zz}^2, $\varepsilon_{r\theta}^2$, $\varepsilon_{\theta z}^2$ and ε_{rz}^2

By using Eqn. (20) and applying Simpson's 1/3 integration rule, could be calculated strain at different z values.

$$\varepsilon=\int \frac{\acute{\varepsilon}}{Vz}dz=\int \frac{\frac{2}{\sqrt{3}}\sqrt{\frac{\varepsilon_{rr}^2+\varepsilon_{\theta\theta}^2+\varepsilon_{\theta\theta}^2+\varepsilon_{r\theta}^2+\varepsilon_{\theta z}^2+\varepsilon_{rz}^2}{2}}}{Vz}dz$$

At different z values from (0-10) strain rate effective, stress and strain values listed in table3.4 below.

Table.3. 4 Strain and Stress values at different z values

Z val.	Pressure(MPa)	Area(mm)	$\acute{\varepsilon}$ in (mm/mm/sec)	σ in MPa	ε in (mm)
0	2.8	314.15	2.415	2.7967	0
2	2.8	314.15	2.448	2.7967	0.8253
4	2.8	314.14	2.448	2.7968	1.0444
6	2.8	310.00	2.448	2.8342	1.2635
8	2.8	290.12	2.448	3.0284	1.4826
10	2.8	219.04	2.448	4.0111	1.7017

2. At 60% area reduction cosine dies

$$R(z) = \frac{R1+R2}{2} + \frac{R1-R2}{2}\cos\left(\frac{\pi}{L}z\right)$$

Where, R1= 10mm

R2 =? L=10mm, $60\% = \frac{A0-A+}{A0} \times 100\%$

$\frac{60\times Ao}{100} = A0 - A_f$, $A_f = A0 - \frac{60A0}{100}$

$A_f = 314-60\pi$

$A_f = 125.5$

$L^2 = A_f/2$

L=11.2mm

R2 = L/2 =5.6mm

$R(z) = f(z) = \frac{10+5.6}{2} + \frac{10-5.6}{2} (\cos\frac{\pi z}{210})$

R (z) = f (z) =7.8+4.4 cos (0.314z)

R’ (z) =-1.38sin (0.314z)

R’’ (z) = -0.43 cos (0.314z)

$R^2(z)$ = 7.8+4.4 cos (0.314z) x 7.8+4.4 cos (0.314z)

= 23.04 $\cos^2$ (0.314z) +78.88 cos (0.314z) +60.84

$R^3(z)$ = 110.59$\cos^3$ (0.314z) +538.7cos (0.314z) + 876.1 cos (0.314z) +4785.5

R^4 (z) = 530.6 cos ^{4} (0.314z) +11208.8 cos^5 (0.314z) + 8461.7cos ^{2} (0.314z) +9111.4 cos (0.314z) + 3701.49

$(R^2(z))^2$= 530.84 cos ^{4} (0.314z) +3634 .8 cos ^{3}(0.314z) +9016.3 cos ^{2} (0.313z) +9566.6 cos (0.314z) +3677.2

$(R^3(z))^2$= 1230.1cos^9 (0.314z) + 119149.6 cos^6 (0.314z) +577802.6cos^3 (0.314z) +1283141 cos^2 (0.314z) +838515.4cos (0.314z) +229010.1.

$(R^4(z))^2$= 781748.6cos^{16} (0.314z) +118999374cos ^{12}(0.314z) +125628230.6cos^9 (0.314z) +8982940cos ^{8} (0.314z) +189684236.6cos^6 (0.314z) +967266.2cos^5 (0.314z) +279778300.1cos ^{4} (0.314z) +237171427.8 cos ^{3} (0.314z) +145659405.8cos^2 (0.3142) +67451512cos (0.314z) +13701028.2

a. Velocity of the billet in different components

- To calculate the power consumption (J) on this die profile, first could be calculate the velocity and the stain rate of the 60% reduction of cosine die at different components.

1. Velocity in the axial direction (z), from eqn.(10)

$$V_z=\frac{V_0 R_1^2}{R^2(z)} = \frac{200}{R^2(z)}$$

$$V_z^2 = \frac{40000}{530.84\cos^4(0.314z) +3639.8\cos^5(0.314z) +9016.5\cos^2(0.314z) +9566.6\cos(0.314z) +3677.2}$$

2. Velocity in the radial direction (r), from eqn.(11)

$$V_r = \frac{\xi V_0 R_1^2 R\prime(z)}{R^2(z)} = \frac{(1)(2)(101)2\ (-1.38\sin(0.314z)}{R^2(z)}$$

$$= \frac{-276\sin(0.3142)}{R^2(z)}$$

$$V_r^2 = \frac{76176\sin^2(0.314z)}{530.84\cos^4(0.314z) +3634.8\cos^8(0.314z) +9016.3\ czs^2(0.314z) +9566.6\cos(0.314z) +3677.2}$$

3. Velocity in the angular direction (θ),from eqn.(12)

$$V_\theta = \frac{V_0 R_1^2 R\prime(z)}{R^3(z)} = \frac{(2)(10)2\ (-1.38\sin(0.3142)}{R^3(z)}$$

$$= \frac{-276\sin(0.3142)}{R^3(z)}$$

$$V_\theta^{\,2} = \frac{76174\sin^2(0.3142)}{12230.1\cos^9(0.314z) + 119199.6\cos^6(0.314z) + 577802.6\cos^3(0.314z) + 1283141\cos^2(0.314z) + 838515.4\cos(0.314z) + 229010.1}$$

Power loss due to frictional resistance by substituting the above velocity values into eqn. (4) it gives as;

$$Ws = \frac{m\sigma y}{\sqrt{3}}\int_0^z\int_0^\theta \sqrt{\left(\frac{76176\sin(0.3142)+40000}{530.84\cos 4(0.3142)+3634.8\cos(0.3142)+9566.6\cos(0.3142)+3672.2}\right) + \left(\frac{6176\sin(0.3142)}{12230.\cos 9(0.3142) +119149.6\cos 6(0.3142\cos 3 +477802.6\cos 3(0.3142) +1283141\cos 2(0.3142) +8388515.4\cos(0.3142) +229010.1}\right)}\, d\theta dz$$

Then, by applying Simpsons 1/3 integration techniques could be determined Ws;

$$Ws = R(z) = \frac{5}{3}[R(0) + 4R(5) + R(10))]$$

$$R(0) = \frac{0.3x103.2\ x5.4}{\sqrt{3}} = 96.52\ MPa$$

$$R(5) = \frac{0.3x103.2\ x4.3}{\sqrt{3}} = 76.86\ MPa$$

$$R(10) = \frac{0.3x103.2x5.4}{\sqrt{3}} = 96.52MPa$$

$$W_s = \frac{5}{3}(96.52 + 4(76.86) + 96.52)$$
$$= 834.14MPa$$

b. Strain rates in different direction

1. Strain in radial direction (r), from eqn.(13)

$$\varepsilon_{rr} = \frac{V_0 R_1^2 R\prime(z)}{R^3(z)} = \frac{-276\sin(0.3142)}{R^3(z)}$$

$$\varepsilon_{rr}^{\,2} = \frac{76176\sin^2(0.3142)}{12230.1\cos^9 + 119144.6\cos^6(0.314z) + 577802.6\cos^3(0.314z) + 1283141\cos^2}$$

(0.314z) +838515cos (0.314z) +2296101

3. Strain rate in axial direction(z), from eqn.(14)

$$\varepsilon_{zz}= \frac{-2V_0R_1^2R\prime(z)}{R^3(z)} = \frac{552\sin(0.3142)}{R^3(z)}$$

$$\varepsilon_{zz}^2= \frac{30470\sin^2(0.314z)}{(R^3(z))^2}$$

4. Strain rate in angular direction(θ), from eqn.(15)

$$\varepsilon_{\theta\theta}=\frac{2V_0R_1^2R'(z)}{R^3(z)} = \frac{-552\sin(0.3142)}{R^3(z)}$$

$$\varepsilon_{\theta\theta}^2 = \frac{30470\sin^2(0.314z)}{(R^3(z))^2}$$

5. Stain rate in both radial and angular direction(rθ), from eqn.(16)

$$\varepsilon_{r\theta} =\frac{2V_0R_1^2R'(z)}{R^3(z)} -3\xi = \frac{138\sin(0.3142)-3R^3(z)}{R^3(z)}$$

$$\frac{-331.77\cos3(0.314z) - 1616.1\cos2(0.314z)-2628.3\cos(0.314z)+138\sin(0.314z)-1435.65}{R^3(z)}$$

$$\varepsilon_{r\theta}^2 = \frac{\begin{array}{c}110038.2\cos9(0.314z)+107218.4\cos6(0.314z)) \\ +4355298.6\cos4(0.314z)+85904379.6\cos3(0.314z) \\ +11548269\cos2(0.314z)+7546637.8\cos-91554.8\sin(0.314z)\cos3(0.314z)) \\ -446005.6\sin(0.314z)\cos2(0.314z) \\ -775410.8\sin(0.314z)(0.314z)\cos(0.314z)+19044\sin2(0.314z) \\ -396339.4\sin(0.314z)+2061090.9\end{array}}{(R^3(z))^2}$$

6. Strain rate in both angular and axial direction(θz), from eqn.(17)

$$\varepsilon_{\theta z}=\frac{-3V_0R_1^2R'(z)}{2R^4(z)}= \frac{129\cos(0.314z)}{R^4(z)}$$

$$\varepsilon_{\theta z}^2 = \frac{16641\cos2(0.314z)}{(R^4(z))^2}$$

7. Strain rate in both radial and axial direction(rz) , from eqn.(18)

$$\varepsilon_{rz} = -\frac{V_0R_1^2R'(z)}{R^3(z)}\left[1+\frac{1}{\xi}\right]$$

$$= \frac{552\sin(0.314z)}{R^2(z)}$$

$$\varepsilon_{rz}^2 = \frac{304704\sin(0.3014z)}{(R^3(z))^2}$$

By substituting of above strain rate in to eqn. (3) can be calculate power loss due to internal deformation for cosine die profile in 60% reduction

W_I=

$$\frac{2\sigma y}{\sqrt{3}}\int_0^z\int_0^r\int_0^\theta\sqrt{½\left(\left(\frac{\begin{matrix}110038.2\cos 9\,(0.314z)\\+107218.4\cos 6\,(0.314z)\\+455298.6\cos 4(0.314z)\\+85904379.6\cos 3(0.314z)\\+11548269\cos 2\,(0.314z)\\+7546637.8\cos(0.314z)\\-91554.8\sin(0.314z)\cos 3(0.314z)\\+446043.6\sin(0.314z)\cos 2(0.314z)\\-725410.8\sin(0.314z)\cos(0.314z))\\+19044\sin(0.314z)-396239.\sin(0.314z)\\+2061090.9\end{matrix}}{(R3\,(z))2}\right)+\left(\frac{716641\cos 2\,(0.314z)}{(R4\,(z))\,2}\right)\right)}\,d\theta drdz$$

Then By applying Simpsons' 1/3 integration rule;

$$WI = R\,(z) = \frac{5}{3}\,[R(0)+4\,R(5)+R(10))]$$

$$R\,(0) = \frac{2x103.2x1.2}{\sqrt{3}} = 143MPa$$

$$R\,(5) = \frac{2x103.2\ x1.25}{\sqrt{3}} = 148.96MPa$$

$$R\,(10) = \frac{2x103.2x1.24}{\sqrt{3}} = 147.76MPa$$

$$W_1 = \frac{5}{3}\,(143 + 4\,(148.96) + 147.76)$$

W_1= 5/3 (143+4 (148.96) +147.76)

= 1477.67MPa

From eqn. (2) $J = W_1 + Ws$ = 1477.67+834.14

= 2311.81MPa

From eqn. (5) $P_{ave} = \frac{J}{\pi V0R^2} = \frac{2311.81}{200\pi}$ = 3.68MPa

F= P_{ave} x Area=3.68 x 100 π =1155.91N

σ = F/Area, Where σ =effective stress at different z values.

From eqn. (19) $\varepsilon_{eff}=\frac{2}{\sqrt{3}}\sqrt{\frac{\varepsilon_{rr}^2+\varepsilon_{\theta\theta}^2+\varepsilon_{zz}^2+\varepsilon_{r\theta}^2+\varepsilon_{\theta z}^2+\varepsilon_{rz}^2}{2}}$ to calculate ε_{eff} at z=0, could be calculated six different strain rate components at this z values.

$$\varepsilon_{rr}{}^2 = \frac{76176 \sin^2 (0.3142)}{12230.1 \cos^9 + 119144.6\cos^6 (0.314z) + 577802.6\cos^3 (0.314z) + 1283141\cos^2 (0.314z) + 838515\cos (0.314z) + 2296101}$$

And similarly, could be calculated $\varepsilon_{\theta\theta}^2$, ε_{zz}^2, $\varepsilon_{r\theta}^2$, $\varepsilon_{\theta z}^2$ and ε_{rz}^2

By using Eqn. (20) and applying Simpson's 1/3 integration rule, could be calculated strain at different z values.

$$\varepsilon=\int \frac{\acute{\varepsilon}}{Vz}dz=\int \frac{\frac{2}{\sqrt{3}}\sqrt{\frac{\varepsilon_{rr}^2+\varepsilon_{\theta\theta}^2+\varepsilon_{\theta\theta}^2+\varepsilon_{r\theta}^2+\varepsilon_{\theta z}^2+\varepsilon_{rz}^2}{2}}}{Vz}dz$$

At different z values from (0-10) strain rate effective, stress and strain values listed in table3.5 below.

Table.3. 5 Strain and Stress values at different z values

Z -value	Pressure(MPa)	Area(mm^2)	$\acute{\varepsilon}$ in (mm/mm/sec)	σ in MPa	ε in (mm)
0	3.68	314.15	4.895	3.6795	0
2	3.68	314.14	4.931	3.6796	0.8467
4	3.68	314.13	4.717	3.6797	1.0955
6	3.68	305.05	4.888	3.7892	1.3443
8	3.68	287.12	4.927	4.0259	1.5331
10	3.68	125.44	4.927	9.2148	1.8419

3. 90% area reduction cosine dies

$$R(z) = \frac{R1+R2}{2} + \frac{R1+R2}{2}\cos\frac{\pi z}{L}$$

$$= \frac{10+2.8}{2} + \frac{10-2.8}{2}\cos\frac{\pi z}{10}$$

$$= 6.4 + 3.6 \cos (0.314z)$$

$$90\% = \frac{A0-Af}{A} \text{ X } 100\%$$

$$A_f = A_0 - \frac{90Ao}{100}$$

$$Af = 31.4mm^2$$

$R'(z) = -1.13 \sin (0.314z)$

$L = \sqrt{Af} = 5.6$

$R''(z) = -0.355 \cos (0.314z)$

$R_2 = 2.8mm$

$R^2(z) = (6.4+ 3.6 \cos (0.314z))^2$

$= 12.9\cos^2 (0.314z) + 46.08 \cos (0.314z) + 40.96$

$R^3 (z) = 46.7\cos^3 (0.314z)\ 7240.5 \cos^2 (0.314z) + 433.8 \cos (0.314z) + 262.4$

$R^4 (z) = 168.1 \cos^4 (0.314z) + 1093.5 \cos^3 (0.314z) + 3157.1 \cos^2 (0.134z) +$

$3720.9 \cos (0.314z) + 1679.4$

$(R^2 (z))^2 = 166.4 \cos^4 (0.314z) + 1188.8 \cos^3 (0.314z) + 3180.2 \cos (0.314z)$

$+29788 \cos (0.314z) + 1677.7$

$(R^3 (z))^2 = 2180.9 \cos^9 (0.314z) + 677010\ cas^6 (0.314z) + 52581269.3 \cos^4$

$(0.314z) + 6313306.8 \cos^3 (0.314z) + 3992195 \cos (0.314z) + 227658.2$

$\text{Cos} (0.314z) + 68853.8$

$(R^4 (z))^2 = 28257.6 \cos^{16} (0.314z) + 367634.8 \cos^{12} (0.314z) + 1195742.3 \cos^9$

$(0.314z) + 1059736 \cos^8 (0.134z) + 6893642.8 \cos^6 (0.314z) + 1250966.6$

$\cos^5 (0.314z) + 18{,}637{,}956.9 \cos^4 (0.314z) + 07130145.6 \cos^{3\,(} 0.314z) + 2820384.4$

a. The velocity of the billet in different components

1. Velocity in axial direction (z) , from eqn.(10)

$$V_z = \frac{V_0 R_1^2}{R^2(z)} = \frac{200}{R^2(z)}$$

$$V_z^2 = \frac{40000}{R^2\ (z)^2}$$

2. Velocity in radial direction (r) , from eqn.(11)

$$Vr = \frac{\xi V_0 R_1^2 R'(z)}{R^2(z)} = \frac{226\sin(0.314z)}{R^2\ (z)}$$

$$V_r^2 = \frac{51076 \sin^2 (0.314z)}{(R^2\ (z))^2}$$

3. Velocity in the angular direction (θ) , from eqn.(12)

$$V_\theta = \frac{\xi V_0 R_1^2 R'(z)}{R^2(z)} = 2\ \frac{(2)\ (10^2)\ (-1.135 \sin (0.314z))}{R^3 (z)}$$

$$= -\frac{226 \sin (0.314z)}{R^3 (z)}$$

$$V_\theta^{\ 2} = \frac{51076 \sin^2 (0.314z)}{(R^3\ (z))}$$

Power loss due to frictional resistance for 90% reduction, from eqn. (3)

$$W_S = \frac{m\sigma y}{\sqrt{3}} \int_0^z \int_0^\theta \sqrt{\frac{51076 \sin 2\,(0.3142)+40000}{166.4 \cos 4\,(0.314z)+1188.8 \cos 3\,(0.314z)+3180.2 \cos 2\,(0.314z)+2974.8 \cos(0.314z)+1677.7} + \frac{51076 \sin 2(0.3142)}{21809 \cos 9\,(0.3142)+67701\,0 \cos 6(0.3142)\;52581269.3 \cos 4\,(0.3142)+631306.8 \cos 3\,(0.3142)+3992195.2 \cos 2\,(0.3142)+227658.2 \cos +68853.8}}$$

To solve Ws, by applied Simpsons' 1/3 integration rule

$$W_S = \frac{5}{3}\,(R(0) + 4R(5) + R(10))$$

$$R(0) = \frac{0.3\text{x}103.2\text{ x}2.08}{\sqrt{3}} = 37.18\text{MPa}$$

$$R(5) = \;= \frac{0.3\text{x}103.2\text{ x}2.12}{\sqrt{3}} = 37.89\text{MPa}$$

$$R(10) = \frac{0.3\text{x}103.2\text{ x}2.09}{\sqrt{3}} = 37.36\text{ MPa}$$

$$W_S = \frac{5}{3}(37.18 + 4\text{x } 37.89 + 37.36)$$

$$= 376.83\text{MPa}$$

b. Strain rates in different components

1. Strain in radial direction (r) , from eqn.(13)

$$\varepsilon_{rr} = \frac{V_0 R1_2\, R'(z)}{R^3(z)} = \frac{200(-1.13\text{ Sin }(0.314z))}{R^3(z)}$$

$$\varepsilon_{rr}^2 = \frac{51076\text{ Sin}^2\,(0.314z)}{(R^3(z))^2}$$

2. Strain rate in axial direction (z) , from eqn.(14)

$$\varepsilon_{zz} = \frac{-2V0R_1^{\,2}R^1(z)}{R^3(z)} =$$

$$\varepsilon_{zz}^{\,2} = \frac{204304\text{ Sin}^2\,(0314z)}{(R^3(z))^2}$$

3. Strain rate in angular direction(θ), from eqn.(15)

$$\varepsilon_{\theta\theta} = \frac{2V_0 R_1^2 R'(z)}{R^3(z)}$$

$$\varepsilon_{\theta\theta}^{\,2} = \frac{204304\text{Sin}^2\,(0.3142)}{(R^3(2))^2}$$

4. Stain rate in both radial and angular direction(rθ), from eqn.(16)

$$\varepsilon_{r\theta} = \frac{-V0R_1^{\,2}R^{1/2}}{2R^3(z)} - 3\xi = \frac{-2\text{x}10^2(-1.13\text{sin})\,(0.314z)}{2R^3(z)} - 3$$

$$= \frac{113 \text{ Sin } (0.314z) - 3R^3 (z)}{R^3 (z)}$$

$$\varepsilon_{r\theta} = \frac{-140cos+(0.3142)-21745.5\cos2(0.3142)13014cas(0.3142)+113\sin(0.3142)-787.2}{R3\ (2)}$$

$$\varepsilon_{r\theta}^2 = \frac{19600 \cos^9(0.314z) + 6088740\cos^6 (0.314z) + 4732311623 \cos^4 (0.314z) + 56819603.4\cos^3(0.314z) + 35929757.2 \cos^2 (0.314z) + 2048924.2 \cos (0.314z) - 31640 \sin (0.314z)\cos^3 (0.314z) - 4914487 \sin(0.314z) \cos^2(0.314z) - 294116.4 \sin(0.314z) \cos (0.314z) + 11769 \sin^2(0.314z) - 177907.25 \sin(0.314z) + 619683.8}{(R^3 (z))^2}$$

5. Strain rate in both angular and axial direction (θz), from eqn. (17)

$$\varepsilon_{\theta z} = \frac{-3V_o R_1^2 R'' (z)}{2R^4 (z)} = \frac{-3(2)(10)^2 (-0.35 \cos (0.314z))}{2R^4 (z)}$$

$$= \frac{106.5 \cos (0.314z)}{R^4 (z)}$$

$$\varepsilon_{\theta z}^2 = \frac{11342.3cos2(0.314z)}{(R4\ (z))\ 2}$$

6. Strain rate in both radial and axial direction (rz), from eqn.(18)

$$\varepsilon_{rz} = \frac{2V_0 R_1^2 R'(z)}{R^3(z)} - 3\xi$$

$$= \frac{452 \sin (0.314z)}{R^3 (z)}$$

$$\varepsilon_{rz}^2 = \frac{204304\sin2(0.314z)}{(R3\ (z))\ 2}$$

By substituting the above stain rate in to eqn. (3) can be calculate power lass due to internal deformation to cosine die profile in 90% reduction.

$$W_I = \frac{2\sigma y}{\sqrt{3}} \int_0^z \int_0^r \int_0^\theta \sqrt{½\left(\frac{\begin{matrix}19600\cos 9(0.3142)\\ +6088740\cos 6(0.3142)\\ +473231162.3\cos 4(0.3142)\\ +56819603.4\cos 3(0.3142)\\ +35929757.2\cos 2(0.3142)\\ +2048924.2\cos(0.3142)\\ +31640\sin(0.314z)\cos 3(0.3142)\\ -491446,\sin(0.314z)\cos 2(0.3142)\\ -294116.4\sin(0.314z)\cos(0.3142)\\ +267149\sin 2(0.3142)\\ -177907.2\sin(0.3142)\\ +619683.8\end{matrix}}{(R3(z))2} + \frac{11342.3\cos 2(0.3142)}{(R4(z))2}\right)} d\theta dr dz$$

Applying Simpson's $\frac{1}{3}$ rule to solve W1;

$$W_I = \frac{5}{3}[R(0) + 4R(5) + R(10))]$$

$$R(0) = \frac{2x103.2}{\sqrt{3}} x2.12 = 252.6 \text{ MPa}$$

$$R(5) = \frac{2x103.2\ x2.1}{\sqrt{3}} = 250.25 \text{ MPa}$$

$$R(10) = \frac{2x103.2x2.1}{\sqrt{3}} = 250.25\text{MPa}$$

$$W_1 = \frac{5}{3}(252.6 + 4(250.25) + 250.25)$$
$$= 2506.39 \text{ MPa}$$

From eqn. (2), $J = W_I + W_S = 2506.39 + 376.83 = 2883.22$MPa

From eqn. (5), $P_{ave} = \frac{J}{\pi V0R^2} = \frac{2883.22}{200\pi}$ =\` 4.59 MPa

F= P_{ave} x Area=4.59 x100π =1441.61N

σ = F/Area, Where σ =effective stress at different z values.

From eqn. (19) $\varepsilon_{eff} = \frac{2}{\sqrt{3}}\sqrt{\frac{\varepsilon_{rr}^2+\varepsilon_{\theta\theta}^2+\varepsilon_{zz}^2+\varepsilon_{r\theta}^2+\varepsilon_{\theta z}^2+\varepsilon_{rz}^2}{2}}$ to calculate ε_{eff} at z=0, could be calculated six different strain rate components at this z values.

$$\varepsilon_{rr}^2 = \frac{51076\ Sin^2(0.314z)}{(R^3(z))^2}$$

And similarly, could be calculated $\varepsilon_{\theta\theta}^2$, ε_{zz}^2, $\varepsilon_{r\theta}^2$, $\varepsilon_{\theta z}^2$ and ε_{rz}^2

By using Eqn. (20) and applying Simpson's 1/3 integration rule, could be calculated strain at different z values. $\varepsilon=\int \frac{\acute{\varepsilon}}{Vz}dz=\int \frac{\frac{2}{\sqrt{3}}\sqrt{\frac{\varepsilon_{rr}^2+\varepsilon_{\theta\theta}^2+\varepsilon_{\theta\theta}^2+\varepsilon_{r\theta}^2+\varepsilon_{\theta z}^2+\varepsilon_{rz}^2}{2}}}{Vz}dz$

At different z values from (0-10) strain rate effective, stress and strain values listed in table3.6 below.

Table.3. 6 Strain and Stress values at different z values

Z -value	Pressure(MPa)	Area(mm)	έ in (mm/mm/sec)	σ in MPa	ε in(mm)
0	4.59	314.15	2.448	4.5889	0
2	4.59	314.14	2.448	4.5890	0.9250
4	4.59	314.11	2.448	4.5895	1.7871
6	4.59	314.04	2.447	4.5905	2.3492
8	4.59	230.31	2.445	6.2594	3.6113
10	4.59	31.36	2.445	45.9697	4.3734

3.4 Third-order polynomial die profile

1. 30% area reduction

This Die profile is represented by the function, from eqn. (8)

$$R(z)=R1+(R1-R2)\left[2\frac{Z^3}{L^3}-3\frac{Z^2}{L^2}\right]$$

At 30% area reduction exit radius, R2=7.4mm

Substitute the given value into the above eqn.it becomes,

$R(z)=10+0.0052z^3-0.078z^2$

$R'(z)=0.0168z^2-0.156z$

$R''(z)=0.336z-0.156$

$R^2(z)=0.0027z^9-0.0082z^6+0.006z^4-1.56z^2+100$

$(R^2(z))^2=0.000007z^{81}-0.000044z^{54}+0.0001z^{36}-0.0001z^{24}-0.008z^{18}+0.000036z^{16}+0.026z^{12}+0.54z^9-0.018z^8-1.6z^6+3.6z^4-312z^2+10000$

$(R^3(z))^2= 0.00000001z^{729}-0.0000001z^{486}+0.0000006z^{324}+0.000006z^{243}-0.000001z^{216}-0.00006z^{162}+0.0000014z^{144}+0.0003z^{108}-0.000001z^{96}+0.002z^{81}-0.0006z^{72}+0.0000003z^{64}-$

$0.022z^{54}+0.0006z^{48}+0.08z^{36}-0.00032z^{32}+0.6z^{27}-0.13z^{24}-4.6z^{18}+0.06z^{16}+13.2z^{12}+87z^{9}-10.4^{8}-643.4z^{6}+947.8z^{4}+10400z^{3}-46800z^{2}+1000000$

$(R^4(z))^2=$ $0.000000000003z^{6561}-0.0000000004z^{4374}+0.000000003z^{2616}+0.00000004z^{2187}-0.000000009z^{1944}-0.000000044z^{1458}+0.00000002z^{1296}+0.0000026z^{972}-0.000000024z^{864}+0.000015z^{729}-0.000009z^{648}+0.00000002z^{576}-0.00021z^{486}+0.000014z^{432}-0.000000008z^{384}+0.0011z^{324}-0.00002z^{288}+0.000000002z^{256}+0.005z^{243}-0.003z^{216}+0.00001z^{192}-0.05z^{162}+0.005z^{144}-0.0000024z^{128}+0.24z^{108}-0.003z^{96}+1.1z^{81}-0.56z^{72}+0.0013z^{64}-10.3z^{54}+0.67z^{48}+40.68z^{36}-0.22z^{32}+434z^{27}-62z^{24}-1522z^{18}+35.6z^{16}+3878z^{12}+22816z^{9}-3096z^{8}-1368896z^{6}+177344z^{4}+2080000z^{3}-6240000z^{2}+100000000$

a. The velocity of the billet at different components

To calculate the power consumption (J) on this die profile, first could be calculate the velocity and the strain rate of the 30% reduction of 3rd order polynomial die at different components.

1. Velocity in the axial direction (z) , from eqn.(10)

$$Vz=\frac{V_0R_1^2}{R^2(z)}=\frac{2x100}{R^2(z)}$$

$$Vz^2=\frac{40000}{(R^2(z))^2}$$

2. Velocity in the radial direction (r), from eqn.(11)

$$V_r=-\frac{\partial\psi}{r\partial z} = \frac{\xi V_0R_1^2R'(z)}{R^2(z)}=\frac{31.2z^2-31.2z}{R^2(z)}$$

$$V_r^2=\frac{973.4z^4-1946.9z^3+973.44z^2}{(R^2(z))^2}$$

3. Velocity in the angular direction (θ), from eqn.(12)

$$V_\theta = \frac{V_r}{r} = \frac{V_0R_1^2R'(z)}{R^3(z)}=\frac{31.2z^2-31.2z}{R^3(z)}$$

$$V_\theta^2=\frac{973.4z^4-1946.9z^3+973.44z^2}{(R^3(z))^2}$$

Then, power loss dace to frictional resistance for 30% reduction is, from eqn. (4)

$$Ws=\frac{m\sigma y}{\sqrt{3}}\int_0^z\int_0^\theta\sqrt{\frac{973.4z^4-1946.9z^3+973.44z^2+40000}{(R^2(z))^2}+\frac{973.4z^4-1946.9z^3+973.44z^2}{(R^3(z))^2}}d\theta dz$$

Applying Simpson's $\frac{1}{3}$ integration rule to solve Ws;

$$Ws=R(z)=\frac{5}{3}[R(0)+4R(5)+R(10))]$$

$$R(0) = \frac{0.3x103.2x2}{\sqrt{3}} = 35.40 \text{ MPa}$$

$$R(5) = \frac{0.3x103.2\ x3.2x10^{-9}}{\sqrt{3}} = 5.7x10^{-8} \text{MPa}$$

$$R(10) = \frac{0.3x103.2x5.5x10^{-14}}{\sqrt{3}} = 9.8x10^{-13} \text{MPa}$$

$$W_s = \frac{5}{3}(35.40 + 4\,(5.7x10^{-8}) + 9.8x10^{-13})$$
$$= 59 \text{ MPa}$$

b. Strain rates in different components

1. Strain in radial direction (r) , from eqn.(13)

$$\varepsilon_{rr} = \frac{V_0 R_1^2 R'(z)}{R^3(z)} = \frac{31.2z^2 - 31.2z}{R^3(z)}$$

$$\varepsilon_{rr}^{\ 2} = \frac{973.4z^4 - 1946.9z^3 + 973.44z^2}{(R^3(z))^2}$$

2. Strain in angular direction (θ), from eqn.(14)

$$\varepsilon_{\theta\theta} = -\frac{V_0 R_1^2 R'(z)}{R^3(z)} = \frac{-62.4z^2 + 62.4z}{R^3(z)}$$

$$\varepsilon_{\theta\theta}^{\ 2} = \frac{973.4z^4 - 1946.9z^3 + 973.44z^2}{(R^3(z))^2}$$

3. Strain in axial direction (z) , from eqn.(15)

$$\varepsilon_{zz} = 2\frac{V_0 R_1^2 R'(z)}{R^3(z)} = \frac{62.4z^2 - 62.4z}{R^3(z)}$$

$$\varepsilon_{zz}^{\ 2} = \frac{3893.76z^4 - 7787.52z^3 + 3893.76z^2}{(R^3(z))^2}$$

4. Strain in radial and angular direction (rθ) , from eqn.(16)

$$\varepsilon_{r\theta} = -\frac{V_0 R_1^2 R'(z)}{2R^3(z)} - 3\xi = \frac{-15.6z^2 + 62.4z - 3R^3(z)}{R^3(z)}$$

$$\varepsilon_{r\theta}^{\ 2} = \frac{\begin{array}{c} 0.00000009z^{729} - 0.0000012z^{486} + 0.0000058z^{324} + 0.00006z^{243} - 0.000013z^{216} \\ -0.0008z^{162} + 0.00001z^{144} + 0.003z^{108} - 0.000012z^{96} + 0.018z^{81} - 0.0068z^{72} + 0.000004z^{64} - 0.0z^{54} + 0.0064z^{48} + 0.9z^{36} \\ -0.0014z^{32} - 0.01z^{28} + 4.6z^{27} - 1.2z^{24} + 0.06z^{19} - 0.396z^{18} + 0.6z^{16} - 0.1z^{13} + 103.32z^{12} - 2.8z^{10} + 783.46z^9 - 77.52z^8 \\ +18.84z^7 - 5303.6z^6 - 18.8z^5 + 6094.36z^4 + 95303.6z^3 - 327356.6z^2 - 93600z + 9000000 \end{array}}{(R^3(z))^2}$$

5. Strain in angular and axial direction (θz) , from eqn.(17)

$$\varepsilon_{\theta z} = \frac{\partial V_\theta}{2\partial z} + \frac{\partial V_\theta}{r\partial\theta} = -\frac{3V_0 R_1^2 R''(z)}{2R^4(z)} = \frac{-93.6z + 46.8}{R^4(z)}$$

$$\varepsilon_{\theta z}^{\ 2} = \frac{8761z^2 - 8761z + 2190}{(R^4(z))^2}$$

6. Strain in radial and axial direction (rz) , from eqn.(18)

$$\varepsilon_{rz} = \frac{\partial V_r}{2\partial r} + \frac{\partial V_z}{\partial r} = -\frac{V_0 R_1^2 R'(z)}{R^3(z)}\left[1+\frac{1}{\xi}\right] = \frac{-62.4z^2+62.4z}{R^3(z)}$$

$$\varepsilon_{rz}^2 = \frac{3893.76z^4-7787.52z^3+3893.76z^2}{(R^3(z))^2}$$

By substituting the above stain rate in to eqn. (3) could be calculated power loss due to internal deformation to 3rd order die profile in 30% reduction.

$$WI = \frac{2\sigma y}{\sqrt{3}}\int_0^z\int_0^r\int_0^\theta \sqrt{½\left(\frac{c}{(R3\ (z))2} + \frac{8761z^4-8761z^3+2190}{(R4\ (z))2}\right)}d\theta drdz$$

Where c =

$$0.00000009z^{729} - 0.0000012z^{486} + 0.0000058z^{324} + 0.00006z^{243}$$
$$-0.000013z^{216}$$
$$-0.0008z^{162} + 0.00001z^{144} + 0.003z^{108} - 0.000012z^{96}$$
$$+0.018z^{81} - 0.0068z^{72} + 0.000004z^{64} - 0.0z^{54} + 0.0064z^{48} + 0.9z^{36}$$
$$-0.0014z^{32} - 0.01z^{28} + 4.6z^{27} - 1.2z^{24} + 0.06z^{19} - 0.396z^{18} + 0.6z^{16} - 0.1z^{13}$$
$$+103.32z^{12} - 2.8z^{10} + 783.46z^9 - 77.52z^8$$
$$+18.84z^7 - 5303.6z^6 - 18.8z^5 + 6094.36z^4 + 95303.6z^3 - 327356.6z^2 - 93600z + 9000000$$

Applying Simpson's $\frac{1}{3}$ integration rule to solve W1;

$$W_I = R\ (z) = \frac{5}{3}\left[R(0) + 4\ R(5) + R(10)\right]$$

$$R\ (0) = \frac{2x103.2}{\sqrt{3}}\ x2.12 = 252.6\ MPa$$

$$R\ (5) = \frac{2x103.2\ x2.24}{\sqrt{3}} = 266.93MPa$$

$$R\ (10) = \frac{2x103.2x2.24}{\sqrt{3}} = 266.93MPa$$

$$W_1 = \frac{5}{3}(252.6 + 4\ (266.93) + 266.93)$$

$$= 2645.4\ MPa$$

From eqn. (2), $J = W_1 + W_S = 2645.4 + 59 = 2704.4\ MPa$

From eqn. (5), $P_{ave} = \frac{J}{\pi V0R1^2} = \frac{2704.4}{200\pi}$ =`4.30 MPa

$$F = P_{ave}\ x\ A = 4.30x\pi R1^2 = 4.30x100\pi = 1352.2N$$

σ = F/Area, Where σ =effective stress at different z values.

From eqn. (19) $\varepsilon_{eff}=\frac{2}{\sqrt{3}}\sqrt{\frac{\varepsilon_{rr}^2+\varepsilon_{\theta\theta}^2+\varepsilon_{zz}^2+\varepsilon_{r\theta}^2+\varepsilon_{\theta z}^2+\varepsilon_{rz}^2}{2}}$ to calculate ε_{eff} at z=0, could be calculated six different strain rate components at this z values.

$$\varepsilon_{rr}^2 = \frac{973.4z^4-1946.9z^3+973.44z^2}{(R^3(z))^2}$$

And similarly, could be calculated $\varepsilon_{\theta\theta}^2$, ε_{zz}^2, $\varepsilon_{r\theta}^2$, $\varepsilon_{\theta z}^2$ and ε_{rz}^2

By using Eqn. (20) and applying Simpson's 1/3 integration rule, could be calculated strain at different z values. $\varepsilon=\int \frac{\acute{\varepsilon}}{Vz}dz=\int \frac{\frac{2}{\sqrt{3}}\sqrt{\frac{\varepsilon_{rr}^2+\varepsilon_{\theta\theta}^2+\varepsilon_{\theta\theta}^2+\varepsilon_{r\theta}^2+\varepsilon_{\theta z}^2+\varepsilon_{rz}^2}{2}}}{Vz}dz$

At different z values from (0-10) strain rate effective, stress and strain values listed in table3.7 below.

Table.3. 7 Strain and Stress values at different z values

Z -value	Pressure(MPa)	Area(mm2)	έ in(mm/mm/sec)	σ in MPa	ε in(mm)
0	4.3	314.15	2.551	4.3043	0
2	4.3	304.29	2.578	4.4438	1.3138
4	4.3	265.90	2.579	5.0854	1.7525
6	4.3	230.97	2.581	5.8544	2.1912
8	4.3	202.51	2.579	6.6772	2.6299
10	4.3	219.04	2.579	6.1733	3.0686

2. At 60% area reduction 3rd order polynomial dies profile

At 60% area reduction exit radius, R2=5.6mm

- Substitute the given Specification of the dimension of the die value into eqn.(8).it becomes,

$$R(z) = 10+0.0088z^3-0.03z^2$$

$$R'(z) = 0.03z^2-0.06z$$

$$R''(z) = 0.05z-0.06$$

$$R^2(z) = 0.00008z^9-0.0006z^6+0.176z^4-0.6z^2+100$$

$(R^2(z))^2 = 0.000000006z^{81}-0.00000001z^{54}+0.000004z^{36}+1.8z^{27}-0.0003z^{18}+0.0008z^{12}+0.05z^9-0.32z^6+0.36z^4+35.2z^3-120z^2+10000$

$(R^3 (z))^2 = 0.0000000000005z^{729} - 0.000000000012z^{486} + 0.00000000009z^{324}$

$+ 0.000000004z^{243} - 0.000000004z^{216} - 0.00000007z^{162} + 0.0000000004z^{144}$

$+ 0.00000055z^{108} + 0.000012z^{81} - 0.0000022z^{72}$

$-0.0013z^{54} + 0.0000008z^{48} + 0.0044z^{36} + 0.0115z^{27} - 0.0012z^{24} - 0.2z^{18} + 0.0004z^{16} + 0.54z^{12} + 8z^9 - 0.4z^8 - 88z^6 + 121z^4 + 5280z^3 - 18000z^2 + 1000000$

$(R^4(z))^2 = 0.00000000003z^{6561} - 0.0000000004z^{4374} + 0.0000000024z^{2616} + 0.00000004z^{2187} - 0.000000009z^{1944} - 0.0000002z^{1458} + 0.0000000184z^{1296} + 0.0000006z^{972} - 0.000000024z^{864} + 0.000015z^{729} + 0.0000021z^{648} + 0.000000018z^{576} - 0.000116z^{486} + 0.001z^{432} - 0.000000008x^{384} + 0.0003x^{324} + 0.000002x^{288} + 0.000000002x^{256} + 0.005x^{243} - 0.0002x^{216} - 0.0000041z^{192} - 0.032z^{162} + 0.000005z^{144} + 0.000002z^{128} + 0.06z^{108} - 0.0001z^{96} + 1.1z^{81} - 0.052z^{72} + 0.0004z^{64} - 6.2z^{54} + 0.0084z^{48} + 6.6z^{36} - 0.024z^{32} + 184.8z^{27} + 3.1z^{24} - 868.82z^{18} + 13.32z^{16} - 1246.2z^{12} + 22816z^9 + 524.8z^8 - 96896z^6 + 93344z^4 + 2080000z^3 - 6240000z^2 + 100000000$

a. The velocity of the die at different components

To calculate the power consumption (J) on this die profile, the velocity and the strain rate of the 60% reduction of 3rd order polynomial die are calculated.

1. Velocity in the axial direction(z) , from eqn.(10)

$$Vz = \frac{V_0 R_1^2}{R^2(z)} = \frac{2x100}{R^2(z)}$$

$$Vz^2 = \frac{40000}{(R^2(z))^2}$$

2. Velocity in the radial direction(r) , from eqn.(11)

$$V_r = -\frac{\partial\psi}{r\partial z} = \frac{\xi V_0 R_1^2 R'(z)}{R^2(z)} = \frac{6z^2 - 12z}{R^2(z)}$$

$$V_r^2 = \frac{36z^4 - 144z^3 + 144z^2}{(R^2(z))^2}$$

3. Velocity in the angular direction(θ), from eqn.(12)

$$V_\theta = \frac{V_r}{r} = \frac{V_0 R_1^2 R'(z)}{R^3(z)} = \frac{6z^2 - 12z}{R^3(z)}$$

$$V_\theta^2 = \frac{36z^4 - 144z^3 + 144z^2}{(R^3(z))^2}$$

Then, power loss dace to frictional resistance for 60% reduction is, from eqn. (4)

$$Ws=\frac{m\sigma y}{\sqrt{3}}\int_0^z\int_0^\theta\sqrt{\frac{36z^4-144z^3+144z^2+40000}{(R^2(z))^2}+\frac{36z^4-144z^3+144z^2}{(R^3(z))^2}}d\theta dz$$

Applying Simpson's $\frac{1}{3}$ integration rule to solve Ws;

$$Ws = R(z) = \frac{5}{3}[f(0)+4f(5)+f(10))]$$

$$R(0) = \frac{0.3x103.2x2}{\sqrt{3}} = 35.75 \text{ MPa}$$

$$R(5) = \frac{0.3x103.2\ x5.47x10^{-22}}{\sqrt{3}} = 9.78x10^{-21}\text{MPa}$$

$$R(10) = \frac{0.3x103.2x5.5x10^{-30}}{\sqrt{3}} = 1.7x10^{-28}\text{MPa}$$

$$W_s = \frac{5}{3}(35.75 + 4(9.78x10^{-21}) + 1.7x10^{-28})$$
$$= 59.58 \text{ MPa}$$

b. Strain rates in different components

1. Strain in radial direction (r) , from eqn.(13)

$$\varepsilon_{rr} = \frac{V_0R_1^2R'(z)}{R^3(z)} = \frac{6z^2-12z}{R^3(z)}$$

$$\varepsilon_{rr}^2 = \frac{36z^4-144z^3+144z^2}{(R^3(z))^2}$$

2. Strain in angular direction (θ), from eqn.(14)

$$\varepsilon_{\theta\theta} = -\frac{V_0R_1^2R'(z)}{R^3(z)} = \frac{12z^2-24z}{R^3(z)}$$

$$\varepsilon_{\theta\theta}^2 = \frac{144z^4-576z^3+576z^2}{(R^3(z))^2}$$

3. Strain in axial direction (z) , from eqn.(15)

$$\varepsilon_{zz} = 2\frac{V_0R_1^2R'(z)}{R^3(z)} = \frac{-12z^2+24z}{R^3(z)}$$

$$\varepsilon_{zz}^2 = \frac{144z^4-576z^3+576z^2}{(R^3(z))^2}$$

4. Strain in radial and angular direction (rθ) , from eqn.(16)

$$\varepsilon_{r\theta} = -\frac{V_0R_1^2R'(z)}{2R^3(z)} - 3\xi = \frac{-3z^2+6z-3R^3(z)}{R^3(z)}$$

$$\varepsilon_{r\theta}{}^2 = \frac{\begin{matrix} 0.000000000004z^{729} - 0.00000000005z^{486} + 0.000000041z^{324} + 0.00000004z^{243} \\ -0.0000004z^{216} \\ -0.0000006z^{162} + 0.000000004z^{144} + 0.000004z^{108} \\ +0.0001z^{81} - 0.00008z^{72} - 0.002z^{54} + 0.000008z^{48} + 0.007z^{36} \\ -0.000024z^{28} + 0.2z^{27} - 0.012z^{24} + 0.0003z^{19} - 2z^{18} + 0.004z^{16} - 0.0007z^{13} \\ +5z^{12} - 0.1z^{10} + 14.4z^9 - 3.6z^8 \\ +0.72z^7 - 840z^6 - 0.72z^5 + 116.4z^4 + 84360z^3 + 179964z^2 - 36000z + 9000000 \end{matrix}}{(R^3(z))^2}$$

5. Strain in angular and axial direction (θz) , from eqn.(17)

$$\varepsilon_{\theta z} = \frac{\partial V_\theta}{2\partial z} + \frac{\partial V_\theta}{r\partial\theta} = -\frac{3V_0R_1^2R''(z)}{2R^4(z)} = \frac{-125+18z}{R^4(z)}$$

$$\varepsilon_{\theta z}{}^2 = \frac{225z^2-540z+324}{(R^4(z))^2}$$

6. Strain in radial and axial direction (rz) , from eqn.(18)

$$\varepsilon_{rz} = \frac{\partial V_r}{2\partial r} + \frac{\partial V_z}{\partial r} = -\frac{V_0R_1^2R'(z)}{R^3(z)}\left[1+\frac{1}{\xi}\right] = \frac{-12z^2+24z}{R^3(z)}$$

$$\varepsilon_{rz}{}^2 = \frac{144z^4-576z^3+576z^2}{(R^3(z))^2}$$

From eqn. (3), $$WI = \frac{2\sigma y}{\sqrt{3}} \int_0^z \int_0^r \int_0^\theta \sqrt{½\left(\frac{c}{(R3\,(z))2} + \frac{225z^2-540z+324}{(R4\,(z))2}\right)}\, d\theta dr dz$$

Where c =

$$\begin{matrix} 0.000000000004z^{729} - 0.00000000005z^{486} + 0.000000041z^{324} + 0.00000004z^{243} \\ -0.0000004z^{216} \\ -0.0000006z^{162} + 0.000000004z^{144} + 0.000004z^{108} \\ +0.0001z^{81} - 0.00008z^{72} - 0.002z^{54} + 0.000008z^{48} + 0.007z^{36} \\ -0.000024z^{28} + 0.2z^{27} - 0.012z^{24} + 0.0003z^{19} - 2z^{18} + 0.004z^{16} - 0.0007z^{13} \\ +5z^{12} - 0.1z^{10} + 14.4z^9 - 3.6z^8 \\ +0.72z^7 - 840z^6 - 0.72z^5 + 584.4z^4 + 82488z^3 + 181836z^2 - 36000z + 9000000 \end{matrix}$$

Applying Simpson's $\frac{1}{3}$ integration rule to solve $W_{I;}$

$$W_I = \frac{5}{3}\,[R(0) + 4\,R(5) + R(10))]$$

$$R\,(0) = \frac{2x103.2x2.236}{\sqrt{3}} = 266.45 \text{ MPa}$$

$$R\,(5) = \frac{2x103.2\ x2.398}{\sqrt{3}} = 285.76\text{MPa}$$

$$R\,(10) = \frac{2x103.2x2.48}{\sqrt{3}} = 295.5 \text{ MPa}$$

$W_1 = \frac{5}{3}(266. + 4\,(285.76) + 295.5)$

$= 2841.65$ MPa

From eqn. (2), $J = W_1 + W_S = 2841.45 + 59.833 = 2901.33$MPa

From eqn. (5), $P_{ave} = \frac{J}{\pi V0 R^2} = \frac{2901.33}{200\pi} = 4.62$ MPa

$F = P_{ave}$ x Area =4.62 x100π =1450.67N

σ = F/Area, Where σ =effective stress at different z values.

From eqn. (19), $\varepsilon_{eff} = \frac{2}{\sqrt{3}}\sqrt{\frac{\varepsilon_{rr}^2+\varepsilon_{\theta\theta}^2+\varepsilon_{zz}^2+\varepsilon_{r\theta}^2+\varepsilon_{\theta z}^2+\varepsilon_{rz}^2}{2}}$ to calculate ε_{eff} at z=0, could be calculated six different strain rate components at this z values.

$$\varepsilon_{rr}^{\ 2} = \frac{36z^4 - 144z^3 + 144z^2}{(R^3(z))^2}$$

And similarly, could be calculated $\varepsilon_{\theta\theta}^2$, ε_{zz}^2, $\varepsilon_{r\theta}^2$, $\varepsilon_{\theta z}^2$ and ε_{rz}^2

By using Eqn. (20) and applying Simpson's 1/3 integration rule, could be calculated strain at different z values.

$$\varepsilon = \int \frac{\acute{\varepsilon}}{Vz} dz = \int \frac{\frac{2}{\sqrt{3}}\sqrt{\frac{\varepsilon_{rr}^2+\varepsilon_{\theta\theta}^2+\varepsilon_{\theta\theta}^2+\varepsilon_{r\theta}^2+\varepsilon_{\theta z}^2+\varepsilon_{rz}^2}{2}}}{Vz} dz$$

At different z values from (0-10) strain rate effective, stress and strain values listed in table3.8 below.

Table.3. 8 Strain and Stress values at different z values

Z -value	Pressure(MPa)	Area(mm)	έ in (mm/mm/sec)	σ in MPa	ε in(mm)
0	4.62	314.15	4.963	4.6178	0
2	4.62	308.85	4.954	4.6970	1.3508
4	4.62	293.21	4.854	4.9475	1.7952
6	4.62	268.04	4.921	5.4121	2.2396
8	4.62	231.92	4.056	6.2550	2.6840
10	4.62	125.44	4.991	11.5646	3.1284

3. At 90% area reduction 3rd order polynomial dies profile

At 90% area reduction exit radius, R2=2.8mm and substitute the given Specification of the dimension of the die value into eqn. (8).it becomes,

$R(z) = 10 + 0.0144z^3 - 0.216z^2$

R' (z) =$0.0432z^2$-0.432z

R'' (z) =0.0864z-0.432

R^2 (z) = $0.00021z^9-0.006z^6+0.047z^4+0.288z^3-4.32z^2+100$

$(R^2 (z))^2 = 0.00000001z^{81}-0.0000008z^{54}+0.000024z^{36}+0.00004z^{27}-0.00032z^{24}-0.016z^{18}+0.0016z^{16}+0.05z^{12}+0.06z^9-0.32z^8-2.4z^6+24z^4+40z^3-800z^2+10000$

$(R^3 (z))^2=$

$$0.000000000001z^{729} - 0.00000000012z^{486} + 0.0000000061z^{324} + 0.000000006z^{243} -0.00000016z^{216} -0.0000006z^{162} + 0.0000024z^{144} + 0.000024z^{108} - 0.00002z^{96} +0.0000096z^{81} - 0.00048z^{72} + 0.000064z^{64} - 0.0012z^{54} + 0.0048z^{48} - 0.368z^{36} -0.0192z^{32} + 0.02z^{27} - 0.48z^{24} - 1.2z^{18} +24z^{12} - 44z^{9} - 160z^{8} -600z^{6} + 6000z^{4} + 9000z^{3} - 120000z^{2} + 1000000$$

$(R^4 (z))^2 = 0.0000000000000001z^{6561}-0.000000000000004z^{4374} + 0.0000000000012z^{2916}+0.0000000000008z^{2187}-0.00000000005z^{1944}-0.00000000014z^{1458}+0.000000002z^{1296}+0.0000000072z^{972}-0.00000002z^{864}+0.0000000032z^{729}+0.0000003z^{648}+0.000000008z^{576}-0.0000005z^{486}+0.000005z^{432}-0.000001z^{384}+0.00003z^{324}-0.000044z^{288}+0.000003z^{256}+0.000006z^{243}-0.000246z^{216}+0.0003z^{192}-0.0082z^{162}+0.005z^{144}+0.03z^{108}-0.02z^{96}+0.0074z^{81}-0.4z^{72}+0.18z^{64}-0.688z^{54}+3.4z^{48}+17.52z^{36}-1792z^{32}+5.6z^{27}-187z^{24}-368z^{18}+1120z^{16}+6256z^{12}+2800z^9-44800z^8-112000z^6+1120000z^4+800000z^3-16000000z^2+100000000$

a. The velocity of the billet at different components

To calculate the power consumption (J) on this die profile, the velocity and the strain rate of the 90% reduction of 3rd order polynomial die are calculated.

1. Velocity in the axial direction (z) , from eqn.(10)

$$Vz = \frac{V_0 R_1^2}{R^2(z)} = \frac{2x100}{R^2(z)}$$

$$Vz^2 = \frac{40000}{(R^2(z))^2}$$

2. Velocity in the radial direction(r) , from eqn.(11)

$$V_r = -\frac{\partial\psi}{r\partial z} = \frac{\xi V_0 R_1^2 R'(z)}{R^2(z)} = \frac{8z^2-80z}{R^2(z)}$$

$$V_r^2 = \frac{64z^4-1280z^3+6400z^2}{(R^2(z))^2}$$

3. Velocity in the angular direction(θ), from eqn.(12)

$$V_\theta=\frac{V_r}{r} = \frac{V_0R_1^2R'(z)}{R^3(z)} =\frac{8z^2-80z}{R^3(z)}$$

$$V_\theta^{\ 2} =\frac{64z^4-1280z^3+6400z^2}{(R^3(z))^2}$$

Then, power loss dace to frictional resistance for 60% reduction is, from eqn. (4)

$$Ws=\frac{m\sigma y}{\sqrt{3}}\int_0^z\int_0^\theta\sqrt{\frac{64z^4-1280z^3+6400z^2+40000}{(R^2(z))^2}+\frac{64z^4-1280z^3+6400z^2}{(R^3(z))^2}}d\theta dz$$

Applying Simpson's $\frac{1}{3}$ integration rule to solve Ws;

$$Ws= \frac{5}{3}[R(0) + 4\,R(5) + R(10))]$$

$$R\,(0) =\frac{0.3x103.2x2}{\sqrt{3}} =35.75\text{ MPa}$$

$$R\,(5) = \frac{0.3x103.2\ x5.25x10^{-9}}{\sqrt{3}} =9.38x10^{-8}\text{MPa}$$

$$R\,(10) = \frac{0.3x103.2x2.8x10^{-14}}{\sqrt{3}} = 5x10^{-13}\text{MPa}$$

$$W_s = \frac{5}{3}(35.75 + 4\,(9.38x10^{-8}) +5x10^{-13})$$
$$= 59.83\text{ MPa}$$

b. Strain rates in different components

1. Strain in radial direction (r) , from eqn.(13)

$$\varepsilon_{rr} = \frac{V_0R_1^2R'(z)}{R^3(z)}=\frac{8z^2-80z}{R^3(z)}$$

$$\varepsilon_{rr}^{\ 2} = \frac{64z^4-1280z^3+6400z^2}{(R^3(z))^2}$$

2. Strain in angular direction (θ), from eqn.(14)

$$\varepsilon_{\theta\theta} = -\frac{V_0R_1^2R'(z)}{R^3(z)} =\frac{16z^2-160z}{R^3(z)}$$

$$\varepsilon_{\theta\theta}^{\ 2}\ \ \varepsilon_{zz}^{\ 2} = \frac{256z^4-5120z^3+25600z^2}{(R^3(z))^2}$$

3. Strain in axial direction (z) , from eqn.(15)

$$\varepsilon_{zz} = 2\frac{V_0R_1^2R'(z)}{R^3(z)} = \frac{-16z^2+160z}{R^3(z)}$$

$$\varepsilon_{zz}^{2} == \frac{256z^4-5120z^3+25600z^2}{(R^3(z))^2}$$

4. Strain in radial and angular direction (rθ) , from eqn.(16)

$$\varepsilon_{r\theta} = -\frac{V_0R_1^2R'(z)}{2R^3(z)} - 3\xi = \frac{-16z^2+160z-3R^3(z)}{R^3(z)}$$

$$\varepsilon_{r\theta}^{2} = \frac{\begin{gathered}0.000000000009z^{729}-0.00000000011z^{486}+0.000000054z^{324}-0.000000064z^{243}\\-0.000014z^{216}\\-0.00002z^{162}+0.00002z^{144}+0.000088z^{108}-0.0002z^{96}\\+0.00014z^{81}-0.0035z^{72}+0.0006z^{64}+0.007z^{54}+0.04z^{48}+0.19z^{36}-0.2z^{32}\\-0.00024z^{28}+0.03z^{27}-4.2z^{24}+0.014z^{19}-3.64z^{18}+21.36z^{16}-0.288z^{13}\\+198.7z^{12}+0.72z^{10}+64.9z^{9}-1315.4z^{8}\\+28.8z^{7}-3888z^{6}-288z^{5}+37456z^{4}+37088z^{3}-352008z^{2}-80000z+9000000\end{gathered}}{(R^3(z))^2}$$

5. Strain in angular and axial direction (θz) , from eqn.(17)

$$\varepsilon_{\theta z} = \frac{\partial V_\theta}{2\partial z} + \frac{\partial V_\theta}{r\partial\theta} = -\frac{3V_0R_1^2R''(z)}{2R^4(z)} = \frac{-27z+120}{R^4(z)}$$

$$\varepsilon_{\theta z}^{2} = \frac{729z^2-6480z+14400}{(R^4(z))^2}$$

6. Strain in radial and axial direction (rz) , from eqn.(18)

$$\varepsilon_{rz} = \frac{\partial V_r}{2\partial r} + \frac{\partial V_z}{\partial r} = -\frac{V_0R_1^2R'(z)}{R^3(z)}\left[1+\frac{1}{\xi}\right] = \frac{-16z^2+160z}{R^3(z)}$$

$$\varepsilon_{rz}^{2} = \frac{256z^4-5120z^3+25600z^2}{(R^3(z))^2}$$

From eqn. (3), $WI = \frac{2\sigma y}{\sqrt{3}}\int_0^z\int_0^r\int_0^\theta \sqrt{½\left(\frac{c}{(R3\,(z))2} + \frac{225z^2-540z+324}{(R4\,(z))2}\right)}d\theta drdz$

Where c

$$= \begin{gathered}0.000000000009z^{729}-0.00000000011z^{486}+0.000000054z^{324}-0.000000064z^{243}\\-0.000014z^{216}\\-0.00002z^{162}+0.00002z^{144}+0.000088z^{108}-0.0002z^{96}\\+0.00014z^{81}-0.0035z^{72}+0.0006z^{64}+0.007z^{54}+0.04z^{48}+0.19z^{36}-0.2z^{32}\\-0.00024z^{28}+0.03z^{27}-4.2z^{24}+0.014z^{19}-3.64z^{18}+21.36z^{16}-0.288z^{13}\\+198.7z^{12}+0.72z^{10}+64.9z^{9}-1315.4z^{8}\\+28.8z^{7}-3888z^{6}-288z^{5}+38288z^{4}+20448z^{3}-352008z^{2}-80000z+9000000\end{gathered}$$

Applying Simpson's $\frac{1}{3}$ integration rule to solve W_I;

$$W_I = \frac{5}{3}\left[R(0) + 4\,R(5) + R(10))\right]$$

$$R(0) = \frac{2x103.2x2.12}{\sqrt{3}} = 252.63 \text{ MPa}$$

$$R(5) = \frac{2x103.2\ x2.58}{\sqrt{3}} = 307.45\text{MPa}$$

$$R(10) = \frac{2x103.2x2.63}{\sqrt{3}} = 313.4 \text{ MPa}$$

$$W_I = \frac{5}{3}(252.63 + 4\,(307.45) + 313.4)$$
$$= 2993.06 \text{ MPa}$$

From eqn. (2), $J = W_I + W_S = 2993.06 + 59.83 = 3052.64\text{MPa}$

From eqn. (5), $P_{ave} = \frac{J}{\pi V0R^2} = \frac{3052.64}{200\pi}$ =` 4.86 MPa

$F = P_{ave}$ x Area =4.86 x100π =1526.32N

σ = F/Area, Where σ =effective stress at different z values.

From eqn. (19), $\varepsilon_{eff} = \frac{2}{\sqrt{3}}\sqrt{\frac{\varepsilon_{rr}^2+\varepsilon_{\theta\theta}^2+\varepsilon_{zz}^2+\varepsilon_{r\theta}^2+\varepsilon_{\theta z}^2+\varepsilon_{rz}^2}{2}}$ to calculate ε_{eff} at z=0, could be calculated six different strain rate components at this z values.

$$\varepsilon_{rr}{}^2 = \frac{64z^4-1280z^3+6400z^2}{(R^3(z))^2}$$

And similarly, could be calculated $\varepsilon_{\theta\theta}^2$, ε_{zz}^2, $\varepsilon_{r\theta}^2$, $\varepsilon_{\theta z}^2$ and ε_{rz}^2

By using Eqn. (20) and applying Simpson's 1/3 integration rule, could be calculated strain at different z values. $\varepsilon = \int \frac{\acute{\varepsilon}}{Vz}dz = \int \frac{\frac{2}{\sqrt{3}}\sqrt{\frac{\varepsilon_{rr}^2+\varepsilon_{\theta\theta}^2+\varepsilon_{\theta\theta}^2+\varepsilon_{r\theta}^2+\varepsilon_{\theta z}^2+\varepsilon_{rz}^2}{2}}}{Vz}dz$

At different z values from (0-10) strain rate effective, stress and strain values listed in table3.9 below.

Table.3. 9 Strain and Stress values at different z values

Z -value	Pressure(MPa)	Area(mm)	έ in (mm/mm/sec)	σ in MPa	ε in (mm)
0	4.86	314.15	2.596	4.8586	0
2	4.86	268.87	2.597	5.6768	1.3610
4	4.86	175.10	2.594	8.7168	2.0132

6	4.86	89.40	2.586	17.0729	2.3748
8	4.86	39.57	2.585	38.5727	5.4440
10	4.86	31.36	2.583	48.6709	5.9230

3.5 Die geometry

Extrusion is of importance to all plastic processing. The required die profile to achieve the desired product dimensions is a very complex task and requires detailed knowledge of material properties and flow, heat transfer phenomena. Extrusion die design is still more an art than a science, even though the latter is becoming more and more relevant for design optimization because of modern advancement in the powerful computation and modeling of complex flow and heat transfer processes, before, through and after the die. The proper design of an extrusion die is extremely important to achieve the desired shape and accurate dimensions of the extruded product. So, could be calculated an extrusion die profile for square section from round billet using cosine function and 3rd order polynomial function. The die profile functions are (C.venkatesh et al. (2014)) written in eqn.7 and 8 above. The die profile function R (z) is similar in both x and y direction. The die profile function satisfies the boundary condition such that at z=0, x=R1 and z=L, x=R2. The exit and entry angles are non-zero angles. The velocity-discontinuity surfaces are normal to the axial flow directions. Where R1 and R2 are semi width of billet and product respectively and L is the die land length.

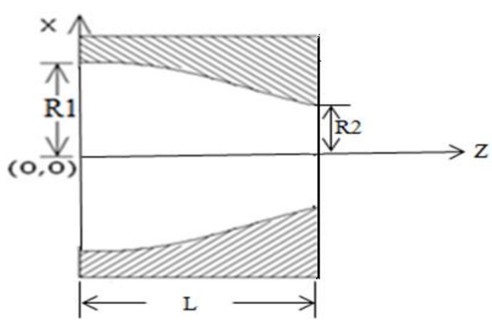

Figure.3. 2 Axisymmetiric dies profile shape

3.5.1 Cosine Die profile

In this section die design for 30%, 60% and 90% reduction considered for cosine die profile and 3rd order polynomial dies profile equation different for different % of reduction shown below.

- For 30% Reduction of Cosine Die profile from eqn.(7)

$$X=Y=R(z)=\frac{R1+R2}{2}+\frac{R1-R2}{2}\cos\left(\frac{\pi z}{L}\right)$$

To calculate the output area of A_f;

$$\% \text{ of Reduction} = \frac{Ao - Af}{Ao} x100\% \quad (21)$$

Here $A_0 = \pi\ (10)^2 mm^2$, $A_f = 14.8x14.8\ mm^2$

R1=10mm and R2= 7.4mm.

So $x = y = R\ (z) = 8.7 + 1.3\cos(\frac{\pi z}{10})$

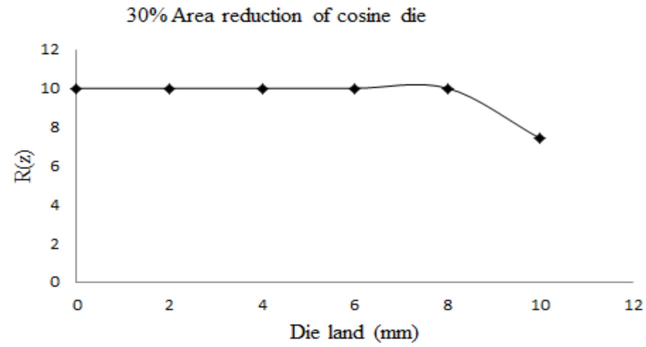

Figure.3. 3 30% area reduction cosine dies profile

- For R= 60% reduction cosine die profile equation

Here $A_0 = \pi\ (10)^2 mm^2$, $A_f = 11.2x11.2\ mm^2$ and $L_0 = 10$ mm

R1=10mm and R2= 5.6mm.

So $x = y = R\ (z) = 7.8 + 2.2\cos\frac{\pi z}{10}$

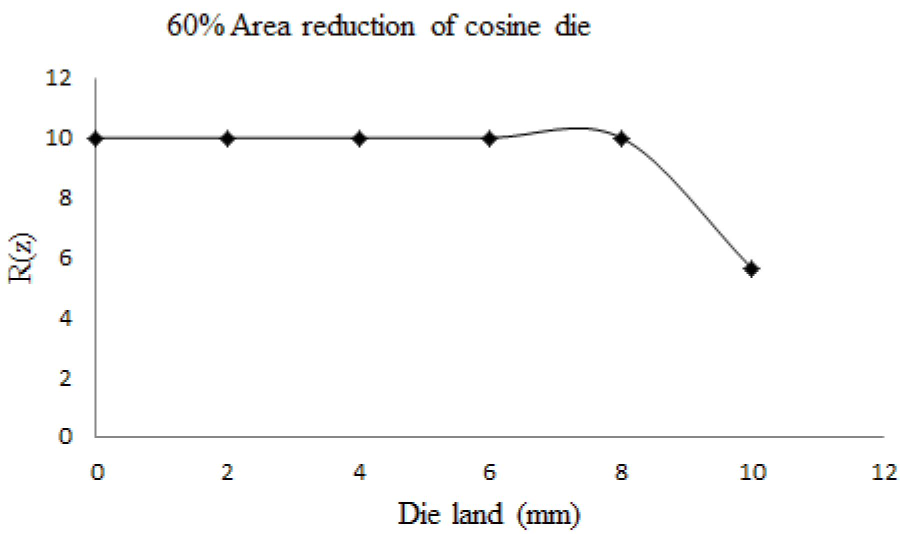

Figure.3. 4 60% area reduction cosine dies profile

- For R= 90% Reduction Cosine Die profile equation

  Here $A_0= \pi\ (10)^2 mm^2$, A_f =5.6x5.6 mm^2 and L_0=10 mm

  R1=10mm and R2= 2.8mm.

  So x = y = R (z) =6.4+3.6 cos $\frac{\pi z}{10}$

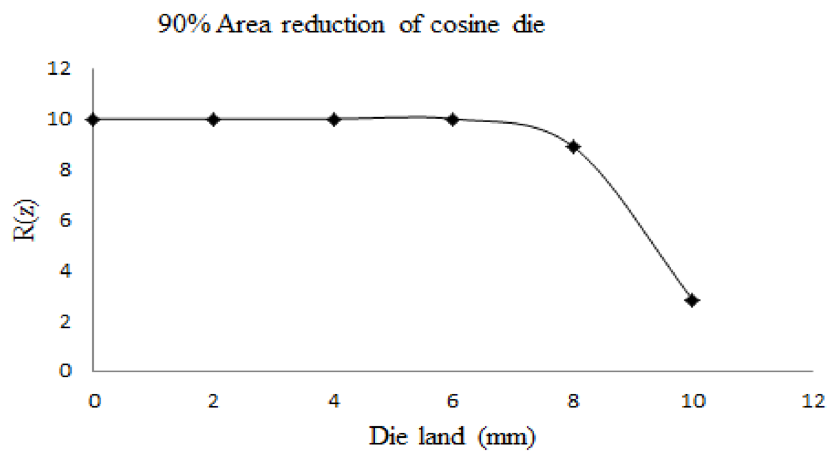

Figure.3. 5 90% area reduction cosine dies profile

Table.3. 10 Dimensions of dies are at different % of area reductions.

Si. No.	% of Area Reduction	Input radius (mm)	Input Area (mm^2)	Output side(mm)	Output Area (mm^2)	Height of Die land (mm)
1	30	10	314.14	14.8	219.04	10
2	60	10	314.14	11.2	125.44	10
3	90	10	314.14	5.6	31.36	10

3.5.2 Third-order polynomial dies profile

The function of 3rd -order polynomial Die profile equation;

$$R\ (z) = R1 + (R1 - R2)\ [2\frac{Z^3}{L^3} - 3\frac{Z^2}{L^2}]$$

❖ For 30% Reduction Third-order polynomial Die profile equation

Here $A_0=\pi\ (10)^2 mm^2$, A_f =14.8x14.8 mm^2 and L_0=10 mm

R1=10mm and R2= 7.8mm.

So x=y=R (z) =10+2.2[$2\frac{Z^3}{10^3}$ -$3\frac{Z^2}{10^2}$]

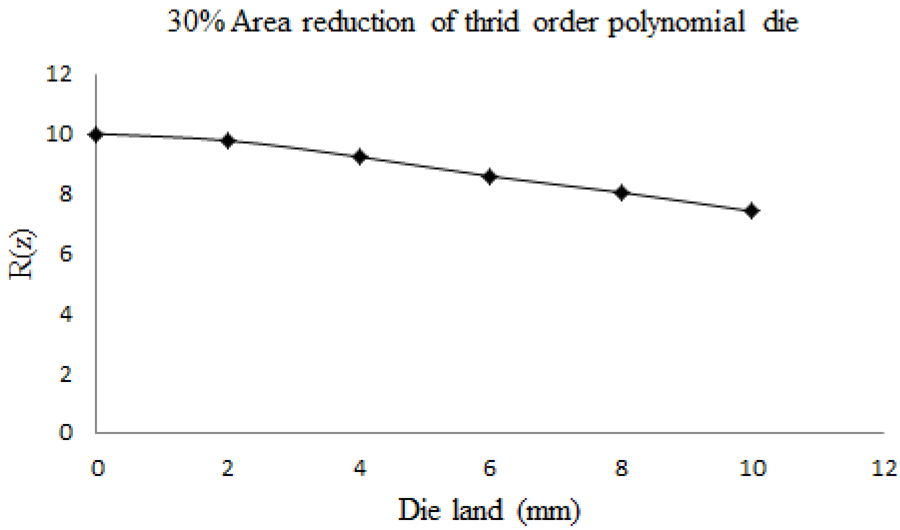

Figure.3. 6 30% Area reduction third-order polynomial Die profile

- For 60% reduction Third-order polynomial die profile equation

  Here $A_0 = \pi\ (10)^2 mm^2$, $A_f = 11.2x11.2mm^2$ and $L_0 = 10$ mm

  R1=10mm and R2= 5.6mm.

  So $x=y=R\ (z) = 10+4.4[2\frac{Z^3}{10^3} - 3\frac{Z^2}{10^2}]$

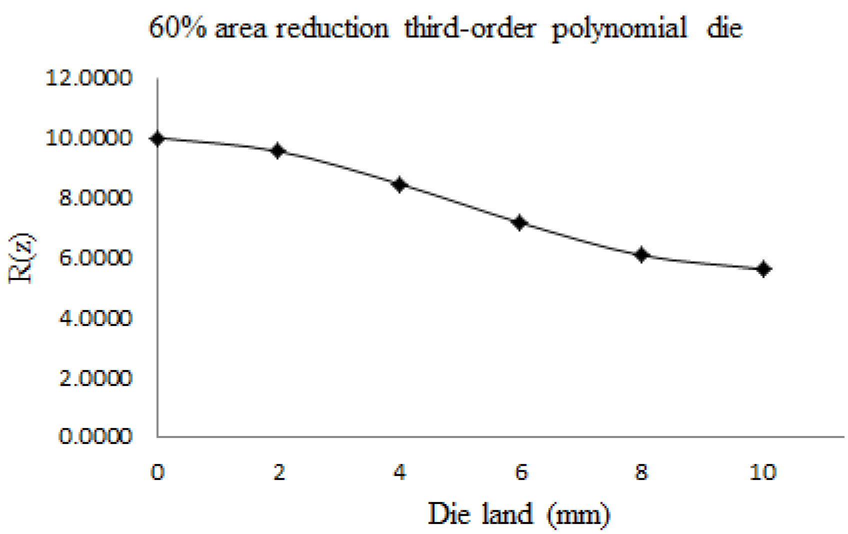

Figure.3. 7 60% Area reduction third-order polynomial dies profile

- For 90% Reduction Third-order polynomial Die profile equation

  Here $A_0 = \pi\ (10)^2 mm^2$, $A_f = 5.6x5.6\ mm^2$ and $L_0 = 10$ mm

  R1=10mm and R2= 2.8mm.

So x = y = R (z) =10+7.2[2$\frac{z^3}{10^3}$ -3$\frac{z^2}{10^2}$]

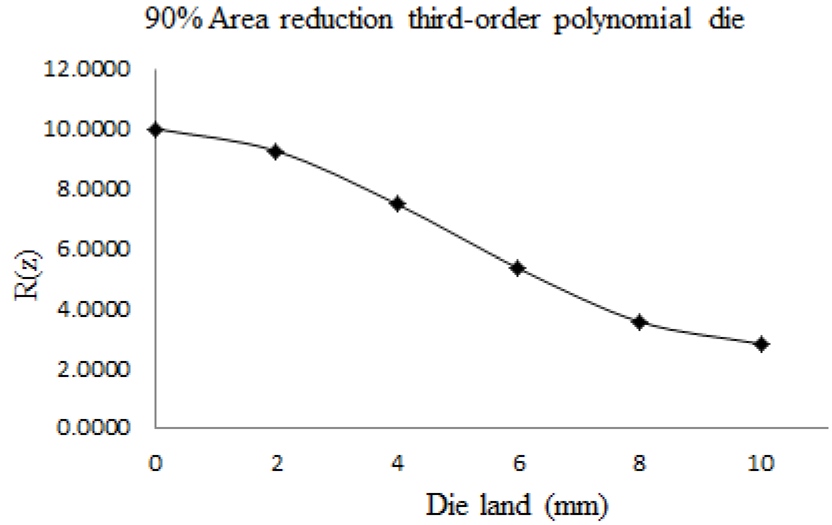

Figure.3. 8 90% Area reduction third-order polynomial dies profile

3.5.3 Solid modeling

For solidwork drawing and simulation have taken die dimensions in the following table based on some previous experimental research results

Table.3. 11 Parts of die dimensions for solidwork drawing and simulations

s/n	Name of parts	Dimension of parts in(mm)		Materials
		Cross section	length	
1	Punch	20	130	H13
2	Container	100	110	H13
3	Billet	20	110	Al/SiC
4	Die	30	20	H13
5	Die holder	100	20	H13
6	Base plate	120	20	H13
7	Bolt	M8	60	Harden steel

The generated points were used to create solid model using solid work software. Solid model generated from solidwork were shown in the following figures (a-r).

3.5.3.1 Cosine Die profile drawing

All drawing dimensions were given below in meters (m).

1. 30% area reduction cosine die

a.

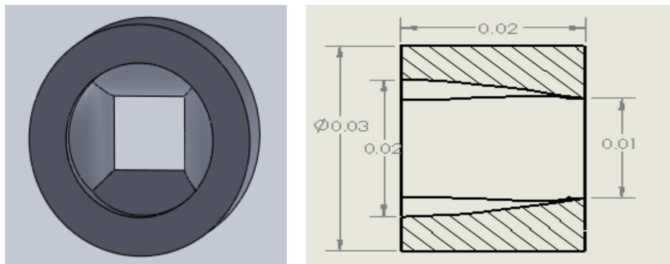

b.

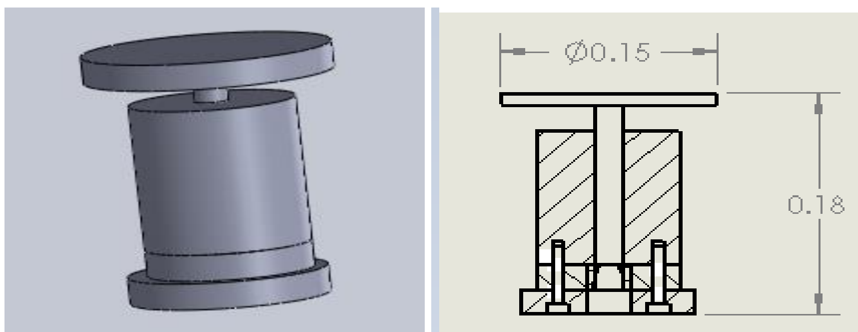

Figure.3. 9 a) Cosine die 3D and 2D section view and b) 3D assembly and 2D sectionsl drawing

1. **60% area reduction cosine die**

c.

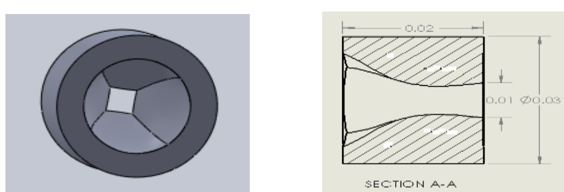

d.

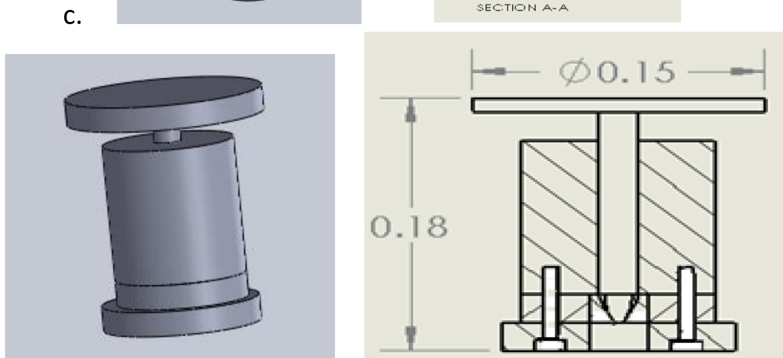

Figure.3. 10 c) Cosine dies 3D and 2D section view and d) 3D assembly and 2D sectionsl drawing

3.**90% area reduction cosine die**

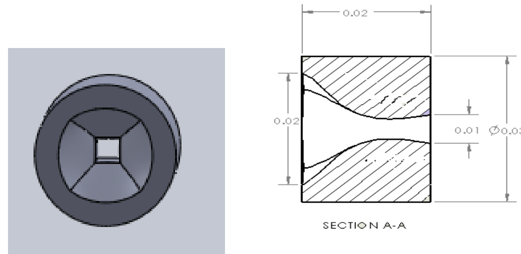

e.

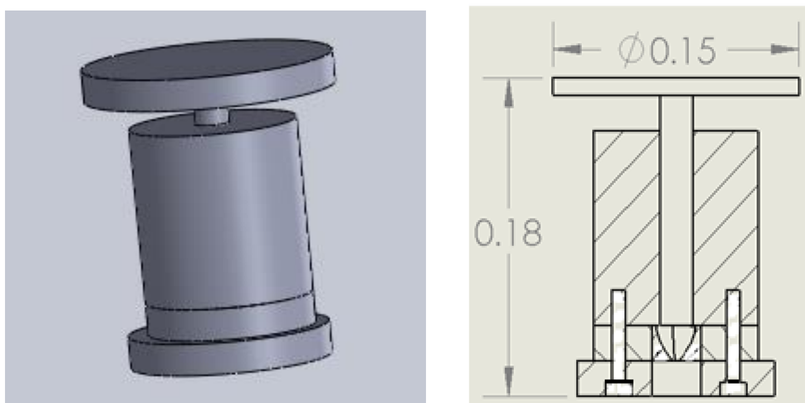

f.

Figure.3. 11 e) 3D and 2D section view of die and f) 3D assembly and 2D sectionsl view drawing

3.5.3.2 Part drawings of the full setup of die

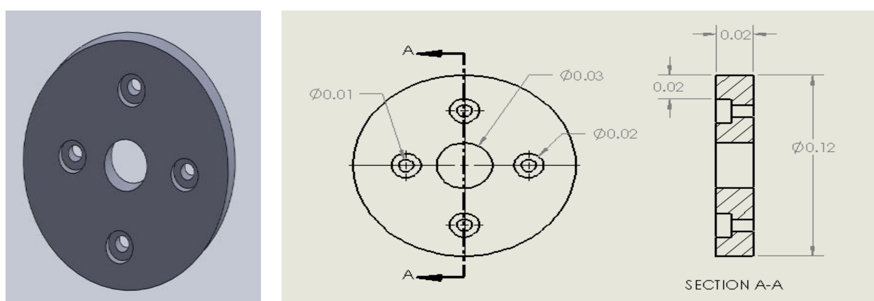

g.

Figure.3. 12 g) baseplate 3D and 2D with section view drawing

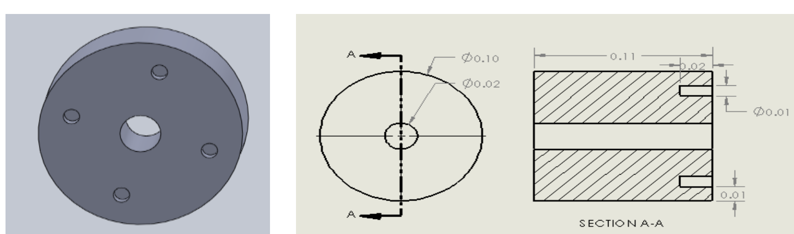

h.

Figure.3. 13 h) Billet container 3D, 2D and section view drawing

i.
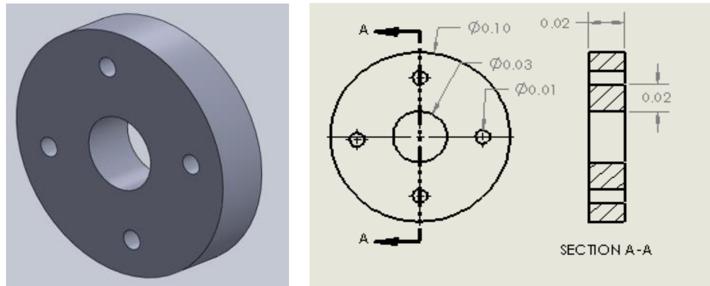

Figure.3. 14 i) Die holder 3D, 2D and section view drawing

j.
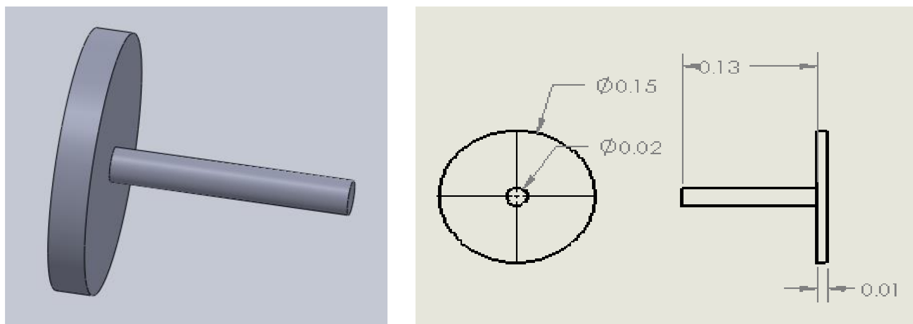

Figure.3. 15 j) Punch 3D, 2D and section view drawing

k.
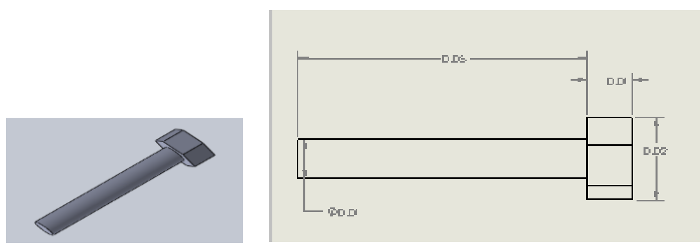

Figure.3. 16 k) Bolt 3D and 2D drawing

3.5.3.3 3rd order polynomial die profile drawings

1. 30% area reduction 3rd order polynomial dies profile

l.
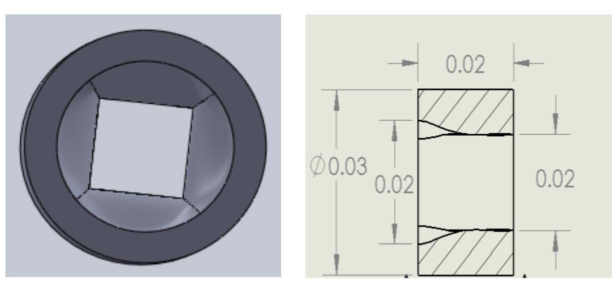

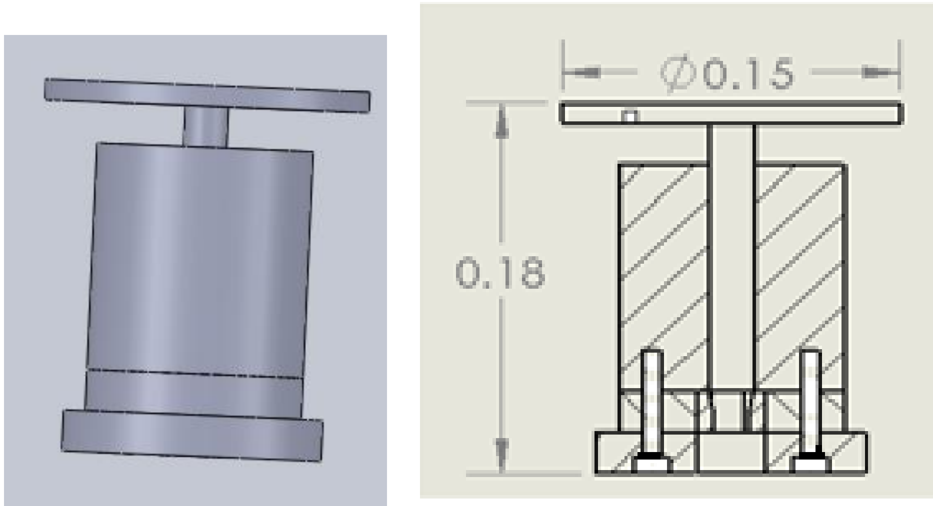

m.

Figure.3. 17 l) 3D and 2D section view of die and m) 3D assembly and 2D sectionsl view drawing

2. 60% area reduction 3rd order polynomial dies profile

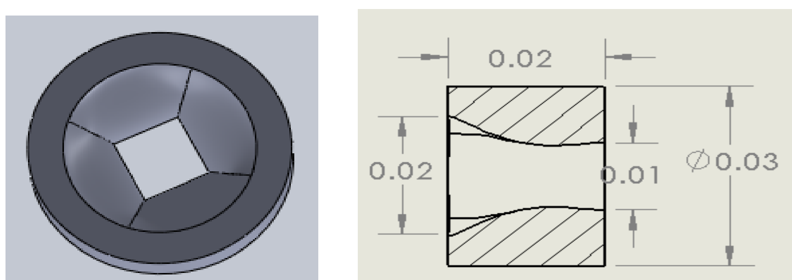

n.

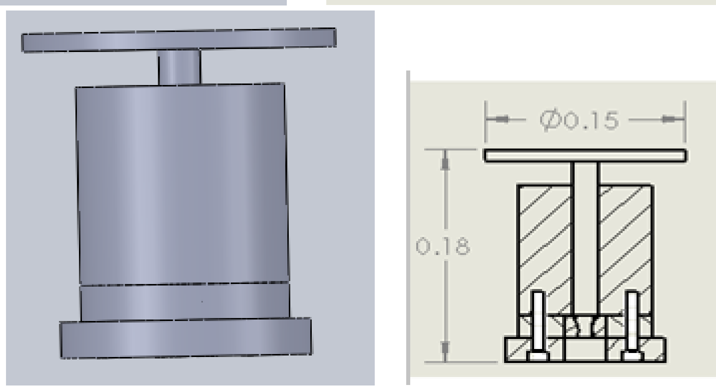

o.

Figure.3. 18 3rd order polynomial dies 3D and 2D section view and f) 3D assembly and 2D sectionsl drawing p.

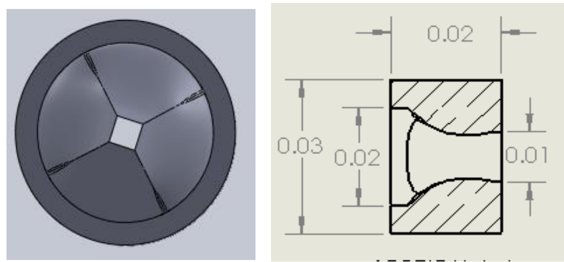

r.

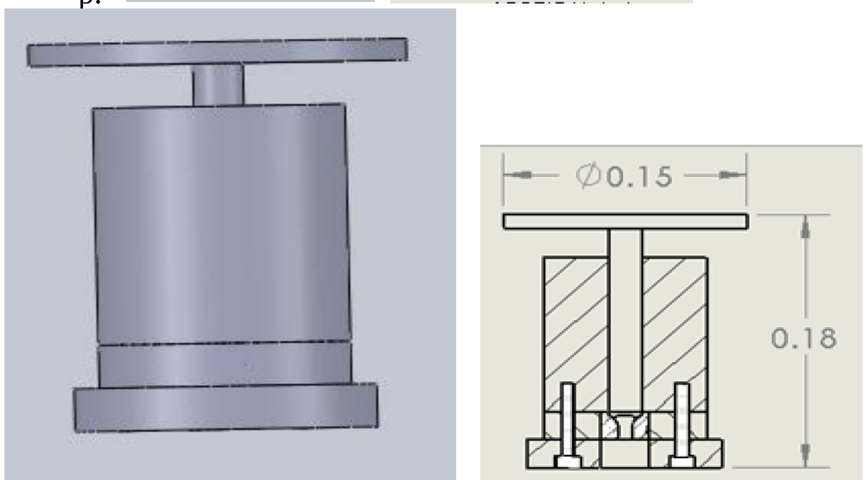

Figure.3. 19 90% area reduction 3rd order polynomial dies 3D,2D and assembly drawing

3.6 Numerical Analysis Method

In numerical analysis FEM modeling is a powerful technique used for different metal deformation problems including extrusion. In the present study, FEM modeling has been carried out for extrusion of square section from circular billet with cosine Die profile and 3rd order polynomial die profile using DEFORM-3D software.

Effective Strain rate ((mm/mm/sec)), effective stress (MPa), load prediction and temperature (C°) distribution obtained during simulation process.

A FEM based program DEFORM-3D software which consists of three special features such as,

1. Pre-processor
2. FEM simulation
3. Post-processor

The block diagram of simulation process in DEFORM-3D software is shown in fig.3.19 below.

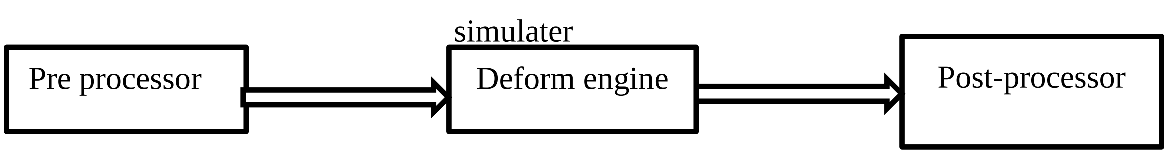

Figure.3. 20 Block Diagram of DEFORM-3D Software process

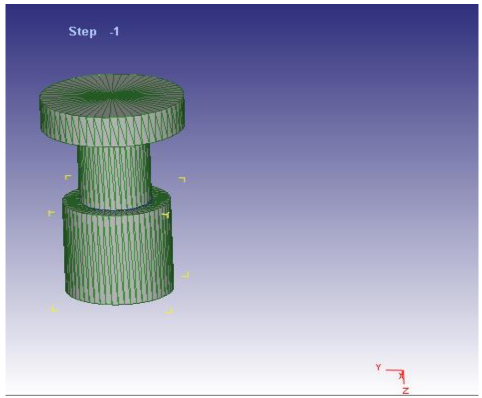

Figure.3. 21 modeling of punch, billet, container and die used in DEFORM-3D Software

1. **Pre-processing**

❖ Input parameters;

- Using Norton –Hoff Law $\sigma=K\,(\varepsilon_0+\varepsilon)^{n}\dot{\varepsilon}^{m}\exp(\frac{\beta}{T_{abs}})$ on the software and could be filled the values of K and n.
- Working Temperature=450^0c
- Speed=2mm/sec
- Friction =0.3

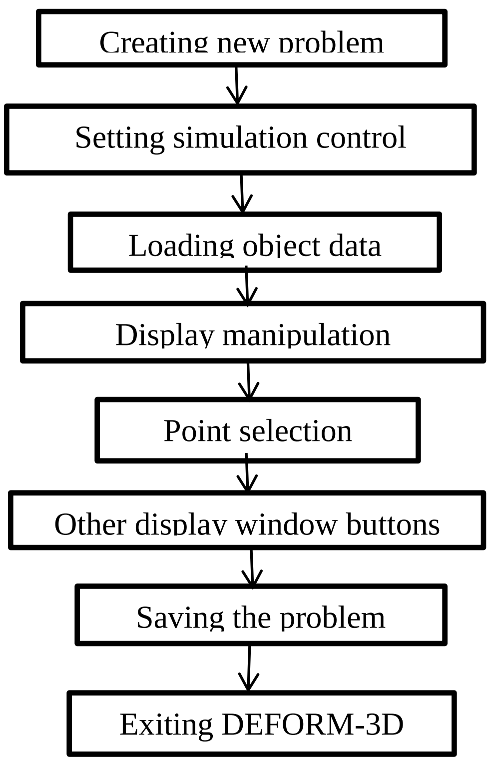

Figure.3. 22 Pre-Processing

2. **Die positioning and Pre-Processing**

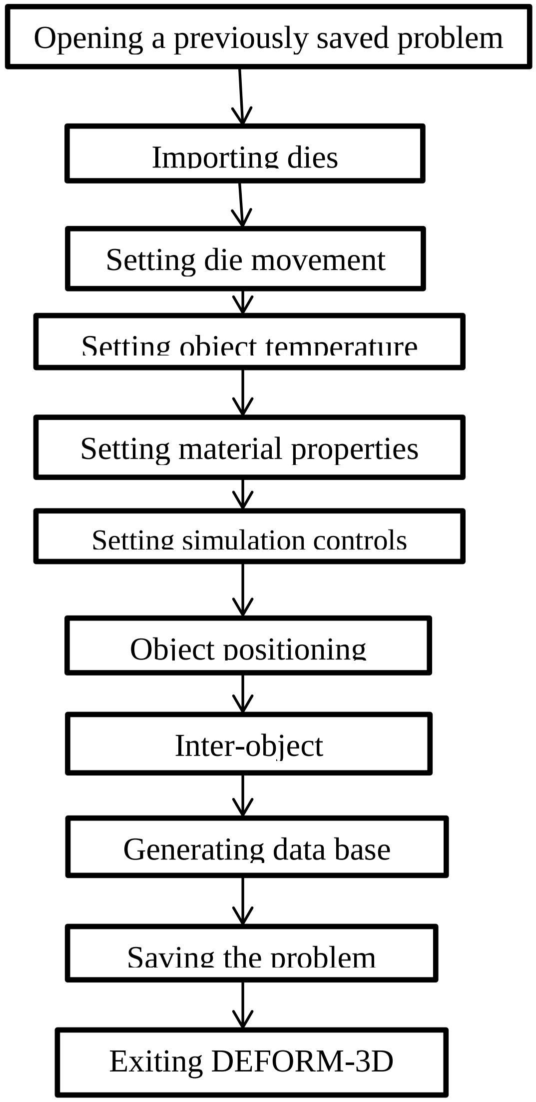

Figure.3. 23 Die positioning and Pre-Processing

3. **Extrusion simulation and post-processing**

In post processing the results, after the simulation has completed, click DEFORM-3D Post under Post processor. In post processing the result optioned by step selection, state variables (like, Strain Rate– Effective, Stress-Effective, Load and Temperature etc.). In point tracking to open the point tracking window by click the icon, and see the graph with point Tracking. In slicing Objects by clicking the icon to open the slicing window then the object can be sliced in several different ways. When finished the process exit the post-processor by clicking the exit icon and back in to the main window, exit DEFORM-3D by clicking exit icon.

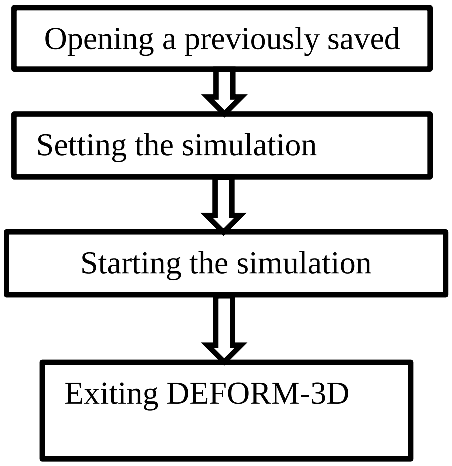

Figure.3. 24 Block Diagram of extrusion simulation and post-processing.

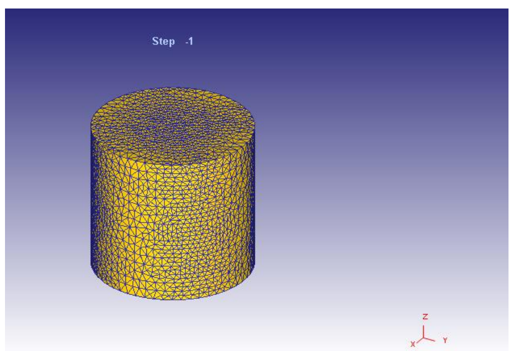

Figure.3. 25 Mesh formulation for circular billet (dia. = 20mm, Size Ratio=1; Number of elements =32000).

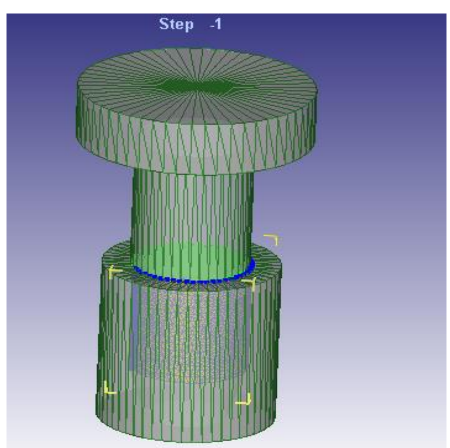

Figure.3. 26 Simulation setup for 30% reduction cosine dies profile

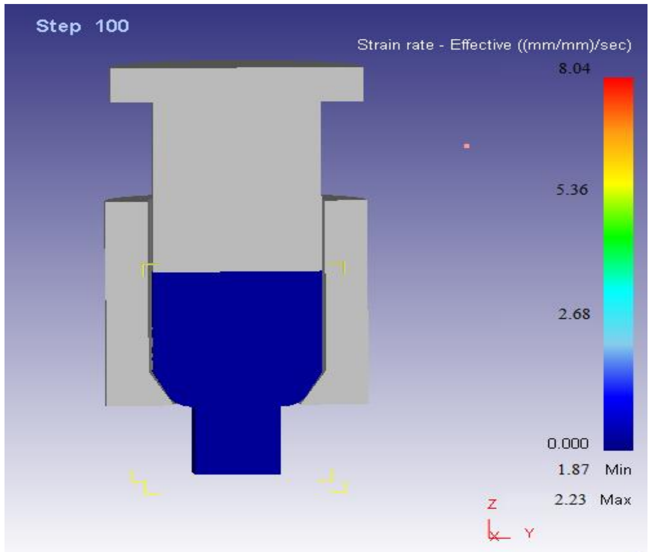

Figure.3. 27 Cosine dies Strain rate effective (30%)

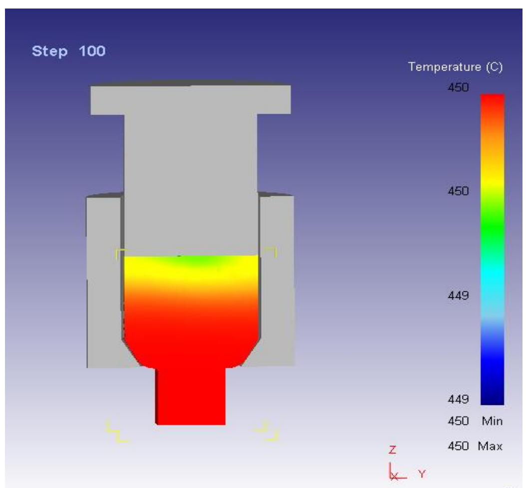

Figure.3. 28 Cosine dies Temperature (30%)

Fig.3.26 has shown the maximum and the minimum strain rate in 30% area reduction of cosine dies. The values are 2.23 and 1.87((mm/mm)/sec) respectively. Fig.3. 27 has shown uniform temperature distribution throughout the system, but some temperatures were loosed due to the instruction between top die and billet materials.

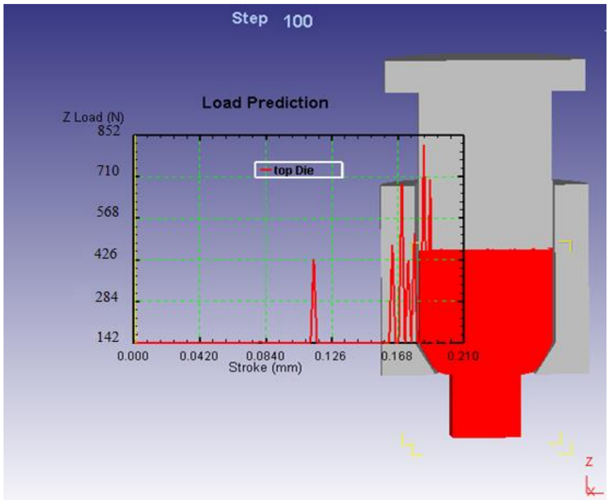

Figure.3. 29 Cosine dies Load prediction (30%)

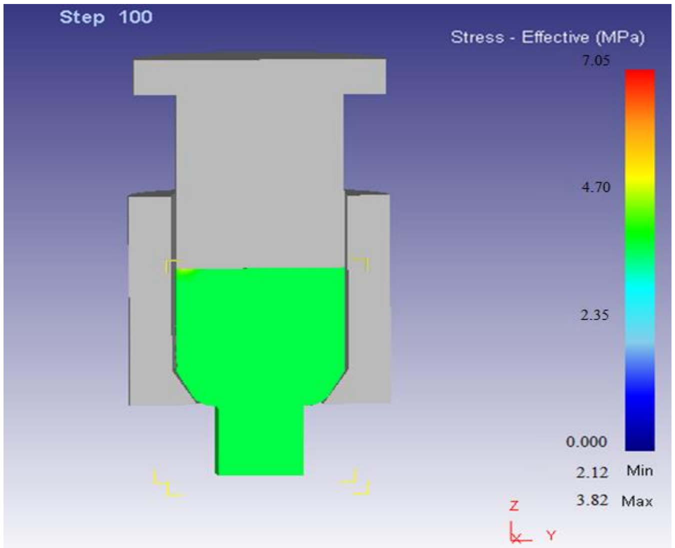

Figure.3. 30 Cosine dies stress effective (30%)

In fig.3.28 has shown above the load prediction of the extrusion and the values of the extrusion load displayed on the graph was 820N. Fig.3.29 shown the maximum and minimum stress effectives on the extrusion process and the values were given 3.82 and 2.12 MPa respectively. The green color shows the maximum stress effective and the blue color shows the minimum stress effective.

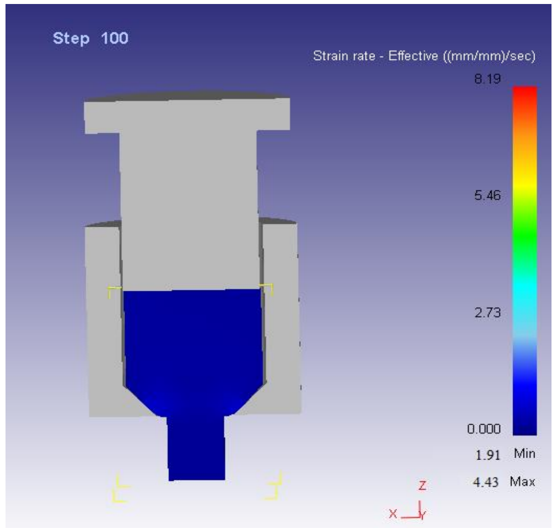

Figure.3. 31 Strain rate effective for 60% reduction cosine die profile

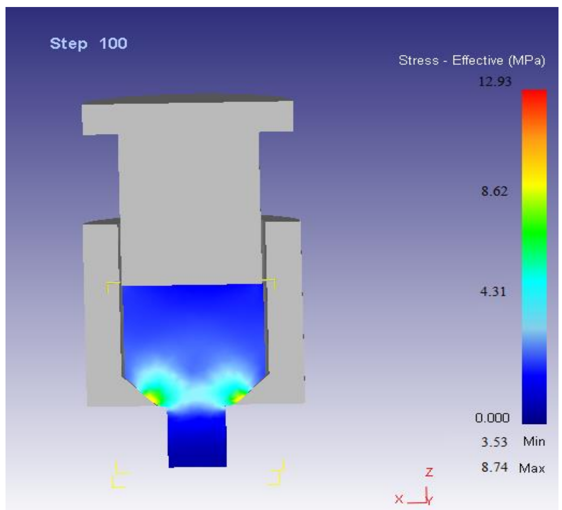

Figure.3. 32 Stress effective for 60% reduction cosine dies profile

Fig.3.30 has shown the maximum and the minimum strain rate in 60% area reduction of cosine dies. The values are 4.43 and 1.91((mm/mm)/sec) respectively. Fig.3.31 shown the maximum and minimum stress effectives on the extrusion process and the values is given 8.74 and 3.53 MPa respectively. The yellow color shows the maximum stress effective and the blue color shows the minimum stress effective.

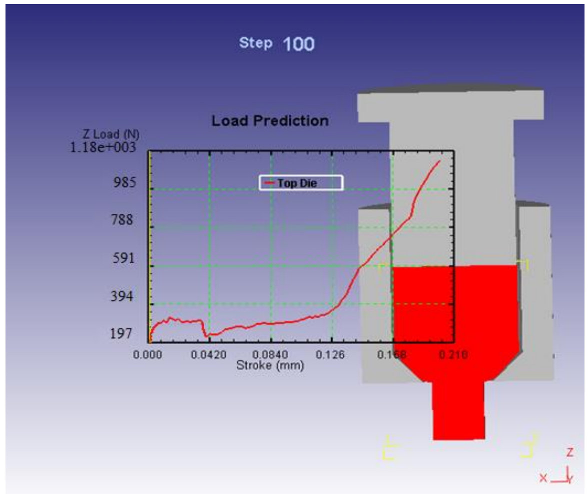

Figure.3. 33 Cosine dies Load prediction (60%)

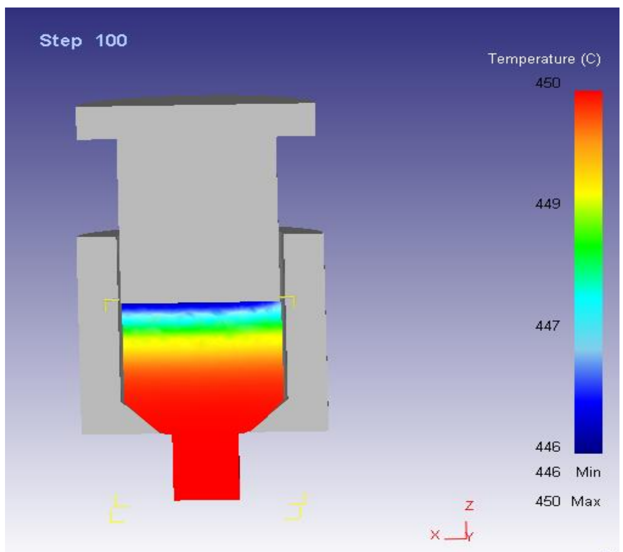

Figure.3. 34 Cosine dies Temperature (60%)

In fig.3.32 has shown above the load prediction of the extrusion and the values of the extrusion load displayed on the graph is 1140N. Fig.3. 33 has shown the uniform temperature distribution throughout the system but some temperatures loosed between top die and billet materials in the system.

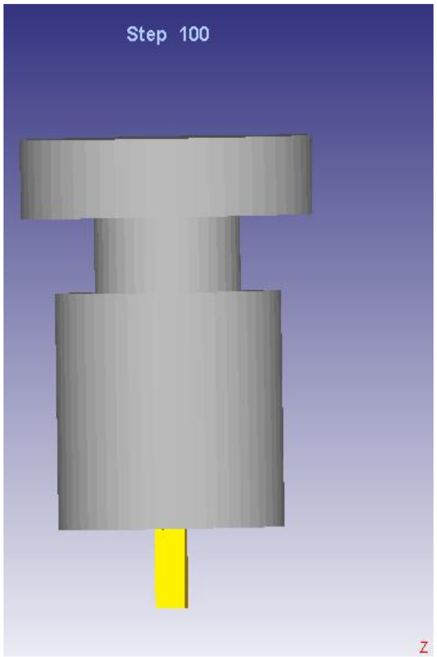

Figure.3. 35 Simulations for 90% reduction cosine die profile

Fig.3.34 above shown the simulation setup of the 90% area reduction of cosine die and it contains top die, billet container with die and billet materials.

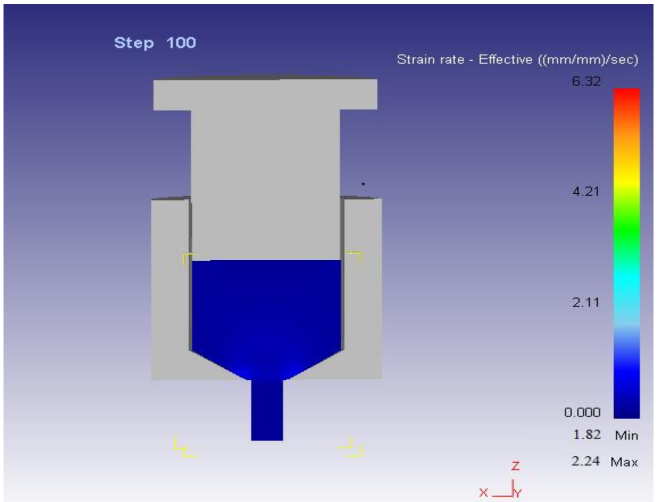

Figure.3. 36 Strain rate effective for 90% reduction cosine die profile

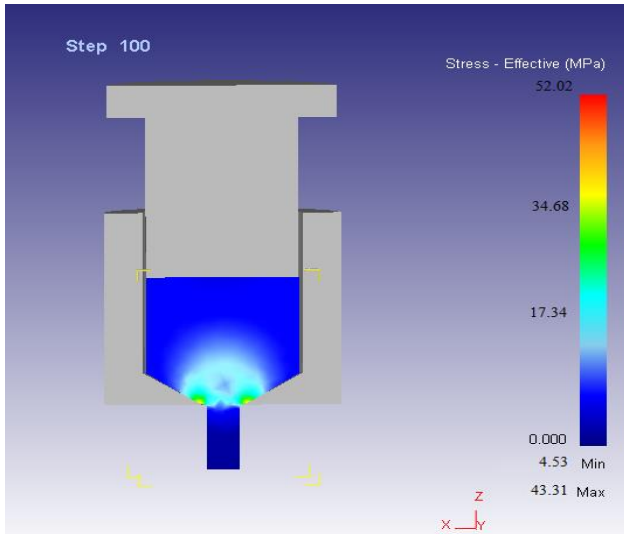

Figure.3. 37 Stress effective for 90% reduction cosine dies profile

Fig.3.35 has shown above the maximum and the minimum strain rate in 90% area reduction of cosine dies. The values are 2.24 and 1.82((mm/mm)/sec) respectively. Fig.3.36 shown above the maximum and minimum stress effectives on the extrusion process and the values is given 43.31and 4.53MPa respectively. The yellow and blue colors are shown the maximum and minimum stress effectives respectively.

In fig.3.37 has shown below the load prediction of the extrusion and the values of the extrusion load displayed on the graph is 1360N. Fig.3. 36 has shown the uniform temperature distribution throughout the system but some temperatures loosed between top die and billet materials in the system.

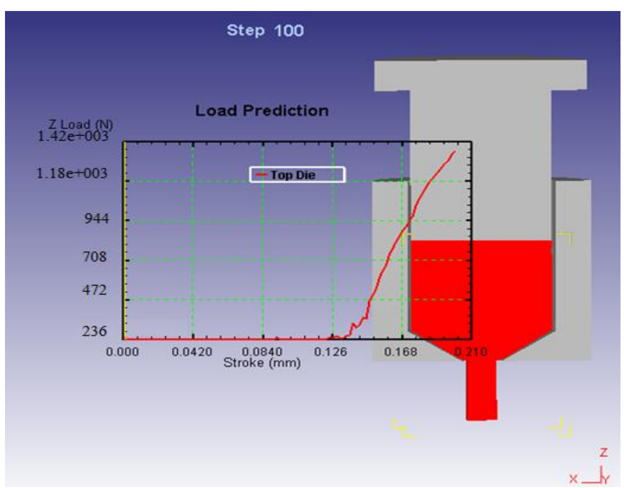

Figure.3. 38 Load prediction for 90% reduction cosine dies profile

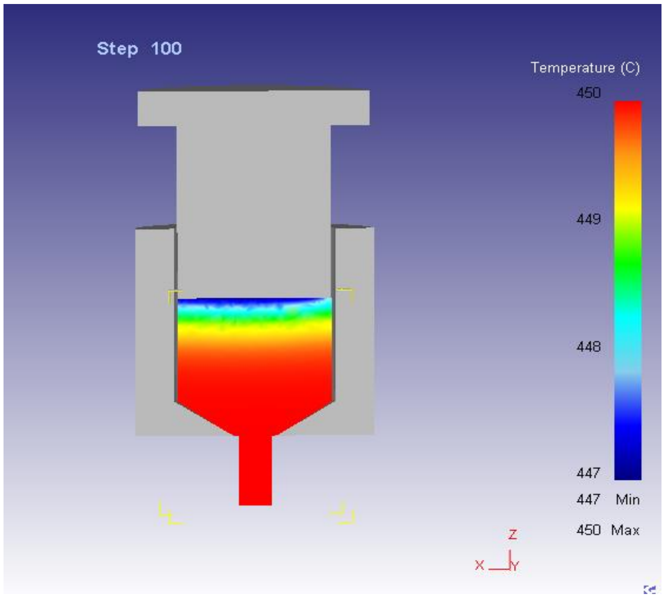

Figure.3. 39 Temperature for 90% reduction cosine dies profile

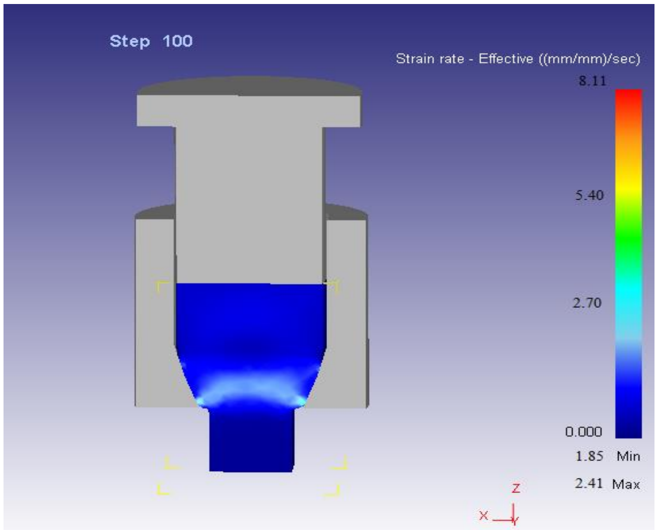

Figure.3. 40 3rd order polynomial dies strain rate effective (30%)

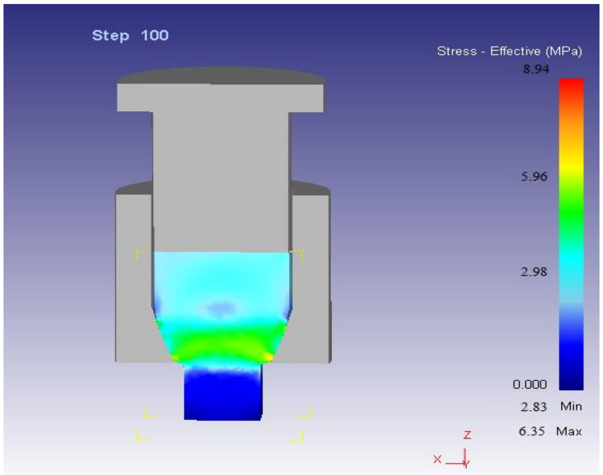

Figure.3. 41 3rd order polynomial dies stress effective (30%)

Fig.3.39 has shown above the maximum and the minimum strain rate in 30% area reduction of 3rd order polynomial dies. The values are 2.41 and 1.85 ((mm/mm)/sec) respectively. Fig.3.40 shown above the maximum and minimum stress effectives on the extrusion process and the values are given 6.35 and 2.83MPa respectively. The yellow and blue colors are shown the maximum and minimum stress effectives respectively.

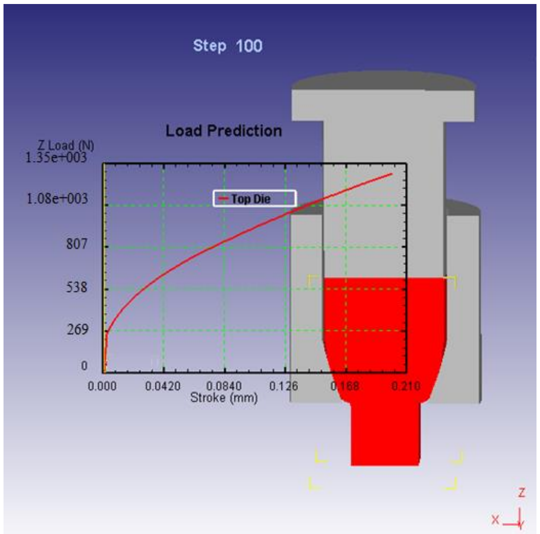

Figure.3. 42 3rd order polynomial dies load prediction (30%)

In fig.3.41 has shown above the load prediction of the extrusion and the value of the extrusion load displayed on the graph is 1290N. Fig.3.42 has shown below, the uniform temperature (450^0c) distribution of the system and minimum temperature is developed at the punch and billet interaction surface which is 446^0c.

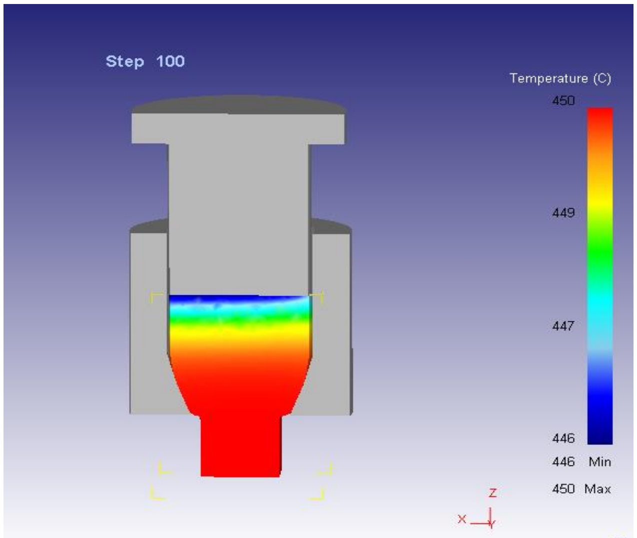

Figure.3. 43 3rd order polynomial dies Temperature (30%)

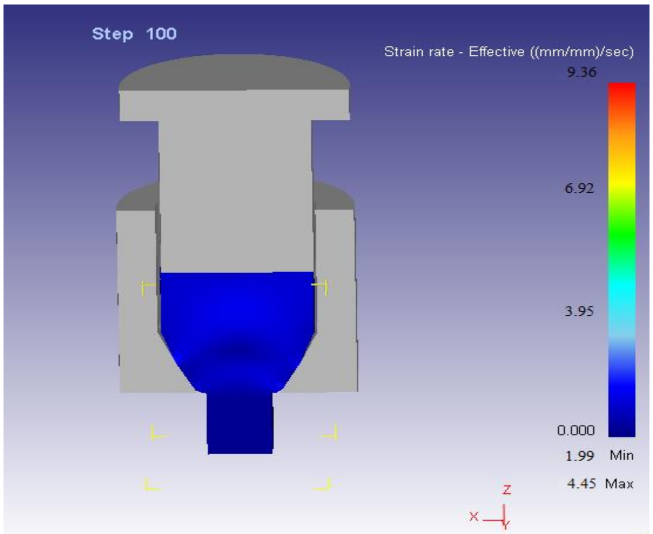

Figure.3. 44 3rd order polynomial dies strain rate effective (60%)

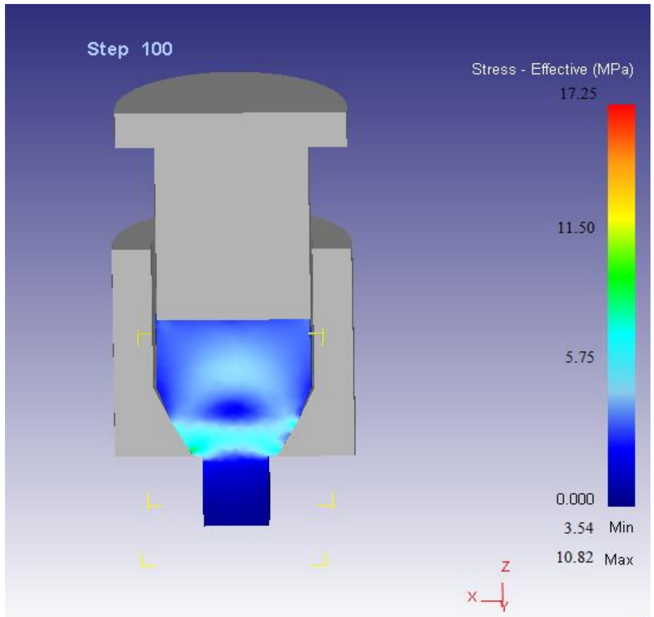

Figure.3. 45 3rd order polynomial dies stress effective (60%)

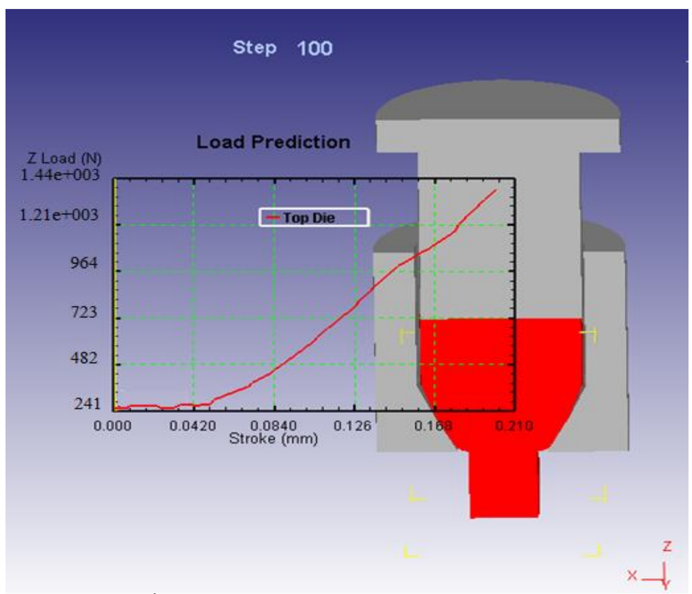

Figure.3. 46 3rd order polynomial dies load prediction (60%)

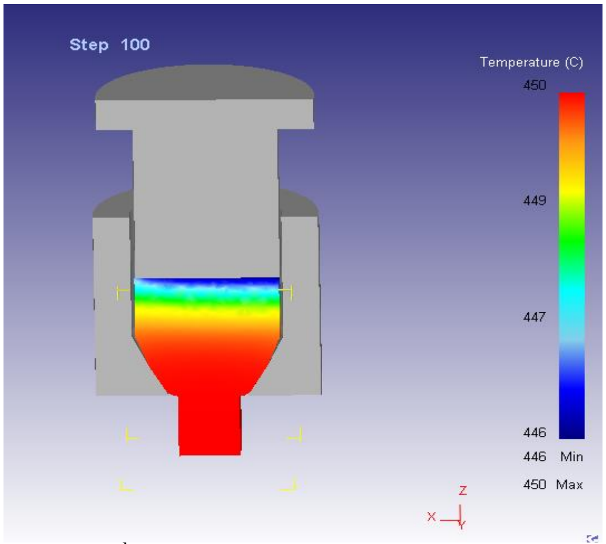

Figure.3. 47 3rd order polynomial dies Temperature (60%)

Fig.3.43 has shown above the maximum and the minimum strain rate in 60% area reduction of 3rd order polynomial dies. The values are 4.45and 1.99((mm/mm)/sec) respectively. Fig.3.44 shown above the maximum and minimum stress effectives on the extrusion process and the values are given 10.82and 3.54 MPa respectively. The green blue colors are shown the maximum and minimum stress effectives respectively. In fig.3.45 has shown above the load prediction of the extrusion and the values of the extrusion load displayed on the graph is 1390N. Fig.3. 46 has shown above, the uniform temperature (450^0c) distribution of the system and minimum temperature is developed at the punch and billet interaction surface which is 446^0c.

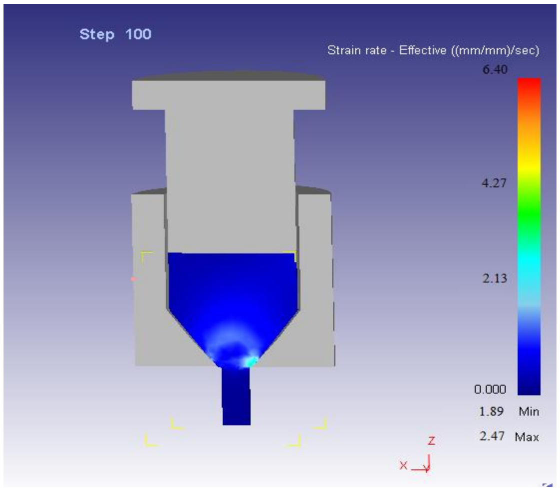

Figure.3. 48 3rd order polynomial dies strain rate effective (90%)

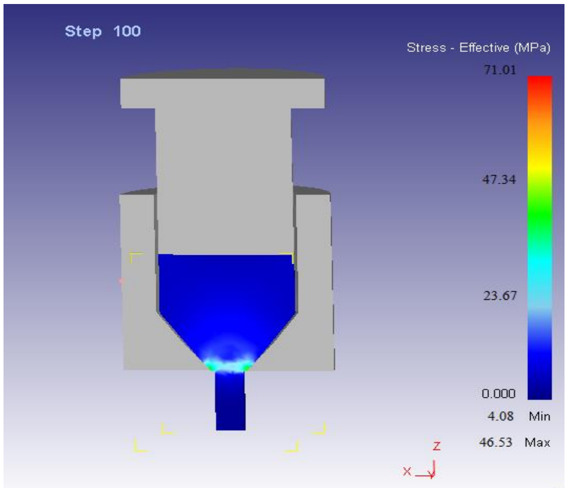

Figure.3. 49 3rd order polynomial dies stress effective (90%)

Fig.3.47 has shown above the maximum and the minimum strain rate in 90% area reduction of 3rd order polynomial dies. The values are 2.47and 1.89((mm/mm)/sec) respectively. Fig.3.48 shown above the maximum and minimum stress effectives on the extrusion process and the values are given46.53 and 4.08MPa respectively. The green and blue colors are shown the maximum and minimum stress effectives respectively.

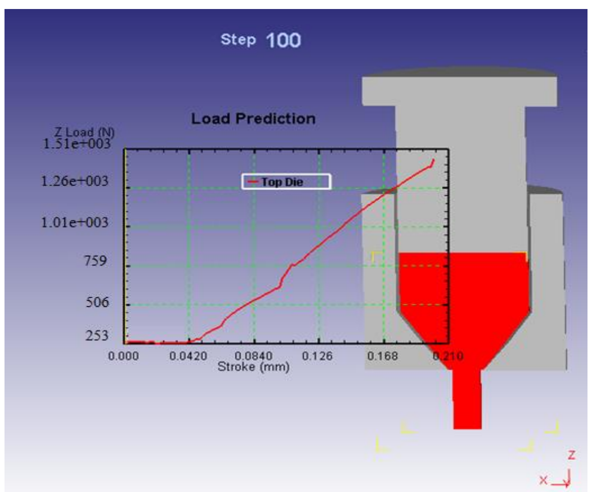

Figure.3. 50 3rd order polynomial dies load prediction (90%)

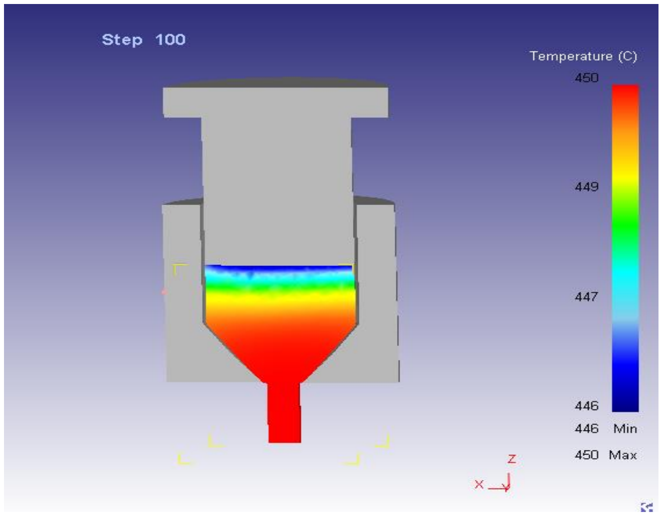

Figure.3. 51 3rd order polynomial dies Temperature (90%)

In fig.3.49 has shown above, the load prediction of the extrusion and the values of the extrusion load displayed on the graph is1460N. Fig.3. 50 has shown above, the uniform temperature (450^0c) distribution of the system and minimum temperature is developed at the punch and billet interaction surface which is 446^0c.

CHAPTER FOUR

RESULT AND DISCUSSION

In this chapter all the results of analytical and numerical analysis are discussed. Results in different reduction conditions are compared with cosine die and 3rd order polynomial die profiles. In cosine and 3rd order polynomial die profiles are taken three different % of area reduction such as: - 30%, 60% and 90%.From this area reduction there were three different extrusion load and effective stress for both cosine and 3rd order polynomial die profiles.

4.1 Upper Bound Analysis Results

Upper bound method is used to analysis the analytical results and the values are shown below tables and graphs.

Table.4. 1 Effective stress and load at different % of area reduction

% of Area reduction	Effective stress(MPa)	Extrusion load(N)
30	4.0111	878.59
60	9.2148	1155.91
90	45.9697	1441.61

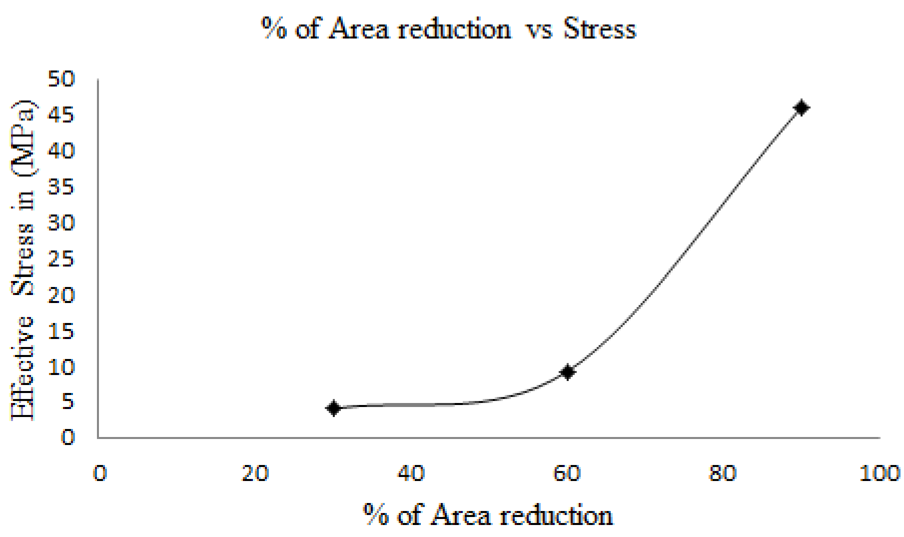

Figure.4. 1 Cosine dies effective stress at different % of area reduction

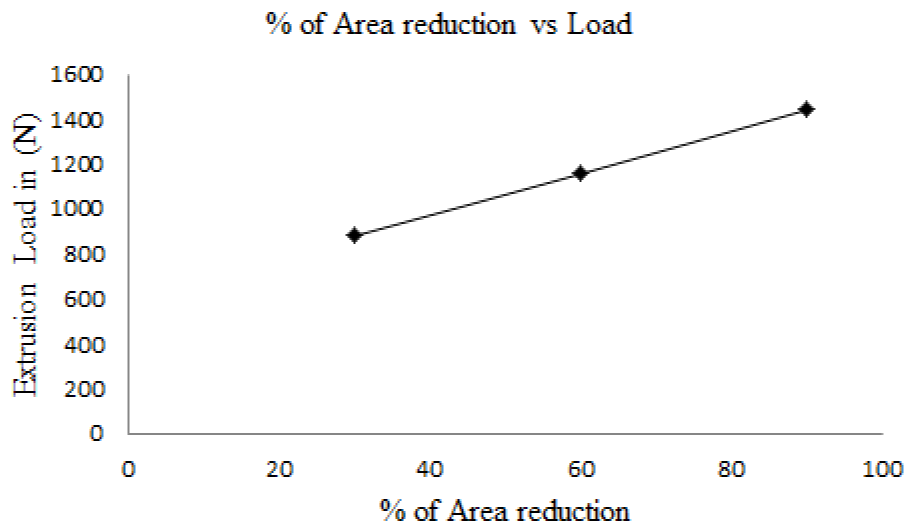

Figure.4. 2 Cosine dies extrusion load at different % of area reduction

Table.4. 2 3rd order polynomial dies Effective stress and load at different % of area reduction

% of Area reduction	Effective stress(MPa)	Extrusion load(N)
30	6.6772	1352.20
60	11.5635	1450.52
90	48.6709	1526.32

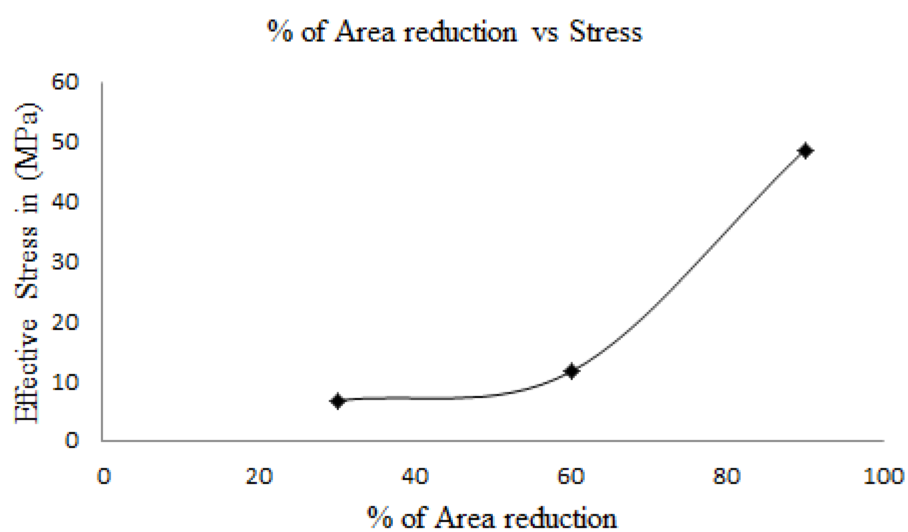

Figure.4. 3 3rd order polynomial dies effective stress at different % of area reduction

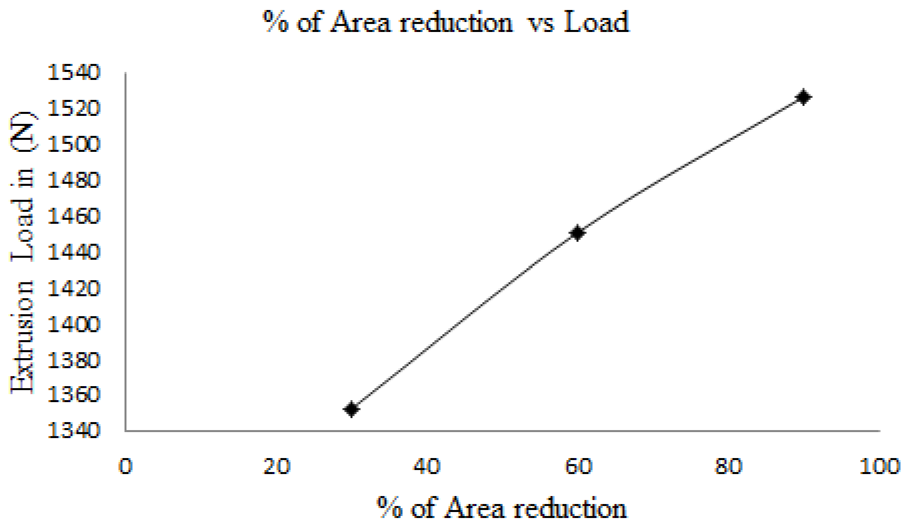

Figure.4. 4 3rd order polynomial dies extrusion load at different % of area reduction

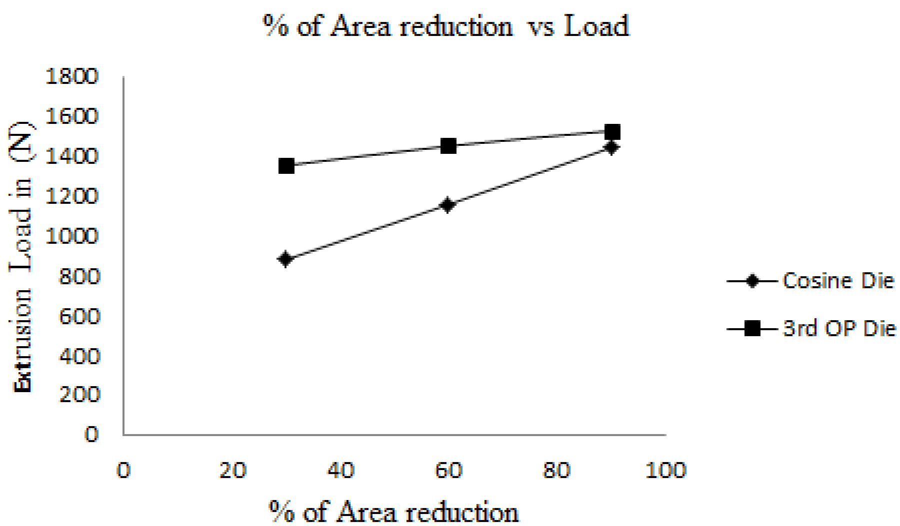

Figure.4. 5 Cosine and 3rd order polynomial dies extrusion load at different % of area reduction

In cosine die profile the stress effective is minimum on 30% of area reduction and maximum on 90% of area reduction. For 3rd order polynomial die profile is similar with cosine die but the value is maximum as compared as cosine die and shown above in fig.4.1 and 4.4 respectively.

The extrusion load is increased with increased the percentage of area reduction for both dies as shown in fig 4.5 and the minimum extrusion load is existed in cosine die profiles. In 3rd order polynomial dies the area reduction is increased from initial to end of the extrusion process. Due to this reason, the deformation is higher than the cosine dies and it needed higher extrusion load to extrude Al6063/20%SiC billet from initial to end of the process.

4.2 Numerical Analysis Results

DEFOEM 3D is used to analysis numerical values and the results are shown below.

Table.4. 3 Effective stress and load at different % of area reduction cosine dies

% of Area reduction	Effective stress(MPa)	Extrusion load(N)
30	3.82	820
60	8.74	1140
90	43.31	1360

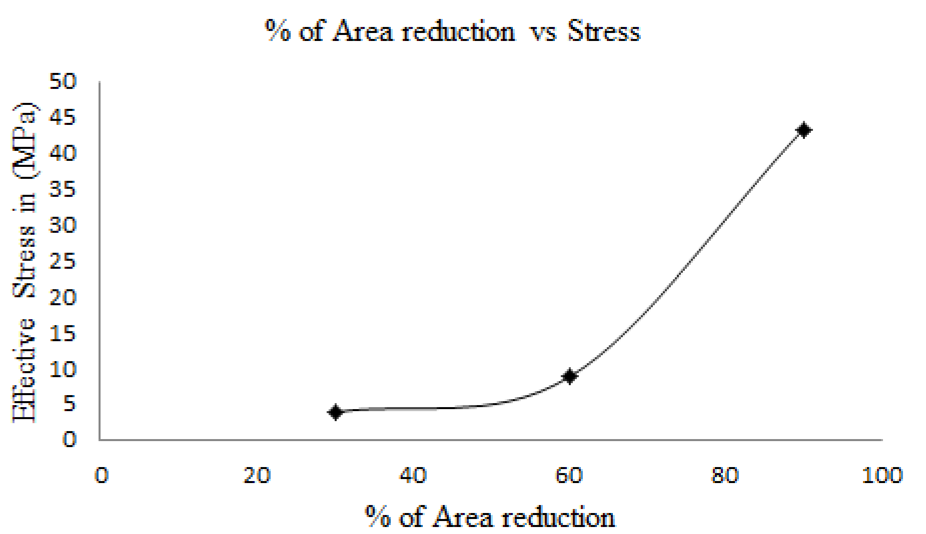

Figure.4. 6 Cosine dies effective stress at different % of area reduction

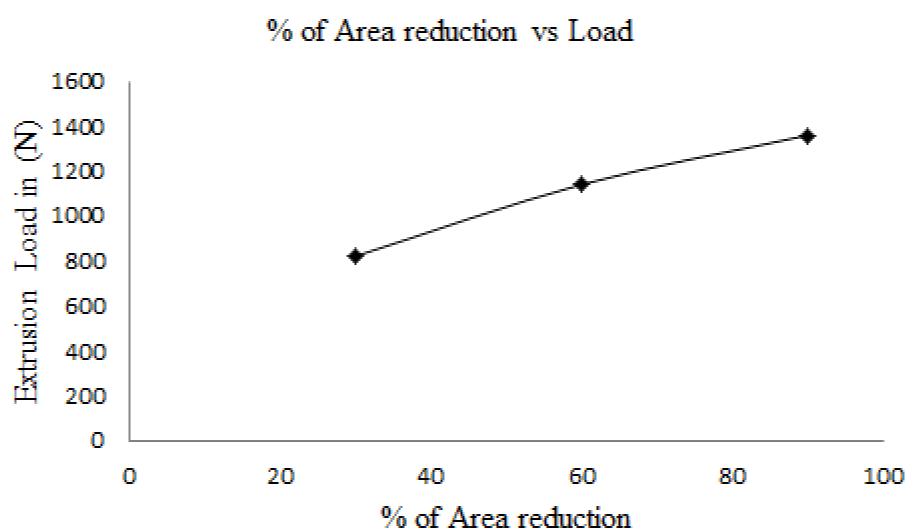

Figure.4. 7 Cosine dies extrusion load at different % of area reduction

Table.4. 4 3rd order polynomial dies Effective stress and load at different % of area reduction

% of Area reduction	Effective stress(MPa)	Extrusion load(N)
30	3.34	1290
60	11.1	1390
90	46.8	1460

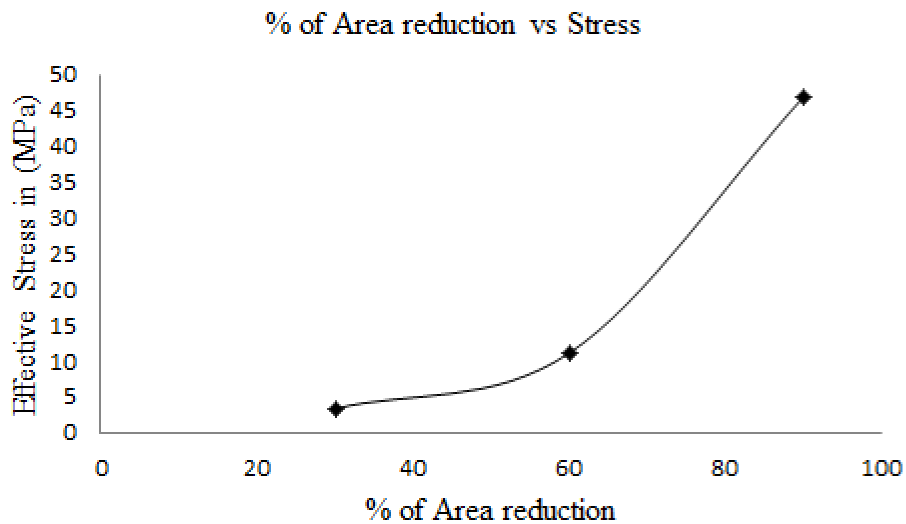

Figure.4. 8 3rd order polynomial dies effective stress at different % of area reduction

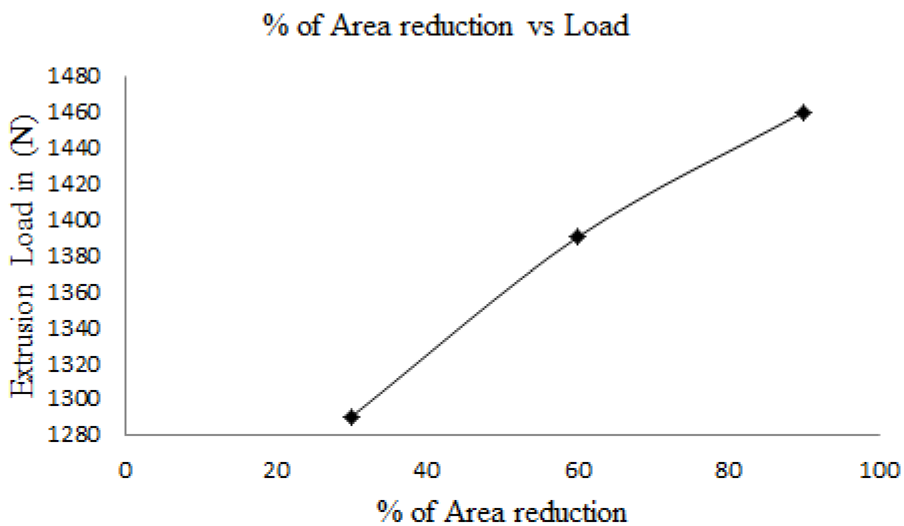

Figure.4. 9 3rd order polynomial dies extrusion load at different % of area reduction

In cosine die profile the stress effective is minimum on 30% of area reduction and maximum on 90% of area reduction. For 3rd order polynomial die profile was similar with cosine die but the value of 3rd order polynomial die is maximum and shown above in fig.4.6 and 4.8 respectively. The value of cosine die stress effective is lower than 3rd order polynomial die profiles. The extrusion load is increased with increased the percentage of area reduction for both dies as shown above in fig 4.7 and fig.4.9 the minimum extrusion load is existed in cosine die profiles.

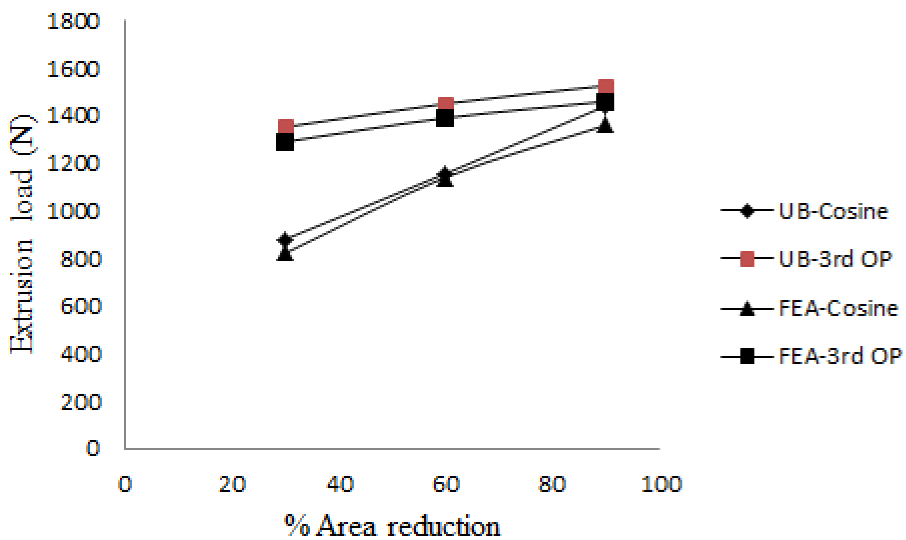

Figure.4. 10 Analytical and Numerical Extrusion Load at different % area reduction

Fig 4.10 above shown analytical and numerical extrusion load at different % area reduction and the results of FEA is minimum values as compare the analytical result values. Generally, due to its low deformation power loss, the cosine die extrusion load is minimum value as compare analytical and numerical analysis results. The cosine die is used as the extrusion load for Al6063/20%SiC composite billet materials. Specially, 30% area reduction cosine die profile has minimum extrusion load as compare other area reduction of cosine and 3rd order polynomial dies and is better to extruded Al6063/20%SiC composite billet materials with optimum extrusion load.

CHAPTER FIVE

CONCLUSION AND RECOMMENDATION

5.1 Conclusion

- For Al6063/20%SiC composite materials which are used to compare cosine and 3rd order polynomial dies to extrude the billet from circular to square shape.
- The cosine die load increased with increased the % of area reduction and similarly, the 3rd order polynomial dies load increased with increased the % of area reduction.
- The results of minimum extrusion load is developed in cosine die profiles as compare from the 3rd order polynomial dies for both analytical and numerical analysis.
- Generally, cosine die profile is used as extrusion die for Al6063/%SiC composite materials to optimum extrusion loads in different % of area reduction of square shape extruded. Specially, 30% area reduction cosine die profile has minimum extrusion load as compare other area reduction of cosine and 3rd order polynomial dies.

5.2 Recommendation

- Cosine die profile could be used as extrusion die for Al6063/20%SiC composite materials to optimum extrusion loads in different % of area reduction of square shape extruded..
- Specifically, could be used 30% area reduction of cosine die has minimum extrusion load from other five dies. Such as; cosine at 60% and 90% area reduction and 3rd order polynomial dies at three different % area reductions. So it used to extrude Al6063/20%SiC composite billet materials with optimum extrusion load.

5.3 Future Work

- For this study depend on theoretical and mathematical analysis results the optimum die profile is selected, so can be check the experimental values with the analytical and numerical values and
- In addition, can be examine the mechanical properties with other die profiles like circular, rectangular, hexagonal and any other die shapes.

6. REFERENCE

[1] A. García-Domínguez, J. Claver, A.M. Camacho, M.A. Sebastián ‘’Comparative Analysis of Extrusion Processes by Finite ElementAnalysis’’- 25th DAAAM International Symposium on Intelligent Manufacturing and Automation, DAAAM,Procedia Engineering 100 (2015) 74 – 83

[2]A. K. Routa K. P. Maityb and S. K. Sahoo (2012) ‘’FEM analysis of Extrusion of Triangular sections from Round Billets through Curved Dies’’- Advanced Materials Research; ISSN: 1662-8985, Vol. 500, pp 391-396

[3] Akshaya Kumar Rout, Kalipada Maity, Sushant Kumar Rath (2010) ‘’A Numerical Investigation of Extrusion through Bezier Shaped Curved Die Profile’’-Key Engineering Materials Vol. 443 (2010) pp 93-97

[4] Aue-u-lan Y., Khansai K., Sinpayakun P., Tragangoon C.(2013) ‘’Investigation of the Parameters Affecting the Die Failure in High Extrusion Ratio of Aluminium Square Hollow Profile by Using Viscoplastic Finite Element Modeling’’- AIJSTPME -6(1): 27-33 27

[5] Beata Pawłowska1(2014) ‘’Metal flow during extrusion of non-circular sections’’ Acta Metallurgica Slovaca, Vol. 20, 2014, No. 1, p. 28-34, p-ISSN 1335-1532 e-ISSN 1338-1156

[6] B.P.P.A. Gouveiaa, J.M.C. Rodriguesa, N. Bay, P.A.F. Martinsa, (2000) ″Deformation analysis of the round-to-square extrusion: a numerical and experimental investigation" Finite Elements in Analysis and Design 35, 269-282

[7] B.P.P.A. Gouveiaa, J.M.C. Rodriguesa, N. Bay, P.A.F. Martinsa,(2001) ″Physical modeling and numerical simulation of the round to square forward extrusion" Journal of materials processing Technology 112,244-251

[8] C. Sun, R. Shen, and M. Song (2012) "Effects of sintering and extrusion on the microstructures and Mechanical properties of a SiC/Al-Cu composite"- Journal of Materials Engineering and Performance, pp 373-381.

[9] C.S Ramesh, Adarsha Hirianiah, Harishanad K.S, Naveen Prakash Noronha (2012) ‘’A review on hot extrusion of Metal Matrix Composites (MMC’s)’’ International Journal of Engineering and Science ISBN: 2319-6483, ISSN: 2278-4721, Vol. 1, Issue 10 PP 30-35

[10] C. Venkatesh · R. Venkatesan(2014) "Design and analysis of optimal die profile for the extrusion of round SiC DRMM Al 6061 Composite billet into hexagonal section’’- Journal of Mechanical Science and Technology 28 (5) 1867-1874

[11] C.W. Wu, R.Q. Hsu (2000) ‘’Theoretical analysis of extrusion of rectangular, hexagonal and octagonal composite clad rods’’-International Journal of Mechanical Sciences 42 (2000) 473-486

[12] Debabrata Rath, Dr. Sushanta Tripathy (2013) "Investigation of Extrusion of lead experimentally from Round section through Equilateral Triangular section Converging dies at different area reductions during Forward Metal Extrusion Process" Research Invent: International Journal Of Engineering And Science Vol.3, Issue, PP, 32-38

[13]DEFORM 3D v11.0 user manual

[14] D. Poirier, R. A. L. Drew, M. L. Trudeau (2010) "Fabrication and properties of mechanically milled alumina/aluminumnano composites". Materials Science and Engineering A, Vol. 527, No. 29-30,pp 7605-7614.

[15] F. Ghaemi, R. Ebrahimi, R. hosseinifar (2013) ‘’Optimization of die profile for cold forward extrusion using an improved slab method analysis’’- IJST, Transactions of Mechanical Engineering, Vol. 37, No. M2, pp 189-202

[16] H.H. kim, J.S.S. babu, and C.G. kang (2014) ‘’Hot Extrusion of A356 Aluminum Metal Matrix Composite with Carbon Nanotube/Al2O3 Hybrid Reinforcement’’ -The Minerals, Metals & Materials Society and ASM International- DOI: 10.1007/s11661-014-2185-5

[17] Jabbar Kasim Jabbar, (2010) "Calculation of relative extrusion pressure for circular section by local coordinates system by Using finite element method (FEM) " Vol. 03 , No. 02 , pp.80-96

[18] Joseph S. Ajiboye ‘’Upper bound analysis of extrusion from square billets through circular and square/rectangular dies’’- Journal of Mechanical Science and Technology 23 (2009) 461-474

[19] K. Abrinia & M. Makaremi(2009) ‘’An analytical solution for the spread extrusion of shaped sections’’Int J Adv Manuf Technol 41:670–676

[20] K.F. Celik, N.R. Chitkara *(*2000) *"*Application of an upper bound method to off-centric extrusion of square sections, analysis and experiments"-International Journal of Mechanical Sciences 42 page 321-345

[21] K.K. Pathak, Vikas Pagey, and V.K. Sethi (2014) "Die and Process Design for Square Rod Extrusion’’-International Conference on Emerging Trends in Computer and Image Dec. 15-16, Pattaya (Thailand)

[22] Mahendra singh pachalasiya, (2013) ‘’modeling of extrusion through curve die’’page, 21-53

[23] Maity K, Chaubey S), Rath S. 2)(2013) "A numerical analysis of extrusion of square section from round billet through mathematically contoured die with design of die profile"- Journal for Technology of Plasticity, Vol. 38,Number 1

[24] Marcelo, Matos Martins, Sérgio Tonini Button (2017) ‘’ Analysis of metal extrusion by the Finite Volume Method’’ International Conference on the Technology of Plasticity, ICTP, 17-22.

[25] Md. Halibut Rahmana,, H. M. Mamun Al Rashedb (2014) "Characterization of silicon carbide reinforced aluminum matrix composites" Procedia Engineering 90 ,103-109

[26] N. Venkata Reddy, P.M. Dixit, G.K. Lal (1995) ’’Die design for axisymmetric extrusion’’ Journal of Materials Processing Technology 55 - 331-339

[27] Peyman Karami, Karen Abrinia, Babak Saghafi (2014) ‘’A new analytical definition of the dead material zone for forward extrusion of shaped sections’’- Meccanica 49:295–304

[28]R. K. Sahoo & P. R. Samantaray & S. K. Sahoo &B. Sahoo & P. K. Kar ‘’Round-to-channel section extrusion through linearly converging die: a three-dimensional analysis’’-Int J Adv Manuf Technol 41:677–683

[29] R. RahmaniFard and F. Akhlaghi(2007) "Effect of extrusion temperature on the microstructure and Porosity of A356-SiCp composites" Journal of Materials Processing Technology, Vol. 187-188,pp 433-436.

[30] R. Venkatesan1 and C. Venaktesh2 (2014) Analytical, numerical and experimental approach for design and development of optimal die profile for the cold extrusion of B4C DRMM Al 6061 composite billet into hexagonal section"-Journal of Mechanical Science and Technology, 5117~5127

[31] Sambit Kumar Mohapatra, Kalipada Maity(2015)’’ Modelling of extrusion of square section of aa-6xxx through cosine and linear converging die’’ Journal for Technology of Plasticity, Vol. 40 ,Number 2

[32] S. K. Mohapatra and K. P. Maity ‘’ Parametric Optimization of Simulated Extrusion of Square to Square Section through Linear Converging Die’’- 5th National Conferences on Processing and Characterization of Materials, doi: 10.1088/1757-899

[33] S. T. Oyinbo, O.M Ikumapayi, J.S Ajiboye, S.A Afolalu (2015) ‘’ Numerical Simulation of Axisymmetric and Asymmetric Extrusion Process Using Finite Element Method, International Journal of Scientific & Engineering Research, Volume 6, Issue 6, ISSN 2229-5518.

[34] Tahir Altinbalik, Onder Ayer (2013) ‘’ Effect of die inlet geometry on extrusion of clover sections through curved dies:Upper bound analysis and experimental verification’’ Trans. Nonferrous Met. Soc. China 23- 1098−1107.

[35] X. Jiang, M. Galano, F. Audebert, "Microstructure and mechanical behavior of 6061 Al alloy reinforced with sic nano particles processed by extrusion and cold rolling "the 19th international conference on composite materials.

[36] Z. W. Wang, M. Song, C. Sun (2010) "Effect of extrusion and particle volume fraction on the Mechanical properties of SiC reinforced Al-Cualloy composites". Materials Science and Engineering A, Vol. 527, No. 24-25, pp 6537-6542.